



University  
of Glasgow

Chaneton, Barbara Julieta (2014) *Targeting cancer cell metabolism as a therapeutic strategy*. PhD thesis.

<http://theses.gla.ac.uk/5762/>

Copyright and moral rights for this thesis are retained by the author

A copy can be downloaded for personal non-commercial research or study, without prior permission or charge

This thesis cannot be reproduced or quoted extensively from without first obtaining permission in writing from the Author

The content must not be changed in any way or sold commercially in any format or medium without the formal permission of the Author

When referring to this work, full bibliographic details including the author, title, awarding institution and date of the thesis must be given

# Targeting Cancer Cell Metabolism as a Therapeutic Strategy

Barbara Julieta Chaneton

This Thesis is submitted to the University of Glasgow in accordance with the requirements for the degree of Doctor of Philosophy in the Faculty of Medicine Graduate School

The Beatson Institute for Cancer Research  
Garscube Estate  
Switchback Road  
Bearsden  
Glasgow

Institute of Cancer Sciences  
College of Medical, Veterinary and Life Sciences  
University of Glasgow  
September 2014



## Abstract

In the past 15 years the field of cancer metabolism has burst providing vast quantities of information regarding the metabolic adaptations found in cancer cells and offering promising hints for the development of therapies that target metabolic features of cancer cells.

By making use of the powerful combination of metabolomics and  $^{13}\text{C}$ -labelled metabolite tracing we have contributed to the field by identifying a mitochondrial enzymatic cascade crucial for oncogene-induced senescence (OIS), which is a tumour suppressive mechanism important in melanoma, linking in this way OIS to the regulation of metabolism.

Furthermore, we have identified the dependency on glutamine metabolism as an important adaptation occurring concomitantly with the acquisition of resistance to vemurafenib (BRAF inhibitor) in melanoma, which opens the possibility to combine therapies targeting glutamine metabolism with BRAF inhibitors, in order to overcome or avoid the onset of resistance in melanoma.

Using the same strategy we have discovered an important mechanism of inter-regulation between glycolysis and amino acid metabolism, identifying the glucose-derived amino acid serine as an activator of the main isoform of pyruvate kinase present in cancer cells, PKM2. In addition, we provide new insights into the mechanism of allosteric regulation of this complex protein and a better understanding of the way it regulates central carbon metabolism.

In summary, our results open new possibilities for the development of cancer therapies that manipulate metabolic adaptations found in cancer cells in order to kill them specifically or halt their growth.

# Table of Contents

Abstract .....	2
Table of Contents .....	3
List of Figures .....	6
Acknowledgements .....	7
Author's Declaration.....	8
Abbreviations .....	9
<b>Chapter 1 - Introduction .....</b>	<b>11</b>
1.1 <i>Cancer Metabolism</i> .....	12
1.1.1 Oncogenes, Tumour Suppressors and Growth Factor Signalling in Cancer Metabolism .....	12
1.1.2 The Warburg Effect and the Regulation of Glycolysis in Cancer .....	12
1.1.2.1 An Example of Complex Regulation in Glycolysis: Pyruvate Kinase M2 .....	17
1.1.3 Glutaminolysis.....	23
1.1.4 The Role of Metabolism in Tumour Initiation and Progression.....	23
1.2 <i>Therapeutic Strategies</i> .....	29
1.2.1 Targeting Glycolysis and the Pentose Phosphate Pathway.....	29
1.2.2 Targeting Pyruvate Metabolism .....	31
1.2.3 Targeting Amino Acid Metabolism.....	32
1.2.4 Targeting Fatty Acid Metabolism.....	33
1.2.5 Targeting the Master Regulators of Tumour Metabolism .....	34
1.3 <i>The Use of Metabolomics and <sup>13</sup>C Tracers to Identify Metabolic Vulnerabilities in Cancer Cells</i> .....	35
1.4 <i>Aims</i> .....	36
<b>Chapter 2 - Materials and Methods .....</b>	<b>37</b>
2.1 <i>Materials</i> .....	38
2.1.1 Reagents .....	38
2.1.2 Primers .....	39
2.1.3 Antibodies.....	39
2.1.4 Vectors and plasmids.....	40
2.1.5 Cell lines .....	40
2.1.6 Equipment .....	40
2.1.7 General buffers and solutions .....	41
2.2 <i>Experimental procedures</i> .....	42
2.2.1 Mammalian cell culture related techniques .....	42
2.2.1.1 Cell culture and storage .....	42
2.2.1.2 Generation of cell lines by shRNA lentiviral infection .....	43
2.2.1.3 Whole cell lysate protein preparation, SDS-PAGE and Western blot .....	44
2.2.1.4 Total mRNA isolation and qPCR .....	45
2.2.1.5 Cell proliferation .....	45
2.2.2 Protein related techniques.....	45
2.2.2.1 Recombinant protein production, isolation and characterization	45
2.2.2.2 <i>In vitro</i> pyruvate kinase activity .....	46
2.2.2.3 UV HPLC Size-exclusion chromatography .....	47
2.2.2.4 Isothermal titration calorimetry .....	48
2.2.2.5 X-ray crystallography .....	48

2.2.2.6 PKM2 mutagenesis.....	49
2.2.3 Metabolic measurements.....	50
2.2.3.1 Metabolic fluxes and exchange rates.....	50
2.2.3.2 Metabolites labelling with $^{13}\text{C}_6$ glucose / $^{13}\text{C}_5$ L-glutamine and extraction.....	50
2.2.3.3 LC-MS metabolomics and metabolites' quantification.....	50
2.2.3.4 Extracellular oxygen and H <sup>+</sup> flux measurements.....	51
2.2.3.5 ATP measurement.....	52
2.2.4 Statistical analysis and data processing.....	52
<b>Chapter 3 - Characterisation of Serine as a Natural Ligand and Allosteric Activator of Pyruvate Kinase M2.....</b>	<b>54</b>
3.1 Introduction.....	55
3.2 Results.....	56
3.2.1 Characterization of HCT116 cells upon PKM2 silencing.....	56
3.2.2 Low PK activity and serine deprivation alter $^{13}\text{C}_6$ -glucose metabolism.....	60
3.2.3 Serine binds to, and activates, PKM2.....	63
3.2.4 PKM2 activation by serine is independent of FBP and does not require tetramerization.....	66
3.2.4.1 <i>In vitro</i> activity.....	66
3.2.4.2 Conformational analysis by UV HPLC-SEC.....	68
3.3 Conclusions.....	70
<b>Chapter 4 - Changes in Glucose Metabolism Related to Oncogene-Induced Senescence (OIS).....</b>	<b>71</b>
4.1 Introduction.....	72
4.2 Results.....	73
4.2.1 BRAF <sup>V600E</sup> -induced senescence increases mitochondrial glucose metabolism.....	73
4.2.2 Mass balance analysis.....	75
4.2.3 Effect of K-RAS <sup>G12V</sup> -induced senescence on glucose metabolism.....	79
4.2.4 Effect of cell cycle arrest on glucose metabolism.....	81
4.3 Conclusions.....	83
<b>Chapter 5 - Resistance to BRAFV600E Inhibition Induces Glutamine Dependency in Melanoma Cell Lines.....</b>	<b>84</b>
5.1 Introduction.....	85
5.2 Results.....	86
5.2.1 BRAF <sup>V600E</sup> inhibition stimulates mitochondrial biogenesis and oxidative metabolism.....	86
5.2.2 BRAF <sup>V600E</sup> inhibition reduces glycolytic flux.....	88
5.2.3 PLX4720-resistant cells display increased glutaminolysis.....	90
5.2.4 Inhibition of glutaminolysis sensitizes PLX4720-resistant cells to PLX4720.....	92
5.3 Conclusions.....	94
<b>Chapter 6 - Discussion and Final Remarks.....</b>	<b>95</b>
6.1 Discussion.....	96
6.1.1 Identification of a new mechanism of allosteric regulation for PKM2.....	97
6.1.2 Therapeutic targeting of metabolic regulators to reactivate senescence.....	99
6.1.3 Inhibition of glutamine metabolism as a therapeutic strategy in PLX- resistant melanoma.....	100
6.2 Final Remarks.....	103

**Bibliography ..... 104**  
**Appendices ..... 120**

## List of Figures

Figure 1:1- Scheme of the central carbon metabolism.....	15
Figure 1:2- The regulation of PDH activity .....	17
Figure 1:3- The effect of PKM2 activity regulation on metabolism .....	22
Figure 1:4- The phosphorylated pathway for serine synthesis .....	26
Figure 1:5- The mTOR signalling pathway .....	28
Figure 3:1- Characterisation of PKM1/2-silenced HCT116 cells.....	58
Figure 3:2- Modulation of central carbon metabolism by PKM1/2-silencing and serine/glycine deprivation.....	62
Figure 3:3- Serine is an allosteric activator of PKM2 .....	64
Figure 3:4- <i>In vitro</i> effects of serine and FBP on PKM2 activity .....	67
Figure 3:5- Oligomeric state of PKM2 in the presence of serine or FBP .....	69
Figure 4:1- Glucose metabolism in BRAF <sup>V600E</sup> -induced senescence .....	74
Figure 4:2- Metabolic model for concerted activation of PDH necessary to drive OIS .....	78
Figure 4:3- Glucose metabolism in K-RAS <sup>G12V</sup> -induced senescence .....	80
Figure 4:4- Glucose metabolism in quiescent cells .....	82
Figure 5:1- BRAF <sup>V600E</sup> inhibition increases mitochondria and the oxidative phenotype in melanoma cell lines.....	87
Figure 5:2- BRAFV600E inhibition results in decreased glycolytic flux.....	89
Figure 5:3- PLX4720-resistance increases glutamine metabolism .....	91
Figure 5:4- Inhibition of glutaminolysis hampers oxidative metabolism and cell viability of PLX4720-resistant cell lines .....	93

## Acknowledgements

Firstly I want to thank my supervisor Eyal Gottlieb and my advisor Karen Blyth for their continuous guidance and endless patience. Eyal, you have been an outstanding boss and the best mentor I could have asked for during these years. Thanks for allowing me to make mistakes and develop my own ideas, thanks for offering me never-ending opportunities to learn and life-long lessons. I will always be grateful for the opportunity you've given me by making me a member of your lab.

From the lab I want to thank 'the guys': The dragon, The Doc, The salmon, Elaine, Laura, Zach, Nadja, Elodie and Simone for their support during the tough times, the long hours of experiments shared and all the good moments we spent together that will always remain with me. I also want to thank to Christian Frezza who taught me almost everything I know about cancer metabolism and who helped me giving the first steps in the lab. Nothing of this would have been possible without you 'Dr. Christian'!

I want to thank my collaborators Joanna Kaplon, Franziska Baenke and Petra Hillman (including all the Astex team). It has been a real pleasure to work with you and learn from you.

Huge thanks to all my dear friends: the Argentineans and the Sicilians that are always there, no matter the distance or time. I want to thank to the many friends that I've met during these years at the Beatson, especially Pearl, Jiska, Martina, Alice, Desi, Gabriele and also many others for making my PhD the most memorable time of my life, you guys will go with me wherever I go.

Finally I want to thank to the most important people in my life: Mabel, mami for supporting me with her endless love and understanding and Kostas, agapi mou, for being the best man I know and making me a better person with his love.

I would also like to thank Cancer Research UK for funding my PhD at the Beatson Institute for Cancer research.

## **Author's Declaration**

I hereby declare that the work presented in this thesis is the result of my own independent investigation unless otherwise stated.

This work has not hitherto been accepted for any other degree, nor is it being currently submitted for any other degree

Barbara Julieta Chaneton

## Abbreviations

2HG, 2 hydroxyglutarate  
 4EBP1, eukaryotic translation initiation factor 4E-binding protein 1  
 ACL, ATP citrate lyase  
 ACN, aconitase  
 ADP, adenosine diphosphate  
 ALD, aldolase  
 ALT, alanine transaminase  
 AKT, protein kinase B  
 AML, acute myeloid leukemia  
 AMP, adenosine monophosphate  
 AMPK, AMP activated protein kinase  
 ASCT, amino acid transporter  
 ATP, adenosine triphosphate  
 BPTES, bis-2-(5-phenylacetamido-1,3,4-thiadiazol-2-yl)ethyl sulfide  
 BSA, bovine serum albumin  
 CCCP, carbonyl cyanide m-chlorophenyl hydrazine  
 c-Myc, V-myc avian myelocytomatosis viral oncogene homolog  
 CS, citrate synthase  
 ENO, enolase  
 ECAR, extracellular acidification rate  
 EGFR, epidermal growth factor receptor  
 ERK, extracellular-signal regulated kinase  
 ETC, electron transport chain  
 F6P, fructose-6-phosphate  
 FAD, flavin adenine dinucleotide  
 FAS, fatty acid synthase  
 FBP, fructose 1,6 bisphosphate  
 FDG-PET, 2-(<sup>18</sup>F)-fluoro-2-deoxy-D-glucose positron emission tomography  
 FH, fumarate hydratase  
 FKBP12, FK506 binding protein 12  
 G6P, glucose-6-phosphate  
 GAPDH, glyceraldehyde 3-phosphate dehydrogenase  
 GBM, glioblastoma multiforme  
 GDH, glutamate dehydrogenase  
 GDP, guanosine diphosphate  
 Glut, glucose transporter  
 GLS, glutaminase  
 GTP, guanosine triphosphate  
 H<sub>2</sub>O<sub>2</sub>, hydrogen peroxide  
 HIF 1 $\alpha$ , hypoxia inducible factor 1 $\alpha$   
 HK, hexokinase  
 HLRCC, hereditary leiomyomatosis and renal cell cancer  
 hnRNP, heterogeneous nuclear ribonucleoprotein

HPLC-MS, high performance liquid chromatography-mass spectrometry  
IDH, isocitrate dehydrogenase  
LDH, lactate dehydrogenase  
LKB1, liver kinase B1  
MCT, monocarboxylate transporter  
MDH, malate dehydrogenase  
ME, malic enzyme  
mTOR, mechanistic target of rapamycin  
NAD, nicotinamide adenine dinucleotide  
NADP, nicotinamide adenine dinucleotide phosphate  
NLS, nuclear localisation signal  
NMR, nuclear magnetic resonance  
OCR, oxygen consumption rate  
OXPHOS, oxidative phosphorylation  
PC, pyruvate carboxylase  
PCR, polymerase chain reaction  
PDC, pyruvate dehydrogenase complex  
PDH, pyruvate dehydrogenase  
PDK, pyruvate dehydrogenase kinase  
PDP, pyruvate dehydrogenase phosphatase  
PEP, phosphoenolpyruvate  
PFK, phosphofructokinase  
PFKFB2, 6-phosphofructo-2-kinase/fructose-2,6-bisphosphatase  
PGK, phosphoglycerate kinase  
PGI, phosphoglucose isomerase  
PGAM, phosphoglycerate mutase;  
PHD, prolyl hydroxylase  
PHGDH, phosphoglycerate dehydrogenase  
PI3K, phosphoinositol 3-kinase  
PK, pyruvate kinase  
PKC $\alpha$ , protein kinase C alpha  
PPP, pentose phosphate pathway  
PSAT, phosphoserine amino transferase  
REDD1, DNA-damage-inducible transcript 4 protein  
ROS, reactive oxygen species  
RTK, receptor tyrosine kinase  
S6, ribosomal protein S6  
S6K, S6 kinase  
SDH, succinate dehydrogenase complex  
SLC1A5, glutamine transporter  
SHMT, serine hydroxymethyl transferase  
TCA cycle, tricarboxylic acid cycle  
TIGAR, TP53-induced glycolysis and apoptosis regulator  
TPI, triose phosphate isomerase  
TSC1/2, tuberous sclerosis 1 and 2

# Chapter 1 - Introduction

## **1.1 Cancer Metabolism**

### **1.1.1 Oncogenes, Tumour Suppressors and Growth Factor Signalling in Cancer Metabolism**

Proto-oncogenes and tumour suppressor genes are main regulators of tissue homeostasis and coordinators of growth signals. Genetic alterations in those can result in constitutively active growth signalling that induces cells to proliferate uncontrollably. As a consequence of this unrestrained proliferation, tumour cells have a remarkably different metabolism to the tissues from which they originated(1). This metabolic reprogramming in cancer cells provides a continuous supply of building blocks and redox potential allowing them to survive and proliferate under strict selective pressure, considering that they require more nutrients and excrete more waste products than normal tissues. In order to divide, cells need to increase in size, and replicate their DNA, processes that require vast amounts of proteins, lipids and nucleotides as well as energy. Therefore, to support these anabolic processes, cells need to increase their uptake of carbon units with amino acids and glucose constituting their main sources(2). The molecular mechanisms underlying metabolic reprogramming in cancer are complex, encompassing alterations in multiple signalling pathways such as those involving hypoxia inducible factor 1 $\alpha$  (HIF-1 $\alpha$ ), phosphoinositol 3-kinase/protein kinase B (PI3K/AKT), mechanistic target of rapamycin (mTOR), AMP-activated protein kinase (AMPK) and V-myc avian myelocytomatosis viral oncogene homolog (c-Myc)(3-7). Moreover, other oncogenes and tumour suppressors have been shown to directly control these pathways, and consequently, most tumour cells display altered glucose and glutamine metabolism compared to normal cells(8).

### **1.1.2 The Warburg Effect and the Regulation of Glycolysis in Cancer**

Almost a century ago, Otto Warburg observed and characterised for the first time one of the most conspicuous features of cancer metabolism: that most cancers utilise high amounts of glucose and secrete it as lactate even in the presence of oxygen, which is referred to as aerobic glycolysis or “the Warburg effect”(9). Instead, normal cells metabolise glucose in the mitochondria via the tricarboxylic acid (TCA) cycle and only under low oxygen, glucose is converted

into lactate (anaerobic metabolism). This dramatic increase in glucose uptake by cancer cells is exploited clinically to visualize tumours by 2-<sup>(18F)</sup>-fluoro-2-deoxy-D-glucose positron emission tomography (FDG-PET).

Glucose enters the cell via one of the tissue specific glucose transporters, which are commonly up-regulated in tumours, *GLUT1* is particularly important under hypoxia(10). Glucose metabolism begins by its phosphorylation by hexokinase (HK, Fig. 1:1) to glucose 6-phosphate (G6P). Hexokinase II (HK2), one of the 4 HK isozymes, is a target of many cancer related transcription factors, including HIF1 $\alpha$  and c-Myc(11). The next step in glycolysis is the isomerisation of G6P to fructose 6-phosphate (F6P) by phosphoglucoisomerase (PGI, Fig. 1:1), which is found up-regulated under hypoxia and in a wide number of cancers (12).

The next step in glycolysis is catalysed by phosphofructokinase 1 (PFK1), a major regulatory protein that is also a HIF1 $\alpha$  and c-Myc target (Fig. 1:1). PFK1 is under complex control, it controls the diversion of glycolytic intermediated into pathways branching from glycolysis, like the pentose phosphate pathway (PPP), as well as regulating the rate of glycolysis according to the energy status of the cell. Interestingly, ATP is a potent PFK1 inhibitor. This so called Pasteur Effect is the most important mechanism by which oxidative phosphorylation (OXPHOS) suppresses glycolysis. A potent allosteric activator of PFK1 is fructose 2,6-bisphosphate (F2,6BP) which is produced by the bi-functional enzyme, 6-phosphofructo-2-kinase/fructose-2,6-bisphosphatase (PFKFB2, Fig. 1:1). PFKFB3 is a form of PFKFB2 that favours the synthesis of F2,6BP increasing glycolytic flux. The increased level of PFKFB3 in tumours, mediated by HIF1 $\alpha$ , has been suggested as a cause for aerobic glycolysis (13). Another isoform of PFKFB2, PFKFB4 has been found to be essential for prostate cancer growth, positioning it as an interesting alternative for therapeutic intervention(14). In addition, a p53 target, TP53-induced glycolysis and apoptosis regulator (TIGAR) indirectly suppresses glycolysis (15). TIGAR shares similarities with the bisphosphatase2 (BPase2) domain of PFKFB2 and it inhibits glycolysis, presumably through the decrease in F2,6BP levels. In this way, PFKFB2 and TIGAR regulate the branching of substrates into the oxidative arm of the PPP, promoting the synthesis of NADPH and ribose 5-phosphate (Fig. 1:1). The diversion of G6P into the PPP increases nucleotide biosynthesis and generates NADPH that it is utilized for the

reduction of oxidised glutathione and to support fatty acid biosynthesis contributing to tumour growth.

Another glycolytic enzyme whose levels can be altered by p53 expression is phosphoglycerate mutase (PGAM, Fig. 1:1) which catalyses the conversion of 3-phosphoglycerate to 2-phosphoglycerate. Cells with low levels of p53 or loss of function mutations have increased PGAM and therefore increased glycolysis (16).

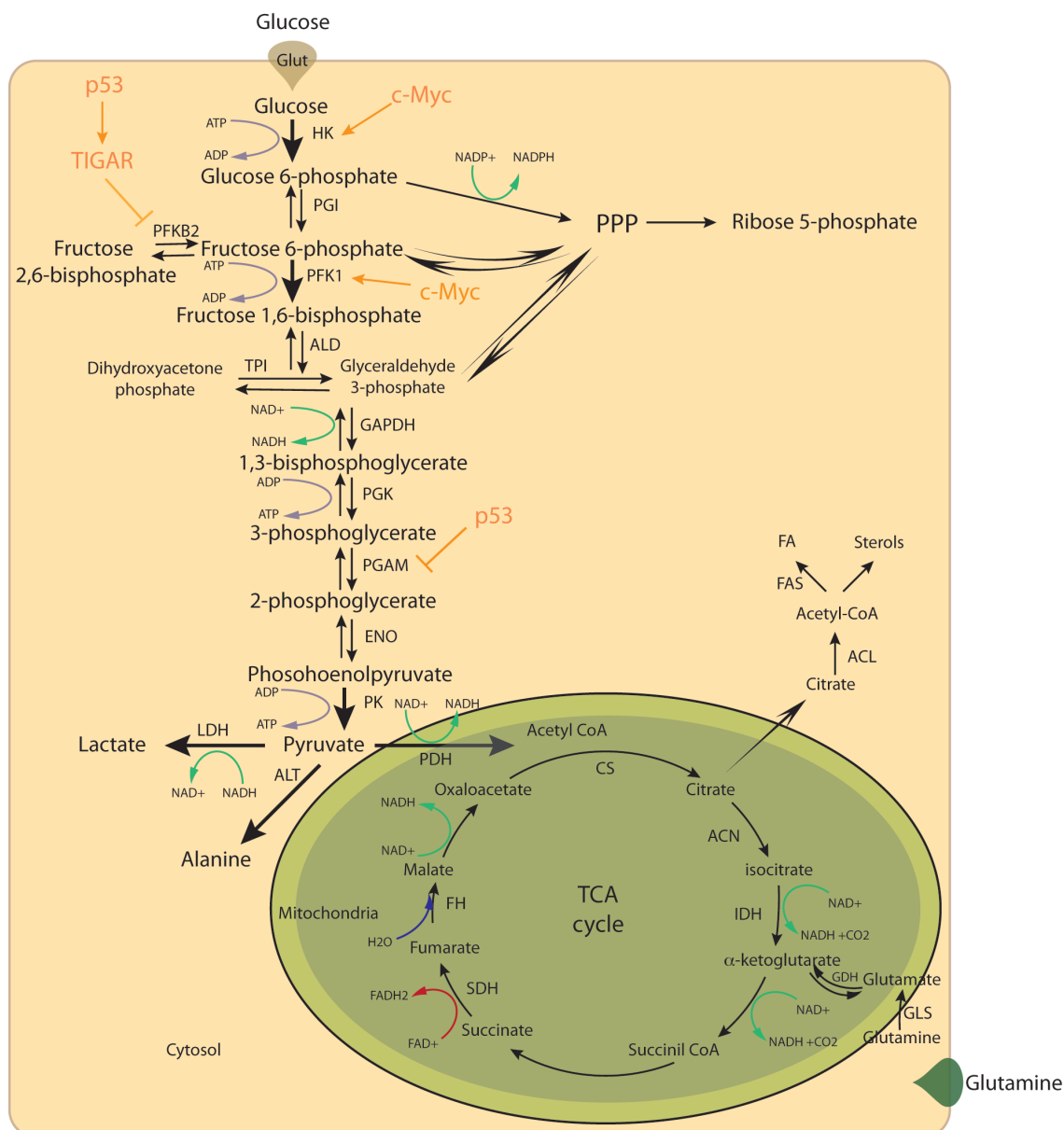


**Figure 1:1- Scheme of the central carbon metabolism**

Summary of the metabolic steps involved in glycolysis, the TCA cycle and pathways branching from them, including examples of their regulation by oncogenes and tumour suppressors. Acetyl-CoA, Acetyl Coenzyme A; ACL, ATP citrate lyase; ACN, aconitase; ADP, adenosine diphosphate ; ALD, aldolase ; ALT, alanine aminotransferase; ATP, adenosine triphosphate; CS, citrate synthase; ENO, enolase; FA, fatty acids; FAD, flavin adenine dinucleotide; FASN, fatty acid synthase; GAPDH, glyceraldehyde 3-phosphate dehydrogenase; GDH, glutamate dehydrogenase ; Glut, glucose transporter; GLS, glutaminase; HK, hexokinase; IDH, isocitrate dehydrogenase; LDH, lactate dehydrogenase; NAD, nicotinamide adenine dinucleotide; NADP, nicotinamide adenine dinucleotide phosphate; PDH, pyruvate dehydrogenase; PDK, pyruvate dehydrogenase kinase; PDP, pyruvate dehydrogenase phosphatase; PFK1, phosphofructokinase; PFKFB2, 6-phosphofructo-2-kinase/fructose-2,6-biphosphatase 2; PGK, phosphoglycerate kinase; PGI, phosphoglucose isomerase, PGAM, phosphoglycerate mutase; PK, pyruvate kinase; PPP, pentose phosphate pathway; TPI, triose phosphate isomerase.

Pyruvate, the final product of glycolysis, can follow several metabolic routes, the major two being its conversion to lactate or acetyl-CoA. The conversion of pyruvate to lactate is carried out by lactate dehydrogenase (LDH, Fig. 1:1). There are two isoforms of LDH (LDHA and LDHB). LDHA is commonly overexpressed in tumours since the recycling of cytosolic NAD<sup>+</sup> via lactate production is vital for glycolysis. LDHA inhibition makes cells more oxidative and slows down proliferation, positioning LDHA as another putative metabolic target for cancer therapy (17).

Pyruvate dehydrogenase (PDH) is the enzyme that catalyses the conversion of pyruvate to acetyl-CoA in the mitochondria, linking glycolysis to the TCA cycle and ATP production by OXPHOS (Fig. 1:2). PDH is part of a complex of enzymes known as the PDH complex (PDC) that regulates PDH activity. There are four isoforms of PDH kinases (PDKs) and two of PDH phosphatases (PDPs) that are associated with the PDC, regulating its phosphorylation and hence, dictating PDH activity. PDK1 is a direct target of HIF1, and therefore hypoxia and some oncogenes inhibit PDH activity and the entry of pyruvate into the mitochondria (18, 19). The phosphorylation of PDH by PDK reduces its activity, decreasing the entry of glucose derived pyruvate into the mitochondria and favouring its conversion to lactate, whereas the dephosphorylation of PDH by PDP actively catalyses the conversion of pyruvate into mitochondrial acetyl-CoA fuelling the TCA cycle (Fig. 1:2). PDK inhibition, hence PDH activation, constitutes a promising metabolic target for cancer therapy (20-22).

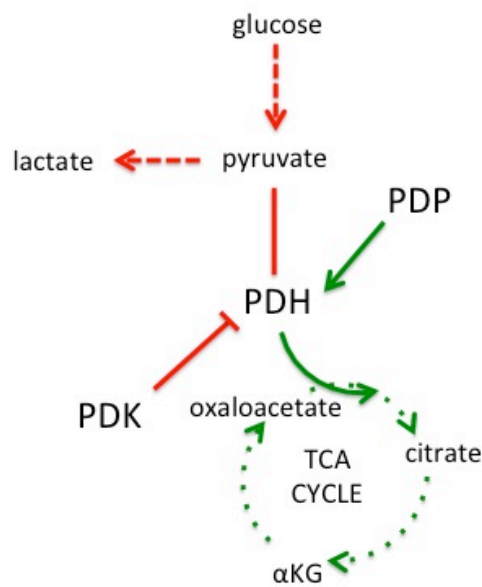


**Figure 1:2- The regulation of PDH activity**

PDH activity, hence the metabolic fate of pyruvate is regulated by phosphorylation events.  $\alpha$ KG, alpha-ketoglutarate; PDH, pyruvate dehydrogenase; PDK, pyruvate dehydrogenase kinase; PDP, pyruvate dehydrogenase phosphatase.

### 1.1.2.1 An Example of Complex Regulation in Glycolysis: Pyruvate Kinase M2

Adapted from Chaneton and Gottlieb, TiBS,2012.

The final enzyme in glycolysis is pyruvate kinase (PK, Fig. 1:1) which catalyses the conversion of phosphoenolpyruvate (PEP) to pyruvate while generating ATP. This enzyme is under complex control, allowing the cell to sense and respond to the energetic and anabolic precursors' levels.

There are four isoforms of PK in mammals and their expression seems to adapt to the specific function and energetic requirements of the different tissues. Given its key role in regulating glycolysis, PK has been conserved throughout evolution. In fact, the four mammalian isoforms are very similar in sequence.

Two genes encode the four isoforms: the PKLR gene produces PKL in the liver and PKR in red blood cells via tissue specific promoters and the PKM gene produces two splice variants: M1, in skeletal muscle, heart and brain; and M2, characteristic of highly proliferating cells during embryonic development and in cancer(23). The M1 and M2 isoforms originate by alternative splicing of two mutually exclusive exons. The PKM gene consists of 12 exons and the two isoforms differ by the presence of exon 9 in M1 or exon 10 in M2. The alternative exons encode for a stretch of 56 amino acids from which 23 are different and they correspond to the regulatory region in the carboxyl-terminus of PKM2 that is partially responsible for its fine regulation(23-25). The alternative splicing of the PKM gene is controlled by the heterogeneous nuclear ribonucleoprotein (hnRNP) family members hnRNPA1, hnRNPA2, and polypyrimidine tract binding protein (PTB; also known as hnRNPI). In addition, c-Myc has been shown to transcriptionally up-regulate hnRNPI, A1 and A2 that bind repressively to the sequences flanking exon 9 consequently favouring PKM2 expression (26-28).

During cancer progression PKM2 arrogates the control of glycolysis from the tissue specific isoform, providing a hint on the importance of this particular isoform in sustaining cell proliferation(29). Furthermore, the replacement of PKM2 by the constitutively active PKM1 slows tumour growth in a xenograft model of lung cancer (30). However, the initial idea that increased aerobic glycolysis in cancer cells is due to a switch in expression of the tissue specific isoform of PK to PKM2 is still under debate. Recently, a large scale study of several normal and tumour tissues, in which PKM1 and PKM2 were quantified using mass spectrometry, showed that in cancer cells there is a proportional increase in the amount of both isoforms. PKM2 seems to be also predominant in normal adult tissues but the concomitant increase of both isoforms found in cancer accentuates the differences in expression between them (31).

Apart from the differential tissue distribution, PK has multiple ways of regulating glycolysis according to tissue's needs. Indeed, all the isoforms, except for PKM1, are allosterically regulated, alternating between a highly active tetramer and a less active dimer (32-34). The tetrameric form of PKM2 has a high affinity for PEP and favours pyruvate and lactate formation, with production of energy. On the other hand, the dimeric form has a low affinity for PEP and is less active at physiological PEP concentrations. When PKM2 is in its less active dimeric form,

all glycolytic intermediates preceding PK become more available as precursors for biosynthetic processes such as, amino acid, nucleic acid and phospholipid synthesis (Fig. 1:3). Therefore, the ratio between the tetrameric and the dimeric forms of PKM2 determines whether glucose is used for energy production or for the synthesis of cellular precursors (30, 35, 36).

In the 1960s the glycolytic intermediate fructose 1,6-bisphosphate (FBP) was identified as a potent activator of PKM2(37). FBP reversibly binds to PKM2 and activates it by favouring the formation of an active tetrameric structure. The dimer to tetramer inter-conversion responds to changes in intracellular glucose concentration. Under physiological glucose concentration, the majority of PKM2 exists in the tetrameric form and around 30% is dimeric. However, when the intracellular concentration of FBP drops, for example after blocking glucose uptake, PKM2 is found mainly in its dimeric state (38). In addition, the binding of tyrosine phosphorylated peptides to PKM2 results in the release of the allosteric activator FBP and the inhibition of PK activity (39). This inhibition is necessary to allow growth factor initiated signalling pathways to channel glycolytic intermediates into biosynthetic processes.

Recently, other post-translational modifications have been found to reduce PKM2 activity, contributing to the idea that PKM2 can be found in an inactive form in proliferating cells. Low PK activity in yeasts increases respiration without increasing reactive oxygen species (ROS) levels and improving resistance to oxidants. This is due to the accumulation of PEP that inhibits triosephosphate isomerase (TPI), a glycolytic enzyme. Moreover, TPI inhibition reduces oxidative stress by increasing the PPP and preventing ROS accumulation (40). Similarly, increased ROS levels in cancer cells, as a result of growth factor signalling or mutations in tumour suppressor and oncogenic pathways, can inactivate PKM2 through oxidation of Cysteine-358. This inactivation causes an accumulation of glycolytic intermediates and hence an increased diversion of carbons into the PPP, which produces NADPH contributing to ROS detoxification. This mechanism allows cancer cells to control ROS and survive under oxidative stress conditions (41).

Acetylation seems to be an alternative post-translational modification that, like the previously described phosphorylation, reduces PKM2 activity, which leads to

increased glycolytic intermediates that are available for biosynthesis in response to nutrient availability. Nevertheless, these modifications are far from being specific for PKM2 since they are also common to a range of other metabolic enzymes (42). Increased glycolysis induces PKM2 acetylation at Lysine-305, this novel mechanism of PKM2 down-regulation when glucose is abundant, has two methods of action. On the one side it reduces PKM2 activity, decreasing PEP affinity while on the other side it favours subsequent PKM2 degradation through chaperone-dependent autophagy (43). Given the fact that this mechanism clearly contrasts the activation of PKM2 that takes place when glucose and therefore FBP are abundant, it would be interesting to understand how acetylation of Lysine-305 may affect FBP binding to PKM2.

During the 1980's *in vitro* measurements of PKM2 activity in the presence of several biologically relevant compounds identified several amino acids and fatty acids as modulators of PKM2 activity. In *in vitro* enzymatic assays, PKM2 seems to increase its activity in response to a number of molecules that contain a hydroxyl group (-OH), such as serine, phosphatidylserine but also methanol and ethanol. PKM2 activity is also inhibited by amino acids like alanine, phenylalanine and tryptophan (44-48). Additionally, PKM2 has been found to interact with several oncogenic proteins and apparently plays a role in the transformation process (49-52). Other signalling cascades that involve tyrosine kinase receptors are commonly amplified in cancer contributing to the regulation of the glycolytic phenotype. Direct PKM2 phosphorylation on tyrosine-105 by FGFR1 prevents FBP binding inhibiting the formation of the fully active tetrameric form. This short-term mechanism of PKM2 inhibition is commonly described in different human cancer cell lines even though the proportion of the phosphorylated/ non-phosphorylated PKM2 is not completely clear(53).

In the cytoplasm, PKM2 can be found as part of a complex with other glycolytic enzymes such as HK, GAPDH, enolase, PGAM and LDH. Only the tetrameric, but not the dimeric form of PKM2 is associated with this glycolytic complex and the dissociation of the tetramer into dimers disrupts the complex. While being part of the glycolytic complex, highly active PKM2 favours lactate production and blocks OXPHOS (54, 55). Dimeric PKM2 has been found in the nucleus where it regulates gene transcription by acting as protein kinase (56). Nuclear translocation of PKM2 is possible thanks to the presence of an inducible nuclear

localisation signal (NLS) in its C-domain, which, in contrast to the classical NLS, is not rich in arginine and lysine (57, 58). A putative translocation mechanism involves PKM2 interaction with the SUMO-E3-ligase PIAS3, which promotes PKM2 sumoylation and its further nuclear translocation (59). In the nucleus PKM2 interacts and activates transcription factors such as Oct-4 contributing to the maintenance of a pluripotent cell status by preventing differentiation (60). Other stimuli that result in nuclear translocation of the dimeric inactive PKM2 are treatment with agents that generate ROS, like H<sub>2</sub>O<sub>2</sub> and UV radiation. The nuclear functions of PKM2 seem to be as varied as its cytoplasmic ones and it has been found to interact with a number of proteins. Another nuclear function of PKM2 includes transactivation of  $\beta$ -catenin upon epidermal growth factor receptor (EGFR) activation (61). Moreover, hydroxylation on prolines-403 and -408 of nuclear PKM2 by PHD3 stimulates its binding to HIF1 $\alpha$ , promoting HIF-1 transcriptional activity of genes encoding glucose transporters and glycolytic enzymes in cancer cells (62). Altogether, these findings certainly confirm that the single exon difference between PKM1 and PKM2 imparts the latter with important regulatory characteristics and functional distinctions.

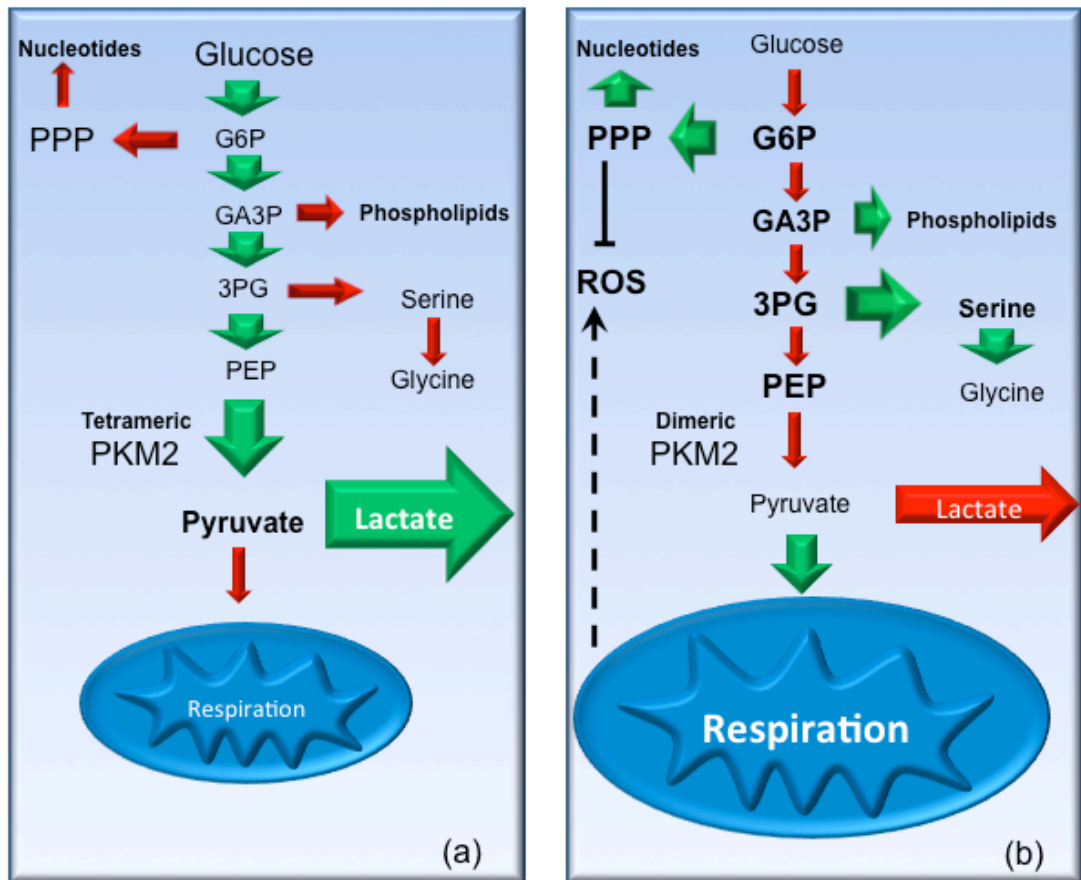


**Figure 1-3- The effect of PKM2 activity regulation on metabolism**

(a) When PKM2 is active, glycolytic rate is high and most of the pyruvate is rapidly converted to lactate while respiration is partially suppressed. (b) A reduction in PKM2 activity leads to a decrease in lactate production associated and the accumulation of upstream glycolytic intermediates with a consequent increase in the synthetic pathways branching from these metabolites. Lower PKM2 activity also increases respiration and with it, the risk of reactive oxygen species (ROS) production. However, high flux via the pentose phosphate pathway (PPP) provides anti-oxidants that counteract the mitochondria-generated ROS. 3PG, 3-phosphoglycerate; GA3P, glyceraldehyde 3-phosphate; G6P, glucose 6-phosphate; PEP, phosphoenolpyruvate. Taken from Chaneton and Gottlieb, *TiBS*, 2012.

### 1.1.3 Glutaminolysis

The other major source of energy and carbons for cancer cells besides glucose is glutamine (63, 64). In addition, glutamine is also an important nitrogen source for cells. As a consequence of the high glucose and glutamine uptake, an associated increased secretion of their metabolic by-products such as lactate, alanine and ammonia is also observed in cancer cells.

Glutamine enters the cell via transporters such as the Na<sup>+</sup>-dependent neutral amino acid transporter ASCT2. Once in the cell glutamine can be deaminated by one of the two glutaminases (GLS or GLS2) producing glutamate and ammonia. Glutamate can be secreted out of the cells or it can enter the TCA cycle through its conversion to  $\alpha$ -ketoglutarate by glutamate dehydrogenase (GDH) or via numerous transamination reactions (Fig. 1:1). Once in the TCA cycle,  $\alpha$ -ketoglutarate is metabolised further to ultimately form oxaloacetate, an important anabolic precursor that will condense with acetyl-CoA to produce citrate. The hint that glutaminolysis is a possible target for cancer therapy came from the observation that GLS is overexpressed in a number of tumours, and its inhibition delays tumour growth(65-67). The use of GLS inhibitors such as compound 968 and Bis-2-(5-phenylacetamido-1,2,4-thiadiazol-2-yl)ethyl sulfide (BPTES) shows promising results in delaying tumour growth(68, 69).

### 1.1.4 The Role of Metabolism in Tumour Initiation and Progression

The link between metabolism and cancer was tremendously tightened when mutations and loss of function of TCA cycle enzymes were found to be the cause of some hereditary forms of cancer. Initially, mutations in the gene encoding for the subunit D of the succinate dehydrogenase complex (SDH) were found to be the underlining cause of the neuronal crest-derived cancer syndrome Hereditary Paraganglioma(70). Soon after this seminal discovery, fumarate hydratase (FH), the enzyme that catalyses the conversion of fumarate to malate, was found mutated in another hereditary disorder called hereditary leiomyomatosis and renal cell cancer (HLRCC)(71). SDH is formed by four subunits: A and B, C and D and is also complex II of the electron transport chain (ETC), where FADH<sub>2</sub> is

generated by succinate oxidation and further oxidised along the ETC (Fig. 1:1). Mutations in FH, or SDHB, C or D are known causes of several familial and sporadic cancers(72). Mutations in these TCA cycle enzymes force cells to rely on a truncated TCA cycle that results in the stabilisation of HIF $\alpha$  subunits, even in the presence of oxygen, giving rise to a pseudo-hypoxic phenotype(73, 74). This phenotype is caused by the increase in succinate (SDH mutations) or fumarate (FH mutations) levels and the consequent inactivation of the oxygen sensing machinery mediated by prolyl hydroxylases (PHDs) (75-77). The fact that mutations in enzymes involved in key metabolic pathways led to tumour predisposition produced the smoking gun, which demonstrated that aberrant metabolism could actually be, in some cases, the cause of cancer. The notion that a cell can adapt to severe metabolic defects, such as the loss of SDH or FH, suggested that a significant metabolic rewiring should be an adaptive response in these cancer types. Furthermore, through a combination of metabolomics, biochemistry and systems biology, using the first cellular syngenic model of FH-deficient epithelial kidney cells, our group predicted and validated the synthetic lethality between the loss of FH activity and the inhibition of the haem biosynthesis/degradation pathway. In FH<sup>-/-</sup> cells, heme oxygenase 1 (HMOX1) helps detoxifying the excess of fumarate via the excretion of bilirubin. The confirmation of this synthetically lethal relationship in a clinical setting may open up new therapies for the treatment of patients with HLRCC(78). In a similar line, fumarate has been shown to induce a protective antioxidant response mediated by Nrf2 in the heart upon an ischemia-reperfusion injury, contributing to the idea that fumarate works as a cytoprotective, which in the context of several mutations can contribute to tumour development(79).

An integrated genomic analysis of human glioblastoma multiforme (GBM) found recurrent heterozygous mutations in the active site of isocitrate dehydrogenase 1 (IDH1), in 12% of GBM patients(80). The same was true for acute myeloid leukemia (AML)(81). In addition, using a metabolomic approach, it was shown that mutant IDH not only has reduced capacity to convert isocitrate to  $\alpha$ -ketoglutarate but it also acquires a novel reductive activity utilising  $\alpha$ -ketoglutarate to produce 2 hydroxyglutarate (2HG)(82). Indeed, the non-invasive detection of 2HG by magnetic resonance has proved to be a valuable diagnostic tool and prognostic biomarker for GBM(83-85). Furthermore, this discovery

granted a novel role for 2HG in the tumorigenesis of GBM and it was dubbed as an “oncometabolite” somewhat similarly to fumarate and succinate. However, intense investigations demonstrated that, unlike fumarate and succinate, 2HG does not inhibit PHDs, on the contrary, it stimulates their activity and reduces HIF levels. Interestingly, 2HG appears to act as a potent modulator of the epigenetic status of the cell by affecting both DNA and histone methylation, suggesting that 2HG can directly impact cellular differentiation and hence increase susceptibility to cancer (86-88). Inhibition of mutant IDH has antineoplastic effects in glioma, apparently through a decrease in 2HG levels and the induction of differentiation (89). Specific chemical inhibitors against mutant IDH1 and IDH2 have been designed and are currently showing positive results in clinical trials (ClinicalTrials.gov NCT01703962 and NCT01915498).

Serine is an important amino acid, not only for protein synthesis, but also for other amino acids, lipids, as well as nucleotide biosynthesis. The endogenous serine synthesis pathway, also called the ‘phosphorylated pathway’ is the main source of serine in several mammalian tissues like the brain, serving also as a source of glycine and one-carbon units for methylation (Fig. 1:4). The up-regulation of this pathway has been associated with the ability of breast cancer cells to metastasise (90). Furthermore, a loss of function screen found that certain breast cancers have PHGDH amplification and rely on endogenous serine production to sustain proliferation(91). Interestingly, using metabolomics it was shown that melanoma and breast cancer cells with PHGDH amplification divert large amounts of glucose-derived carbons into serine and glycine biosynthesis (92). In addition to the endogenous serine synthesis pathway, serine metabolism also seems to be important for cancer cells, contributing to redox balance by glutathione production, protein and nucleotide biosynthesis as well as providing methylene groups for methylation. Furthermore, p53 has been related to the ability of cells to survive to serine starvation (93, 94).

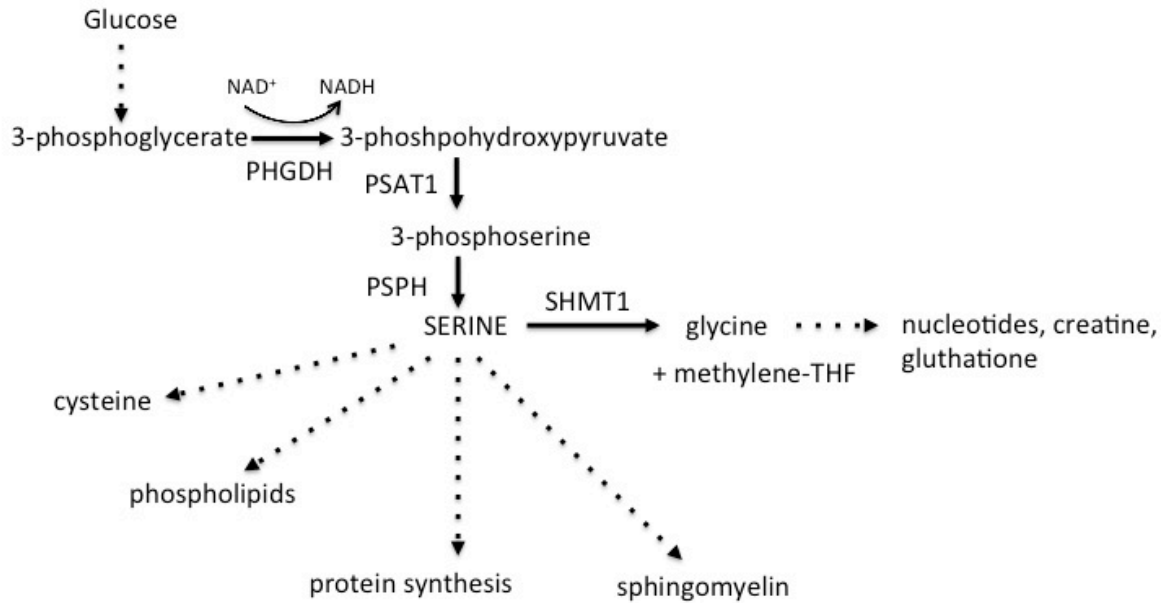


**Figure 1:4- The phosphorylated pathway for serine synthesis**

Scheme of the serine synthesis pathway from glucose and the main biosynthetic pathways in which L-serine is involved. PHGDH, phosphoglycerate dehydrogenase; PSAT1, 3-phosphoserine  $\alpha$ -ketoglutarate aminotransferase; PSPH, 3-phosphoserine phosphatase; SHMT1, serine hydroxymethyl transferase 1; methylene-THF, methylene tetrahydrofolate. Dotted lines indicate multiple step reactions.

mTOR is a key metabolic regulator that promotes protein synthesis and cell growth when energy and nutrients are in plenty. Upon energy depletion, mTOR is inhibited by the activation of the LBK1/AMPK pathway (6, 95). mTOR forms two complexes: mTOR complex 1 (mTORC1, Fig. 1:5), controls protein synthesis and cell cycle progression. Rapamycin, a compound originally isolated from *streptomyces hygroscopicus* inhibits mTORC1 by binding to FKBP12 (FK506-Binding Protein 12) resulting in the dissociation of Raptor from the mTORC1 complex (96). In response to nutrients and growth signalling, mTORC1 activates S6K and inhibits 4EBP1, both regulators of mRNA translation (97). The second complex, mTORC2, interacts with AKT and is composed by mTOR, RICTOR and DEPTOR among other proteins. mTORC2 was initially thought to be insensitive to

rapamycin and it is involved in the regulation of cytoskeleton and metabolism (98).

Upstream of mTORC1 is TSC1/2, an inhibitor of mTORC1 kinase activity that transduces growth factor signalling through AKT and ERK pathways, hypoxia through the HIF1 target REDD1 and energy status through AMPK(99, 100). Some amino acids and their transporters can also regulate mTOR activity (Fig. 1:5)(101). In spite of the importance of glutamine as an energy source, leucine seems to be necessary and sufficient for mTORC1 activation (102). mTORC1 activation by TSC1/2 loss is able to drive tumorigenesis, modulating apoptosis, cellular senescence, and response to treatment(103-105). AKT inhibits TSC1/2 controlling mTOR activity and it has been shown that rapamycin treatment alleviates the cancer phenotype in some activated AKT tumours (106, 107). Furthermore, PTEN-deficient cancer cells have constitutively active AKT and mTORC1 associated with poor prognosis (108).

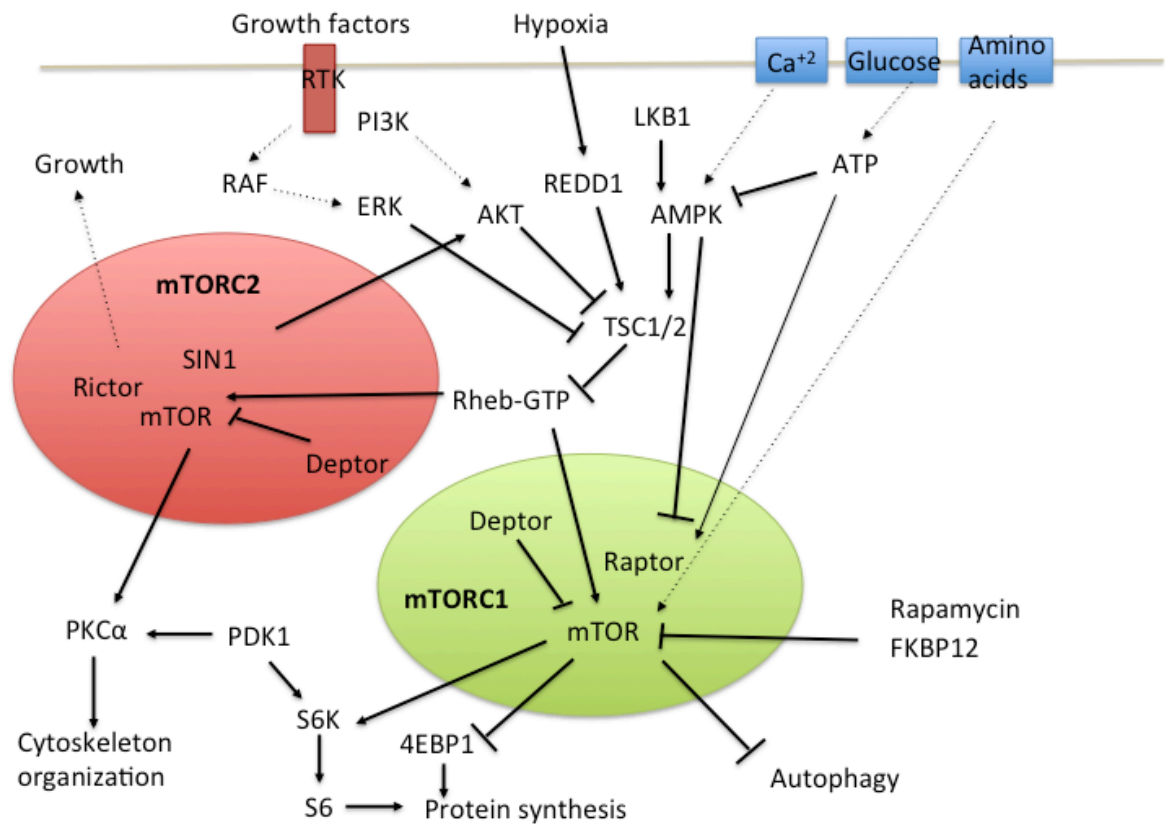


**Figure 1:5- The mTOR signalling pathway**

Scheme showing how the mTOR machinery integrates growth signals and nutrient levels in order to regulate cell metabolism. 4EBP1, Eukaryotic translation initiation factor 4E-binding protein 1; AKT, protein kinase B; AMPK, AMP regulated kinase; ATP, adenosine triphosphate; ERK, extracellular-signal regulated kinase; FKBP12, FK506 binding protein 12; LKB1, liver kinase B1; mTOR, mechanistic target of rapamycin; mTORC1/2, mTOR complex 1 and 2 respectively; PI3K, Phosphatidylinositol 3-kinase; PKC $\alpha$ , protein kinase C alpha; PDK1, pyruvate dehydrogenase kinase 1; REDD1, DNA-damage-inducible transcript 4 protein; RTK, receptor tyrosine kinase; S6, ribosomal protein S6; S6K, S6 kinase; TSC1/2, tuberous sclerosis 1 and 2 respectively.

## 1.2 Therapeutic Strategies

Studies of the unique metabolism of cancer started in the early 1920s when Otto Warburg proposed that tumours, unlike most normal cells, utilize glycolysis rather than OXPHOS for ATP production. The consequences of this metabolic adjustment are conspicuously high glucose uptake and lactate secretion(9). In all tissues glucose is first partly oxidised to pyruvate in the cytosol in an oxygen independent ATP-generating process. Although normal tissues like brain and heart also exhibit high rates of glucose metabolism, the main difference between normal tissue and cancer cells is that in normal cells, pyruvate is mainly oxidised in the mitochondria for energy production while in the latter it is reduced in the cytosol and secreted as lactate. These observations were debated for decades, after which, the methodological investigation of the molecular basis of aerobic glycolysis in cancer began, and with it, a new era of research on cancer metabolism.

The vast majority of metabolic pathways in which cancer cells rely are also essential for the survival of normal cells and hence are not, in principle, suitable drug targets. However, the presence of a specific enzyme isoform or changes in the activity of a pathway may allow targeting them. Since the early development of chemotherapy in the 1950s until now, cancer therapy has largely focused on targeting the rapid proliferation of tumour cells. For instance, by using antimetabolites such as methotrexate, which interferes with the use of folic acid by cancer cells, blocking in this way DNA synthesis and halting cell proliferation. Nonetheless, this unspecific approach has a vast number of undesirable side effects(109).

### 1.2.1 Targeting Glycolysis and the Pentose Phosphate Pathway

Several genetic modifications occurring during tumorigenesis contribute to glucose addiction. For instance, mutations in the tumour suppressor gene Von-Hippel-Lindau (VHL) make renal cell carcinomas (RCC) highly dependent on glycolysis. A high-throughput screen for compounds that synergise with VHL loss identified a candidate drug that directly inhibits GLUT1, selectively killing VHL

deficient cells *in vitro*, and retarded RCC growth in a murine model(110). Oncongenic BRAF and RAS have been associated with increased GLUT1 expression in tumours and specific GLUT1 inhibitors underwent clinical trials (111-113). Hexokinase controls the first step in glycolysis, phosphorylating glucose to G6P and it is up-regulated by both HIF1 $\alpha$  and c-Myc. On the one hand, several inhibitors of hexokinases such as lonidamine, 2-deoxyglucose and 3-bromopyruvate started clinical trials but they have now been abandoned and there is still a need to determine if their effect on tumour growth is the result of their specific action on hexokinase(114-116). Glycolytic inhibitors, like 2-deoxyglucose, do not show significant effect on tumour growth, but can re-sensitise tumours to chemo- and radiotherapy apparently by reducing ATP levels in the tumours(117-119).

The diversion of G6P from glycolysis into the PPP produces on the one hand, NADPH for lipid and nucleotide biosynthesis and ROS protection, and on the other hand, ribose 5-phosphate for nucleotide biosynthesis. At present, there are no specific inhibitors for this pathway undergoing clinical trials although its inhibition will likely mimic the effect of antimetabolites and, by decreasing NADPH levels, alter cellular redox balance and block lipid biosynthesis. In spite of this, pre-clinical data on glycolytic modulators show that they can act on the PPP pathway by reducing the amount of glucose derived carbons flowing into this pathway, such as PGAM1 inhibitors and PKM2 activators(16, 120).

6-Phosphofructo-1-kinase (PFK1) catalyses the addition of a second phosphate group to F6P and it is a rate-limiting step in glycolysis, being very active in cancer cells. F2,6BP is a potent allosteric activator of PFK1 and it is the product of a family of bifunctional enzymes known as PFKFBPs. It has been shown that a small molecule inhibitor of PFKFB3 decreases F2,6BP levels reducing PFK1 activity and glycolytic flux, with cytostatic effects(121).

The final and most important enzyme from an energetic point of view in glycolysis is PK. For this reason, PK activity is strictly controlled, among other ways by isoform selection and by allosteric regulation. The glycolytic intermediate, F1,6BP, binds to and allosterically activates a specific isoform of PK highly expressed in proliferating cells, PKM2. This feed-forward mechanism links the two rate-limiting steps in glycolysis enabling co-ordinated glycolytic

flux in PKM2 expressing cells. Therefore, PKM2 constitutes an interesting target for cancer therapy and understanding its regulation *in vivo* is of paramount importance to design drugs that can modulate its activity in tumours.

It has been shown in cancer cells that PKM2 binding to phospho-tyrosine residues in other proteins can interfere with the feed-forward effect of F1,6BP resulting in reduced PK activity (39). The multiple ways in which PKM2 is regulated gave rise to an increasing interest in modulating its activity. To that end, both PKM2 inhibitors and activators have been designed in order to modulate PKM2 activity in cancer cells in an attempt to halt tumour growth (120, 122-124).

Initially, an inhibitor to PK (TLN-232) was taken to phase II clinical trials but was then dropped. However, since it was noticed that cancer cells expressing the constitutively active isoform PKM1 have reduced tumour growth capacity *in vivo* compared to PKM2 expressing cells, an opposite therapeutic approach towards PKM2 has been adopted (30, 125). To this end, a number of PKM2 activators have been designed and characterised (120, 126-129). They increase the affinity for PEP as the natural activator FBP does without altering the  $K_m$  for ADP. PKM2 activation has emerged as an appealing therapeutic opportunity in an attempt to normalise cancer cell metabolism back to a normal cell status, and it has proved successful in combination with serine starvation halting cell proliferation (124).

One of the causes of the limited effect that glycolytic inhibitors have shown in cancer treatment could be the strong increase in glutaminolysis displayed by some tumours, and therefore the ability of tumours with functional mitochondria to produce ATP by OXPHOS. Therefore, the use of anti-glycolysis treatment could lead to the depletion of muscle glutamine stores and loss of adipose and muscle tissue (cachexia) due to increased tumour demand (130).

### **1.2.2 Targeting Pyruvate Metabolism**

Pyruvate is generated in the cytosol by oxidation of glucose during glycolysis, yielding two moles of pyruvate for every mole of glucose consumed. In most tissues pyruvate is converted to acetyl-CoA in the mitochondria by pyruvate dehydrogenase (PDH). A greater proportion of the pyruvate produced in tumour cells is redirected into lactate production, due to the increased activity of two

key enzymes: PDK, which phosphorylates and inhibits PDH activity, and LDHA, which converts cytosolic pyruvate to lactate (18, 19, 131)(18, 19, 130). The increase in lactate production and consequent decrease in pyruvate entering the TCA cycle has proved to be crucial for tumours, as LDHA or PDK inhibition reduce tumour growth in xenograft models(17, 132). In particular, the PDK inhibitor DCA showed anti-cancer effects in pre-clinical studies and it is already a prescription drug for the treatment of lactic acidosis, being well tolerated in patients with GBM(133). However, neither DCA nor other PDK inhibitors have been approved yet for cancer therapy and there are no effective therapies targeting LDHA.

Lactate is secreted with protons (H<sup>+</sup>) out of the cells via the monocarboxylate transporter 4 (MCT4) preserving the intracellular pH at expense of creating an acidic tumour microenvironment. H<sup>+</sup> are also exported using the Na<sup>+</sup>/H<sup>+</sup> exchanger 1 (NHE1 or SLC9A1). Small molecule inhibitors targeting NHE1, such as cariporide are in clinical trials as cardioprotective agents but they are not being tested as anti-tumour agents in the clinic (134, 135). Cancer cells can take-up lactate from the tumour microenvironment using MCT1, converting it back to pyruvate for further oxidation and it has been shown that inhibition of MCT1 results in reduced tumour growth in xenografts and re-sensitisation to radiation (136). Currently AZD3965, a chemical MCT1 inhibitor is being tested in patients with advanced solid tumours and lymphomas (ClinicalTrials.gov NCT01791595).

Extracellular acidification has been shown to increase the motility of cells both *in vitro* and *in vivo* (137-139). Therefore, targeting tumour acidification has multiple benefits: it inhibits glycolytic energy production, decreases immunosuppression and also inhibits tumour cell invasion (140, 141). Indisulam is an inhibitor of the tumour-associated isoform of carbonic anhydrase (CA IX), currently in phase II clinical trials for the treatment of melanoma and breast cancer (142-145).

### **1.2.3 Targeting Amino Acid Metabolism**

Tumours require high levels of exogenous essential and non-essential amino acids, in particular glutamine, which is the most concentrated amino acid in human plasma(146). Glutamine has multiple uses for cancer cells: besides protein synthesis, its amine group can be used to generate most of the non-

essential amino acids by transamination, it can also replenish the TCA cycle and it is also important for nucleotide biosynthesis. Tumour cells use large amounts of glutamine, depleting it from the blood of cancer patients (147). Phenylacetate reduces bioavailability of glutamine, inhibiting cancer cells proliferation and promoting differentiation (148-150). However the removal of glutamine directly from the plasma may also increase the rate at which the body depletes its own muscle stores (cachexia).

Glutaminolysis is the catabolic conversion of glutamine into glutamate by glutaminase (GLS or GLS2) which is up-regulated by c-Myc (151). Although a number of anti-glutaminolysis compounds have been developed, they were found to be toxic or raised an immune response(152). The recent renewed interest in the glutaminolytic pathway has led to the development of more specific GLS inhibitors like compound 968 and BPTES, to which glioma cells expressing mutant IDH1 seem to be particularly sensitive to(67, 153). In addition, GLS inhibition halts the growth of xenografts from c-Myc-expressing B cells (69).

Although asparagine is not usually an essential amino acid in humans due to the presence of asparagine synthetase (ASSN), certain tumour types like leukaemia have little ASSN activity and require exogenous asparagine. This has led to the use of asparaginase, the enzyme that converts asparagine to aspartate and ammonia, for the treatment of childhood acute lymphoblastic leukemia (ALL)(154, 155). Likewise, while in normal tissue arginine is not an essential amino acid, some hepatocellular carcinoma (HCC), mesothelioma and melanomas do not express argininosuccinate synthetase (ASS), and therefore are auxotrophic for arginine and hence are sensitive to its depletion in plasma(156, 157). Arginine deiminase has proved effective in the treatment of unresectable melanoma (ClinicalTrials.gov NCT00450372) and it's currently being tested in several other tumour types.

#### **1.2.4 Targeting Fatty Acid Metabolism**

Endogenous fatty acids are synthesised from TCA cycle derived citrate and NADPH, which can be produced by the PPP and other enzymes. Once in the cytosol, citrate is broken down into acetyl-CoA and oxaloacetate by ATP citrate lyase (ACL). Fatty acid synthesis starts with acetyl-CoA carboxylase (ACC)

converting acetyl-CoA to malonyl-CoA, and this is followed by a series of steps in which malonyl-CoA is converted to palmitate by fatty acid synthase (FASN). Many tumours express high levels of FASN, including breast, colorectal and endometrial cancers (158-160). Orlistat, a FASN inhibitor used for the treatment of obesity, appears to kill tumour cells directly, as well as sensitises them to other therapies such as 5-Fluorouracil and trastuzumab (Herceptin)(161, 162).

The inhibition of other enzymes involved in lipid metabolism, such as ATP citrate lyase (ACL), choline kinase, acetyl-coA carboxylase (ACC), monoglyceride lipase (MGLL) and 3-hydroxy-3-methylglutaryl-CoA reductase (HMGCR) has proved effective as cancer treatment in preclinical settings and these enzymes are the focus of drug development, some of them like in the case of statins are currently undergoing clinical trials (ClinicalTrials.gov NCT01428869, NCT01992042)(163-167).

### **1.2.5 Targeting the Master Regulators of Tumour Metabolism**

A number of therapeutic strategies that target upstream regulators of metabolic pathways are being tested. Targeting HIF can prevent metabolic adaptation to hypoxia and the metabolic shift observed in pseudo-hypoxic tumours, but HIF1 inhibitors like Acriflavine and PX-478 never reached the clinical stage or were discontinued for undisclosed reasons(168). The PI3K/AKT pathway is often activated and it is known to contribute to the cancer metabolism phenotype (169). AKT up-regulates glycolysis by accumulating glucose transporters in the plasma membrane and altering the expression or localisation of enzymes such as HK and PFK (170-173). Furthermore, the PI3K/AKT pathway also activates mTOR, contributing to cancer cells growth and PTEN loss-mediated PI3K/AKT activation cooperates with BRAF<sup>V600E</sup> in melanomagenesis (100, 174). PI3K inhibitors promote tumour regression by reversing some of the metabolic features of cancer, (169). However, inhibition of the PI3K/AKT pathway can also contribute to tumour regression in a non-metabolic fashion, as this pathway is pro-tumorigenic promoting cell growth and proliferation (175). Despite these observations, clinical trials using rapamycin on PTEN-deficient tumours have not provided positive results, which may be due to the AKT inhibition by S6K (5). mTORC1 inhibition with rapamycin and therefore, loss of S6K activity would

cause AKT re-activation, which may account for poor results in clinical trials(176, 177).

Another important regulator of mTOR is AMPK, which is activated under low energy conditions, leading to a metabolic adaptation characterised by increased catabolism and decreased anabolism, partially via the inhibition of mTOR(6). Oncogenic events such as BRAF over-activation inhibit the LKB1/AMPK pathway, maintaining high levels of mTOR activity and contributing to the development of melanoma(178, 179). The AMPK activator metformin, used for the treatment of type II diabetes, has shown to have prophylactic and therapeutic effects on cancer with particularly positive results in breast cancer (180-184). The anti-cancer effect of metformin is independent of glycaemia and seems to be mediated by the inhibition of mitochondrial complex 1(185, 186). Metformin is currently in phase I and II clinical trials for cancer treatment (ClinicalTrials.gov NCT02109549). In light of this, it is clear that targeting these pathways may have important clinical benefits for cancer treatment.

### **1.3 The Use of Metabolomics and <sup>13</sup>C Tracers to Identify Metabolic Vulnerabilities in Cancer Cells**

Metabolomics is the discipline that aims to identify and characterize all known small molecule metabolites (less than 1 kDa) present in a system (e.g.: a cell or body fluids); currently allowing for the simultaneous measurement of hundreds of metabolites(187). The use of metabolic profiling in cancer provides more accurate knowledge on the biological state of a tumour, i.e. progression, drug metabolism, etc., compared to the genomic approach.

The initial metabolomics approaches were based on nuclear magnetic resonance (NMR) but they are now complemented with the use of mass spectrometry (MS), which provides higher sensitivity, better resolution, and a wider range of metabolites detection(188). MS is coupled to a separation method such as liquid or gas chromatography. Liquid chromatography (LC) is a very robust system that allows for the separation of a wide range of metabolites(189). The LC-MS platform offers the possibility to perform targeted analyses of metabolic

pathways by using  $^{13}\text{C}$ -labelled metabolites such as glucose and glutamine (190). This strategy allows for the calculation of intracellular metabolic fluxes and, by making use of partially labelled substrates, for the identification of alternative metabolic pathways(191). By applying these recent advances in the field of metabolomics in the context of cancer research we have been able to characterize the metabolism of a wide variety of tumours, identifying adaptations and vulnerabilities, opening in this way new possibilities for the development of more efficient cancer therapies.

## 1.4 Aims

The general aim of this work was to identify metabolic enzymes that are important for cancer metabolism and that could be exploited as possible therapeutic targets.

Specific aims:

- 1- Characterize metabolic changes associated with oncogene-induced senescence and understand how changes in metabolism can modulate senescence in order to inhibit tumour progression.
- 2- Explore the role of PKM2 in cancer metabolism and identify new mechanisms of regulation. Understand how changes in PKM2 activity affect glycolysis and the pathways branching from it.
- 3- Identify metabolic adaptations to currently available therapies in order to overcome resistance in melanoma.

## Chapter 2 - Materials and Methods

## 2.1 Materials

Materials and methods were taken from Chaneton et al, 2012. Nature.

### 2.1.1 Reagents

All reagents were purchased from Sigma-Aldrich unless specified below:

Fisher Scientific: HPLC grade methanol, HPLC grade acetonitrile, NaCl, NaOH, Sodium dodecyl sulphate (SDS).

Invitrogen: NuPAGE Novex 4-12% Bis-Tris Protein Gels, 1.0 mm, 10 well, NuPAGE MOPS SDS Running Buffer (20X), NuPAGE LDS sample buffer (4x), HEPES, L-glutamine, DMEM, RPMI, ENZcheck reverse transcriptase assay kit, DH5 $\alpha$  competent cells, trypsin, ZOOM strips pH 3-10NL for IEF.

Life technologies: Fast SYBR<sup>®</sup> Green Master Mix, SuperScript<sup>®</sup> VILO<sup>™</sup> Master Mix, High-Capacity RNA-to-cDNA<sup>™</sup> Kit

Eppendorf: UVette

Promega: Kinase-Glo<sup>®</sup> Luminescent Kinase Assay

Qiagen: RNeasy Mini Kit, QIAEXII Gel Extraction Kit, QIAshredder, Ni-NTA Agarose beads

Stratagene: QuikChange II site directed mutagenesis kit

Seahorse Bioscience: Seahorse media, XF calibrant and XF24 plates

Millipore: Nitrocellulose membrane 0.22  $\mu$ m

Cambridge Isotope laboratories: U13C glucose, U13C glutamine.

GE Healthcare: Fetal bovine serum.

Thermo Scientific: Bicinchoninic Acid Assay (BCA), BSA standard.

Merck: ZIC-pHILIC column (4.6 mm×150 mm, guard column 4.6 mm×10 mm) HPLC column

Agilent Technologies: BioSec3 column (Agilent SEC-3,300A,7.8x300mm)

Eppendorf single sealed cuvettes, UVette (Eppendorf UK Limited)

## 2.1.2 Primers

qPCR primers:

β-actin-Forward Primer: 5'- TCCATCATGAAGTGTGACGT-3'; β-actin-Reverse Primer: 5'- TACTCCTGCTTGCTGATCCAC-3'; PKM1-Forward Primer: 5'- GAGGCAGCCATGTTCCAC-3'; PKM1-Reverse Primer: 5'- TGCCAGACTCCGTCAGAACT-3'; PKM2- Forward Primer: 5'- CAGAGGCTGCCATCTACCAC-3'; PKM2- Reverse Primer: 5'- CCAGACTTGGTGAGGACGAT-3'. PKL Forward Primer: 5'- CTGGTGATTGTGGTGACAGG-3' PKL Reverse Primer: 5'- TGGGCTGGAGAACGTAGACT-3' PKR Forward Primer: 5'- CAATTTGGCATTGAAAGTGG-3' PKR Reverse Primer: 5'- CCTGTCACCACAATCACCAG-3'

Site directed mutagenesis primers (sequence of mutated bases shown in uppercases bold): H464A: 5'gctcgtcaggcc**GC**cctgtaccgtggc3', S437Y: 5'accaagtctggcaggt**At**gctcaccaggtgg3'.

## 2.1.3 Antibodies

PKM1 antibody was custom-made by PolyPeptide Laboratories (Strasbourg, France) using the following peptide sequence: CLVRASSHSTDLMAMAMGS. The PKM2 (cat #3198) and PKM1/2 (#3186) antibodies were purchased from Cell Signalling Technology (Danvers, MA, USA). The anti-actin antibody (mouse monoclonal AC-40) was purchased from Sigma (Gillingham, UK). The donkey-anti rabbit (926 32213) or donkey-anti mouse (926 32212) secondary antibodies were purchased from LI-COR Biosciences.

PGAM1 and its phosphorylated forms were detected by Western blot using goat anti-PGAM1 (Novus) 1:1000 and Donkey anti-Goat (LI-COR Biosciences) 1:1000 antibodies.

#### **2.1.4 Vectors and plasmids**

shRNA (shCntrl) (sc-108080) or PKM1/2 shRNA (shPKM) (sc-62820) lentiviral particles were purchased from Santa Cruz Biotechnology, Santa Cruz, CA, USA. PKM1/2 shRNA (shPKMa) were bought from Openbiosystems (TRCN0000037610 and TRCN0000037611). pLKO scramble shRNA (Openbiosystems) was used as a control (shCntrl).

Lentiviral envelope and packaging helper plasmids: pLP/VSVG (lentiviral packaging plasmid for expression of the vesicular stomatitis virus G glycoprotein, Invitrogen) and psPAX-2 (2nd generation lentiviral packaging plasmid, Addgene).

Bacterial expression plasmids pET28a\_LIC\_wtPKM2, pET28a\_LIC\_H646A\_PKM2, pET28a\_LIC\_S437Y\_PKM2 were derived from pET28a\_LIC purchased from Structural Genomics Consortium, Toronto, CA.

pMSCV-blast-BRAFV600E and pMSCV-blast were previously described (Kuilman et al., 2008).

#### **2.1.5 Cell lines**

HCT116, HT29, SW620, HEK293T, Tig3, A375 and Colo829 were purchased from ATCC

#### **2.1.6 Equipment**

7500 Fast Real-Time PCR System (Life Technologies Corporation Carlsbad, California)

Odyssey CLx Infrared Imaging System (LI-COR Biosciences)

XCell SureLock Mini-Cell Electrophoresis System and blot module (Invitrogen)

Seahorse flux analyser XF24 (Seahorse Bioscience)

Agarose gel caster and tanks (Biorad)

Exactive™ Plus Orbitrap Mass Spectrometer (Thermo Scientific)

Veritas microplate luminometer (Turner Biosystems)

MicroCal VP-ITC

Hiload Superdex 16/60 S75 size exclusion chromatography

CASY cell counter and analyser (Roche Applied Science)

SpectraMax Plus 384 Absorbance Microplate Reader (Molecular Devices)

Eppendorf Biophotometer (Eppendorf UK Limited)

## **2.1.7 General buffers and solutions**

**RIPA buffer:** 50mM Tris-HCl, 150mM NaCl, 1% Triton x100, 1.0% NP-40, 0.1% SDS, pH 8.0, 1:100 protease inhibitors cocktail (Sigma, Gillingham, UK).

**Metabolomics extraction buffer:** 50% HPLC grade methanol, 30% HPLC grade acetonitrile, 20% milliQ water.

**Phosphate buffered saline (PBS):** 137mM NaCl, 2.7mM KCl, 10mM Na<sub>2</sub>HPO<sub>4</sub>, 2mM KH<sub>2</sub>PO<sub>4</sub>, pH 7.4.

**1X Blotting buffer:** 25mM Tris, 192mM glycine, 0,01%SDS, pH 8.3.

**LB-Broth:** 10g/l tryptone, 5g/l yeast extract, 10g/l NaCl.

**LB agar plates:** LB medium, 15 g/l bacto agar.

**Tris-acetate-EDTA 1X (TAE):** 40mM Tris, 20mM acetic acid, 1mM EDTA, pH 8.

**PE:** PBS, 0.01% EDTA.

**Trypsin (1X):** 10% 10X trypsin, 90% PE.

**PBST:** PBS, 0.05% Tween-20.

**Blocking buffer for western blot:** 5% Milk in PBST.

**Standard medium:** high glucose DMEM, 10% FBS, 2mM L-glutamine.

**Protein SEC buffer:** Tris-HCl 25mM, NaCl 150mM; pH 7.6

## **2.2 Experimental procedures**

### **2.2.1 Mammalian cell culture related techniques**

#### **2.2.1.1 Cell culture and storage**

HCT116 and HT29 colon cancer cells were cultured in high glucose DMEM supplemented with 10% FBS (heat inactivated at 56 °C for 45 min prior to use) and 2mM L-glutamine at 37 °C and 5% CO<sub>2</sub>. SW620 colon cancer cells were maintained in RPMI supplemented with 20% FBS and 2mM L-glutamine at 37 °C and 5% CO<sub>2</sub>.

The human diploid fibroblast (HDF) cell line Tig3 expressing the ecotropic receptor and hTERT was cultured in high glucose DMEM supplemented with 10% FBS and 2mM L-glutamine at 37 °C and 5% CO<sub>2</sub>. Infections with K-RAS<sup>G12V</sup>, BRAF<sup>V600E</sup>-encoding or control virus were performed as described in section 2.2.1.2 for lentiviral infection, using Phoenix packaging cells instead of HEK293T for the generation of ecotropic retroviruses. After 5 days of selection, HDF were seeded for assays.

A375 and Colo829 cells were purchased from the ATCC and maintained in RPMI both supplemented with 10% FBS, 1mM sodium pyruvate and 2mM L-glutamine. A375 and Colo829 cells were cultured in increasing concentrations of PLX4720 (from 0.1-1µM) to generate resistant clones (A375/R and Colo829/R

respectively). Cells able to grow in the continued presence of  $1\mu\text{M}$  of PLX4720 emerged after ~2 months of culture. PLX4720 was synthesized in house.

To split cells, media was removed and cells washed once with PBS (20ml per  $175\text{cm}^2$  flask), cells were dissociated with 1X trypsin (4ml per  $175\text{cm}^2$  flask), the flask returned to  $37^\circ\text{C}$  until the cells have completely detached, trypsin was neutralized by adding 14ml of full culture media and the cells in suspension were then spun down for 5 min at 1000rpm, re suspended in culture media and re plated at the needed concentration.

Frozen cell stocks were generated by re-suspending the pellets obtained after trypsinization in freezing media (90% FBS, 10% DMSO) to a concentration of  $1 \times 10^6$  cells/ml. They were further aliquoted into cryovials for storage, at  $-80^\circ\text{C}$  at first and in liquid nitrogen for long-term storage.

Lentiviral particles containing pLKO-shRNAs were produced in HEK293T cells by transfection using the  $\text{CaPO}_4$  protocol (see 2.2.1.2 section). Cells were cultured in DMEM supplemented with 10% FCS and 2mM glutamine and grown at  $37^\circ\text{C}$  at 5%  $\text{CO}_2$ .

#### **2.2.1.2 Generation of cell lines by shRNA lentiviral infection**

For stable PKM1/2 silencing, HCT116, SW620 and HT29 cells were infected with control shRNA (shCntrl) or PKM1/2 shRNA (shPKM) lentiviral particles according to the manufacturer's instructions. Infected cells were selected using  $6\mu\text{g}/\text{ml}$  puromycin and shPKM clones were analysed for PKM1 and PKM2 expression levels using Western blot analysis and qPCR. A different set of plasmids containing PKM1/2 shRNA (shPKMa) and pLKO scramble shRNA (shCntrlA) was used to generate independent cell lines. HCT116 cells were infected with both pLKO-shPKM1/2 or pLKO-shSCR and selected using  $2\mu\text{g}/\text{ml}$  puromycin for 2 weeks and PKM1/2 silenced clones were analysed for PKM1 and PKM2 expression levels using Western blot analysis and qPCR.

For lentiviral production,  $2 \times 10^6$  HEK293T cells were seeded in 10cm plates and cultured overnight. The next day, cells were transfected using  $10\mu\text{g}$  of DNA,  $7.5\mu\text{g}$  of psPAX-2 and  $4\mu\text{g}$  pLP/VSVG. The combined DNA was prepared in  $500\mu\text{l}$

of 2X HBS, 60 $\mu$ l of 2M CaCl<sub>2</sub> and water up to a volume of 1ml. The mix DNA/CaPO<sub>4</sub> was incubated for 30 min at 37°C and then added dropwise onto the HEK293T cells. Next day in the morning (no more than 18hr after transfection) media was replaced and left for 24hr for lentiviral production. At this point the target cells were plated and next day they were infected using the filtered supernatant (0.45 $\mu$ m pore size) from HEK2937 containing the lentiviral particles. The infection was repeated after 24hr for a total time of 48hr. Before using the cells for experiments they were screened for viral titer using the ENZcheck reverse transcriptase assay according to manufacturer's instructions (Invitrogen).

### **2.2.1.3 Whole cell lysate protein preparation, SDS-PAGE and Western blot**

4x10<sup>5</sup> cells were plated in a 6 well plate and after 2 days they were washed with 2ml of ice cold PBS prior lysis in 300 $\mu$ l of RIPA buffer (Section 2.1.7). Protein concentration was determined using the Bicinchoninic Acid Assay (Thermoscientific, Waltham, MA) using BSA as standard, according to manufacturer's instructions. Absorbance at 562nm was determined using Molecular Devices SpectraMax Plus 384 Absorbance Microplate Reader and SoftmaxPro software.

Equal amounts of protein were prepared in NuPAGE LDS sample buffer (4x) with 5%  $\beta$ -mercaptoethanol, loaded into a NuPAGE Novex 4-12% Bis-Tris Protein Gel and electrophoretically separated at 200V for 45 min using 1X NuPAGE MOPS SDS Running Buffer (Invitrogen). After SDS-PAGE, proteins were transferred to a 0.22 $\mu$ m nitrocellulose membrane (Millipore, Billerica, MA) in 1X blotting buffer (Section 2.1.7) using the XCell SureLock Mini-Cell Electrophoresis System and blot module (Invitrogen) for 1.5hr at 25V. The membrane was then blocked for an hour in blocking buffer (Section 2.1.7) and probed overnight with the specific primary antibody, at 1:1000 in 5% non-fat milk in PBST (Section 2.1.7). After 1hr incubation with the corresponding fluorescent secondary antibody (LI-COR Biosciences), the infrared scanning was performed using the LI-COR Odyssey scanner, Channel 800, Brightness: 50, Contrast: 50, Sensitivity: auto, resolution: 169.492 micron, Pixel area: 0.02873, Intensity: 5 and acquired using Odyssey software version 3. Images were then exported as TIFF and cropped using Adobe Photoshop CS4.

#### **2.2.1.4 Total mRNA isolation and qPCR**

mRNA extraction and qPCR analyses.  $4 \times 10^5$  cells were plated in a 6 well plate and were lysed after 2 days in RLT buffer (Qiagen, West Sussex, UK). Lysates were passed through QiaShredder columns (Qiagen, West Sussex, UK) and mRNA was isolated using the RNeasy kit (Qiagen, West Sussex, UK) following the manufacturer's instructions. RNA was quantified and quality controlled using an Eppendorf Biophotometer and Eppendorf single sealed cuvettes, UVette (Eppendorf UK Limited, Endurance House, UK). For qPCR analyses 1  $\mu$ g of mRNA was retro-transcribed into cDNA using High Capacity RNA-to-cDNA (AB, Life Technologies Corporation Carlsbad, California). In brief, 0.5  $\mu$ M primers, 1X Fast SYBR Green Master mix (AB, Life Technologies Corporation Carlsbad, California) and 1  $\mu$ L of a 1:10 dilution of cDNA in a final volume of 20  $\mu$ L were used. Real-time PCR was performed on the 7500 Fast Real-Time PCR System (Life Technologies Corporation Carlsbad, California) and expression levels of the indicated genes were calculated using the  $\Delta\Delta C_t$  method by the appropriate function of the software using actin as calibrant. The PCR program was: 20 seconds at 95°C followed by 40 cycles of 3 seconds at 95°C and 30 seconds at 60°C. Finally the melting curve was performed, which was used to confirm the presence of single PCR products.

#### **2.2.1.5 Cell proliferation**

shPKM and control HCT116, HT29 or SW620 cells were seeded into a 24 well plate at a density of  $1 \times 10^4$  cells/well in 500 $\mu$ l of full media or media without serine and glycine. Cells were counted in triplicates every 24hr for 5 days using a CASY cell counter and analyser (Roche Applied Science).

### **2.2.2 Protein related techniques**

#### **2.2.2.1 Recombinant protein production, isolation and characterization**

In order to produce PKM2 WT, H464A, and S437Y, N-terminal His-tagged fusion proteins (Section 2.1.4) were expressed in BL21(DE3) bacteria and then purified using Ni-NTA Agarose beads (Qiagen). Briefly, BL21(DE3) recombinant bacteria expressing the proteins of interest from previously generated glycerol stocks were inoculated in 5 ml of LB medium with kanamycin 50 $\mu$ g/ml and incubated

overnight at 225 rpm/37 °C. The following day, the culture was transferred to 1 litre of LB medium and incubated for approximately 3hr or until OD<sub>λ600</sub> reached 0.8. Bacteria were induced to produce the recombinant proteins with IPTG (0.2 M) and left overnight at 20 °C. The next day, cells were pelleted at 4,000 g for 15 minutes (all centrifugation steps were performed at 4 °C) and re-suspended in buffer 1 (Tris-HCl 25 mM, NaCl 150 mM; pH 7.6) containing imidazole (20 mM), lysozyme (1mg/ml), and PMSF (1.5 mM). Imidazole prevents unspecific binding of His rich proteins to the Ni beads, lysozyme breaks down the cell wall, and PMSF (phenylmethylsulfonyl fluoride) is a protease inhibitor. Samples were snap-frozen in liquid nitrogen and stored overnight at -80 °C. The next day, samples were thawed, PMSF added (1.5mM) and sonicated in ice for 1 minute in 8 seconds pulse/pause cycles and pelleted at 15,000 g for 30 minutes. Ni beads (in 50% EtOH) were equilibrated in 14 ml of buffer 1 with 20mM imidazole by centrifugation at 1,000 rpm for 5 minutes to remove EtOH and cell lysates were mixed with the beads and incubated on a shaker for 2 hours at 4 °C to allow binding of the His-tagged proteins to the Ni beads. After incubation, beads were spun down at 1,000 rpm for 5 minutes and washed three times in buffer 1 with 20mM imidazole, and a fourth time in buffer 1 without imidazole containing 2mM CaCl<sub>2</sub>. Beads were re-suspended in 500 µl buffer with CaCl<sub>2</sub> and 100 µl thrombin (0.72 µg/ml) and left rocking overnight at 4 °C to allow cleavage of the purification tag. Next day, beads were pelleted at 6,000 g for 1 minute and supernatant with cleaved protein was quantified using the Bradford protein assay with the following formula:

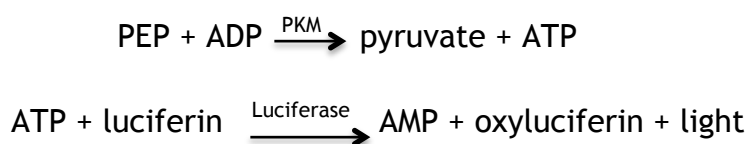
$$\text{Protein (mg/ml)} = (\text{Absorbance } (\lambda 595)) / (0.071 \times \text{volume } (\mu\text{l}))$$

After protein purification, samples were separated on a NuPage 4-12% Bis-Tris gel and compared to commercially bought PKM1 (rabbit muscle, Sigma) to determine whether the purification process was successful and the presence of contaminants or degradation products present in the sample.

#### **2.2.2.2 *In vitro* pyruvate kinase activity**

PKM2 WT, H4646A and S437Y were expressed and purified as described in section 2.2.2.1. Rabbit muscle PKM1 was obtained from Sigma; PKL/R was purchased from Abcam. Enzyme activity was measured *in vitro* with a coupled assay

quantifying the ATP generated by pyruvate kinase during the conversion of PEP to pyruvate using the luminescent Kinase-Glo Plus reagent (Promega). The reaction buffer was made of 50mM Tris pH 7.5, 100 mM KCl, 10mM MgCl<sub>2</sub>, 200μM PEP, 200μM ADP, 3% DMSO and either 10nM PKM2, 4nM PKM1, 10nM PKL/R, 10nM PKM2-H464A or 30nM PKM2-S437Y in the presence of increasing concentrations of FBP (0.01, 0.03, 0.1, 0.3, 1, 3, 10, 50 μM) or serine (0.03, 0.1, 0.3, 1, 3, 10, 30, 100 mM). Reactions (25 μL) were incubated for 20 minutes on a shaker at room temperature, before addition of 25 μL Kinase-Glo Plus reagent and incubation for another 10 minutes before measurement. Luminescent signal was quantified on a Veritas microplate luminometer (Turner Biosystems) using GLOMAX software (version 1.9.2) and normalized to control wells containing no enzyme. Activation curves were fitted to a four-parameter logistic equation and Km curves were fitted to a Michaelis-Menten equation using Prism 5 (GraphPad).



### 2.2.2.3 UV HPLC Size-exclusion chromatography

A Dionex HPLC system was used for all chromatographic analyses, consisting of an automated sample injector, solvent pump, thermo controlled column chamber, and a UV detector. An Agilent Bio SEC-3 (300 Å) column was used. In addition, an ISCO Foxy Jr fraction collector was used to collect separated protein fractions. Dionex Chromeleon software (version 6.7) was used to control the instruments, acquire the data, visualize and quantify the peak areas. An isocratic HPLC method was employed with a mobile phase of Tris-based buffer (Tris-HCl 25 mM, NaCl 150 mM; pH 7.6). Purified protein (20 mg/ml) was injected at a volume of 5 μl with a pump flow of 500 μl/minute. The column temperature was held constant at 22 °C and ultraviolet signal was recorded at 220 nm. Activators were added to the buffer at 500 μM, 1 mM, 5 mM, 50 mM (serine), and 250 μM (FBP). Separated protein fractions were collected every 15 seconds from retention time 14:00 minutes to 18:00 minutes, corresponding to tetrameric and dimeric PKM2, resulting in 16 fractions.

The fractions were precipitated using trichloroacetic acid (TCA) solution (Sigma). Briefly, 40% TCA was added to the protein samples at a 1:1 volume ratio, incubated for 10 minutes at 4 °C, and spun down at 14,000 rpm for 10 minutes. The pellet was washed with 10% TCA and a second time with water before being re-suspended and heated at 70 °C for 10 minutes in SDS loading buffer with 5%  $\beta$ -mercaptoethanol. Samples were separated on a 10% NuPAGE Bis-Tris gel, transferred to a PVDF membrane, and incubated overnight at 4 °C with primary rabbit PKM1/2 antibody at 1:2000 (# 3186, Cell Signalling). The next day, protein was incubated with a fluorescent secondary donkey anti-rabbit antibody (926 32213, LI-COR Biosciences) and visualized using a LI-COR Odyssey scanner.

#### **2.2.2.4 Isothermal titration calorimetry**

ITC experiments were performed on a MicroCal VP-ITC at 25°C in a buffer comprising 50mM Tris, 100mM KCl, 10mM MgCl<sub>2</sub> and 1mM TCEP at pH 7.5. For titrations the L-serine concentration was 5mM in the injection syringe and the PKM2 concentration was 28 $\mu$ M in the sample cell. The protein concentration refers to the monomer. PKM2 was incubated for 30 minutes with an excess of FBP (200 $\mu$ M) prior to the L-serine titration performed in the presence of FBP. The K<sub>d</sub> value for L-serine binding was significantly higher than the PKM2 concentration used, making it difficult to accurately determine the stoichiometry value. Therefore, the stoichiometry parameter was fixed at 1 for the purpose of data analysis using the single-site binding model in Origin 7.0. This work was performed at Astex Pharmaceuticals.

#### **2.2.2.5 X-ray crystallography**

A publically available human PKM2 expression construct was obtained from the Structural Genomics Consortium (SGC). His6-hPKM2 was purified using NiNTA affinity capture and Hiload Superdex 16/600 S75 size exclusion chromatography. hPKM2 was crystallised using hanging drop vapour diffusion. Protein solution 10 mg/ml, 25mM Tris/HCl pH 7.5, 100mM KCL, 5mM MgCl<sub>2</sub>, 10% (v/v) glycerol was mixed in a (1:1) ratio with reservoir solution containing 100mM KCl, 200mM ammonium tartrate, 24% (w/v) PEG3350. Crystals were soaked overnight in a solution containing 30mM L-Serine, cryoprotected and flash frozen in liquid N<sub>2</sub>.

X-ray diffraction data were collected from a single crystal at 100K at Beamline-I03 at the Diamond Light Source. Diffraction data were processed using XDS AutoPROC from Global Phasing and SCALA (CCP4). Molecular replacement was performed using model 3H6O (SGC) in CSEARCH and maximum likelihood refinement carried out using a mixture of automated and manual refinement protocols employing Refmac (CCP4) and AutoBuster from Global Phasing. Ligand fitting was performed using Autosolve and manual rebuilding. Simulated annealing was not employed. The four PKM2 monomers comprising the tetramer in the asymmetric unit were refined as independent entities, but NCS restraints were imposed in AutoBuster using the 'ncsauto' command. Refinement of the structure in the absence of NCS restraints gave ( $R_f=23.7$ ,  $R=17.7$ ) and with 'ncsauto' gave ( $R_f=22.7$ ,  $R=17.9$ ), showing a small, but significant, reduction in  $R_f$  using 'ncsauto' restraints. At the 'effective resolution' of 2.36Å there are ~86000 unique reflections. The refinement included ~16600 non-hydrogen atoms. B-factors were refined isotropically giving a total of ~66500 parameters for all non-hydrogen atoms in the PKM2 tetramer. The four serine molecules were refined as independent ligands. This work was performed at Astex Pharmaceuticals.

#### **2.2.2.6 PKM2 mutagenesis**

hPKM2 point mutant constructs were generated using a Stratagene QuikChange II site directed mutagenesis kit (#200524). PCR protocols were as defined in the product manual. The following forward DNA primers, and their reverse complemented primer counterparts, were used for the mutagenesis reactions (sequence of mutated bases shown in uppercase bold): H464A: 5'gctcgtcaggccGCcctgtaccgtggc3', S437Y: 5'accaagtctggcaggtAtgctcaccaggtgg3'. Primers were purchased from Sigma (UK). The previously described SGC hPKM2 construct was used as the DNA template within the PCR reactions. The presence of the point mutations was confirmed by DNA sequencing of the DNA constructs (Beckman Coulter Genomics Inc., Takeley, UK) and in-house LC-MS of the purified recombinant proteins. The mutant proteins were expressed and purified identically to the wild type protein. This work was performed at Astex Pharmaceuticals.

## **2.2.3 Metabolic measurements**

### **2.2.3.1 Metabolic fluxes and exchange rates**

Cells were incubated for 48h in full culture media and metabolite's exchange rates were calculated by comparing the peak area for each metabolite in full culture media kept under the same conditions for 48h without cells and considering the average cell number during the culture time. Metabolites present in the culture media were extracted by adding 20µl of culture media into 980µl of ice cold extraction buffer, composed by a 50:30:20 ratio of methanol:acetonitrile:water (Section 2.1.7) centrifugation for 10min at 16000rpm, 4°C and LC-MS analysis.

### **2.2.3.2 Metabolites labelling with $^{13}\text{C}_6$ glucose / $^{13}\text{C}_5$ L-glutamine and extraction**

Cells were plated at a density of  $4 \times 10^5$  onto 6 well plates and cultured in standard medium (Section 2.1.7) for 24 hours. The medium was then replaced by 2ml of fresh medium containing 5mM unlabelled glucose and 3 hours later 5mM of  $^{13}\text{C}_6$  glucose (Cambridge Isotope Laboratories, Inc) was added; alternatively, medium was replaced by 2ml of standard medium containing 2mM  $^{13}\text{C}_5$  L-glutamine instead of normal L-glutamine. Cells were incubated in one of the above media for the indicated time prior to extraction. For extraction, cells were washed twice in PBS and metabolites were extracted in ice-cold extraction buffer (Section 2.1.7), quickly scraped and incubated on a dry ice/methanol bath for 20min. The insoluble material was spun down in a cooled centrifuge at 16000g for 15 minutes at 0°C and the supernatant collected for subsequent LC-MS analysis. The volume of extraction solution was calculated according to the cell number and, extrapolated using a "counter dish" cultured under the same experimental conditions as the sample dishes. A volume of 1 ml of extraction solutions per  $2 \times 10^6$  cells was used.

### **2.2.3.3 LC-MS metabolomics and metabolites' quantification**

Metabolites were separated by liquid chromatography (LC) using a Sequant ZIC-pHILIC column (2.1mm x 150mm, 5µm polymeric beads, guard column Sequant Zic-pHILIC guard peek 2.1mm x 20mm, Millipore) using formic acid, water, acetonitrile as components of the mobile phase. Detection of metabolites was

performed using mass spectrometry (MS) in a Thermo Scientific Exactive high-resolution mass spectrometer with electrospray (ESI) ionization, examining metabolites in both positive and negative ion modes, over the mass range of 75-1000 m/z.

For intracellular and extracellular metabolite's quantification,  $1 \times 10^6$  cells were plated onto 6cm plates in triplicates and cultured in standard medium (Section 2.1.7). Two additional plates were grown as counter plates. The medium was replaced after 24 hours by 10 ml of fresh standard medium, and cells were incubated for another 24 hours before extraction (Section 2.2.3.1). Standard compounds were weighed separately and dissolved together in water to make solution A (where each metabolite has a concentration between 1mM and 10mM). 1ml of solution A was added to 49 ml of dilution solvent (50:50 acetonitrile:water) to make stock solution B (where each metabolite had a concentration between 20 $\mu$ M and 200 $\mu$ M). For quantification, cells or media extracts (200 $\mu$ l) were mixed with 800 $\mu$ l of dilution solvent, containing 0, 4, 20, 100, 300 or 500 $\mu$ l of stock solution B. Dilutions were analysed by LC-MS. The concentration of each metabolite in the extract was calculated according to a linear regression fit. All dilution series were performed in triplicates using 3 biological replicates.

#### **2.2.3.4 Extracellular oxygen and H<sup>+</sup> flux measurements**

For the measurement of oxygen consumption rate (OCR) and extracellular acidification rate (ECAR),  $3 \times 10^4$  cells were plated onto XF24 plates (Seahorse Bioscience, North Billerica, MA) in 100 $\mu$ L of DMEM (10% FBS, 2mM Glutamine) and incubated at 37°C, 5% CO<sub>2</sub> overnight. At the same time, the probes were equilibrated by adding 1ml of XF calibrant to each well of the cartridge plate of an XF24 Assay Kit (Seahorse Bioscience, North Billerica, MA) and the plate was then placed at 37°C in a CO<sub>2</sub>-free incubator overnight. The following day, the media on the plate containing cells was replaced with 675 $\mu$ L of unbuffered assay media (Seahorse Bioscience, North Billerica, MA) supplemented with 2mM L-glutamine, 25mM glucose and 2% FBS (pH was adjusted to 7.4 using sodium hydroxide 0.5mM) and cells were then placed at 37°C in a CO<sub>2</sub>-free incubator for 30 minutes. Basal OCR and ECAR were measured using the optical fluorescent oxygen/hydrogen sensor XF24 Seahorse plate reader. The mito stress kit was

used with the following concentrations: 1 $\mu$ M Oligomycin, 1 $\mu$ M CCCP and 1 $\mu$ M antimycin A. Each measurement cycle consisted of 3 minutes mixing, 3 minutes waiting and 4 minutes measuring. OCR and ECAR were normalised to cell number. To obtain the mitochondrial-dependent OCR, only antimycin A-sensitive respiration was used. Homogeneous plating and cell count were assessed by fixing the cells with 10% trichloroacetic acid for 1 hour at 4°C and then staining the fixed cells with 0.47% solution of Sulforhodamine B (SRB) (Sigma, Gillingham, UK)(192).

### **2.2.3.5 ATP measurement**

To measure intracellular ATP levels, 6x10<sup>5</sup> cells were seeded on a 6 well plate the day before the experiment. Cells were then washed twice with PBS in order to remove dead cells, and then lysed using the ATP-release buffer (Sigma, Gillingham, UK). ATP was then measured using a luciferase-based assay according to the manufacturer's instructions using the adenosine 5' - triphosphate (ATP) bioluminescent somatic cell assay kit FLASC (Sigma). Values were normalised to the total protein content of the cell lysate as measured by BCA assay (Thermoscientific, Waltham, MA) using BSA as standard.

### **2.2.4 Statistical analysis and data processing**

For general statistical analyses, data were analysed and presented with Graphpad Prism 5.01 software (GraphPad Software Inc, CA, USA). The data (mean  $\pm$  s.e.m.) are representative of 3-5 independent experiments, performed in technical triplicates if not differently indicated.

The metabolomics data processing workflow started by first converting the vendor specific raw data files from the mass spectrometer into the mzXML open data format, using the msconvert utility from the ProteoWizard Library and Tools collection (<http://proteowizard.sourceforge.net/>). The set of all chromatographic peaks in each of the converted raw files were then extracted using the CentWave feature detection algorithm from XCMS. The resulting data were stored in the PeakML file format and the rest of the processing was handled by the scriptable mass spectrometry data processing tool mzmach.R (<http://mzmach.sourceforge.net/>).

The next step in the workflow involved aligning and combining the chromatographic features between biological replicates of a single sample. The PeakML files thus created were subjected to an additional filtering procedure to discard all peaks that were not reproducibly detected in all biological replicates involved. Chromatographic peaks of individual samples were then aligned together based on their retention time and m/z values, and combined into a single PeakML file. Peak sets that do not include peaks from every sample were filled in by extracting ion chromatograms within the retention time and mass window of the corresponding peak set directly from the raw data files. From these peak sets, only those that had more peaks than the number of replicates minus one were selected for further analysis. Putative identification of the peak sets were made by matching the detected masses to that of the compounds relevant to this study. Isotope peaks were extracted by identifying the peaks that fell in the retention time window of the identified unlabelled peak and correspond to the estimated mass window (2 ppm) of the isotope. All isotope identification and quantification of the ratios were performed by the `PeakML.Isotope.TargettedIsotopes()` function of the `mzmatch.R` library. Detailed documentation and tutorials for which are available at [http://mzmatch.sourceforge.net/isotopes\\_targetted.html](http://mzmatch.sourceforge.net/isotopes_targetted.html).

## **Chapter 3 - Characterisation of Serine as a Natural Ligand and Allosteric Activator of Pyruvate Kinase M2**

### 3.1 Introduction

In recent years, pyruvate kinase (PK), the enzyme that catalyses the final and rate-limiting step of glycolysis by dephosphorylating phosphoenolpyruvate (PEP) to pyruvate, has emerged as a key regulator of the glycolytic phenotype found in cancer cells. Mammalian cells express four isoforms of PK in a tissue-dependent manner, which are encoded by two different genes: *PKLR* (producing PKL and PKR) and *PKM* (producing PKM1 and PKM2). All isoforms show tissue specificity, however, PKM2 is highly expressed in all tissues during embryogenesis as well as in rapidly proliferating cells (193). The expression of PKLR isoforms is regulated by tissue-specific transcription factors, while the expression of PKM isoforms is controlled by alternative splicing (23, 194). Interestingly, tumour cells predominantly express high levels of PKM2, which was thought to result in the glycolytic phenotype of cancer cells (30, 36, 195).

Conformational differences between the PKM isoforms arise from the presence of exon 10 in PKM2, which allows it to alternate between a dimeric and a tetrameric form, unlike PKM1, which always forms an active tetramer(25). Of all PK isoforms, PKM1 has the highest affinity for its substrate PEP and therefore, is found in tissues that have to rapidly generate large quantities of energy (193). It is constitutively active and not subject to phosphorylation or allosteric regulation (25, 196, 197). In contrast, the different conformations of PKM2 show large functional differences. Kinetic studies showed that the affinity for PEP is much higher in the tetrameric form compared to the dimeric form, with a sufficiently high  $K_m$  to render the dimeric form nearly inactive at physiological concentrations of PEP(198). As a consequence, when PKM2 exists predominantly as a dimer, the intermediates upstream of PEP accumulate and are available for biosynthetic processes in the expense of ATP. However, when PKM2 is predominantly tetrameric, the flux through glycolysis is dramatically increased, favouring the generation of ATP.

The conformational switch of PKM2 from dimer to tetramer can be induced by the allosteric regulator fructose-1,6-bisphosphate (FBP), an upstream intermediate of the glycolytic pathway(38). The low activity of PKM2 in its

dimeric confirmation results in a build-up of upstream FBP levels, until a critical concentration is reached, after which FBP induces a conformational switch in PKM2 towards the highly active tetramer. As a consequence, glucose goes through the full glycolytic pathway and ATP is generated. Simultaneously, FBP is consumed and levels drop below this critical concentration, causing PKM2 to dissociate into the inactive dimer. This makes glycolytic intermediates available for biosynthetic processes instead of energy production. Via this feedback mechanism, PKM2 acts as a metabolic sensor as well as a key regulator of glucose-derived carbons towards either energy production or biosynthesis (199).

## **3.2 Results**

### **3.2.1 Characterization of HCT116 cells upon PKM2 silencing**

PKM2 is a highly regulated allosteric enzyme that responds not only to its substrates, PEP and ADP, but also to other metabolites, with the glycolytic intermediate FBP being the strongest activator. Additionally, PKM2 activity is dependent on its oligomeric state and post-translational modifications such as phosphorylation and acetylation (38, 43, 53). Overall, PKM2 is considered a slow enzyme compared to the alternatively spliced and constitutively active variant PKM1 or the other two variants PKL/R. It has been proposed that the predominance of PKM2 in proliferating cells supports the build-up of glycolytic intermediates that can be diverted into other anabolic pathways (199). To test this hypothesis we used HCT116 cells (human colon carcinoma cell line) that express high levels of PKM2 (Fig. 3:1a). Pyruvate kinase activity was reduced in these cells via stable expression of short hairpin RNA against PKM1 and PKM2 (shPKM1/2) (Fig. 3:1a and 3:1b). Despite a marked reduction in RNA and protein levels of PKM1/2 compared to cells expressing non-targeting shRNA (shCntrl), no compensatory transcriptional induction of the PKL/R isoforms was observed (Fig. 3:1c). Importantly, the stable silencing of PKM1/2 did not alter the steady-state levels of ATP (Fig. 3:1d). Since PK catalyses an important ATP-producing step within glycolysis, one might predict an increase in oxidative phosphorylation in shPKM1/2 cells. Indeed, the oxygen consumption rate of these cells doubled (Fig. 3:1e) while lactate production and secretion decreased dramatically in

shPKM1/2 cells (Fig. 3:1b, 3:1f). All the above results are consistent with the lack of changes observed in the proliferation rate of these cells upon PKM inhibition (Fig. 3:1g). Overall, this demonstrates that despite the predominant expression of the slower enzyme PKM2, HCT116 cells still require a significant level of PK activity to undergo aerobic glycolysis and that they are able to adapt their metabolism according to changes in PK activity in order to continue proliferating.

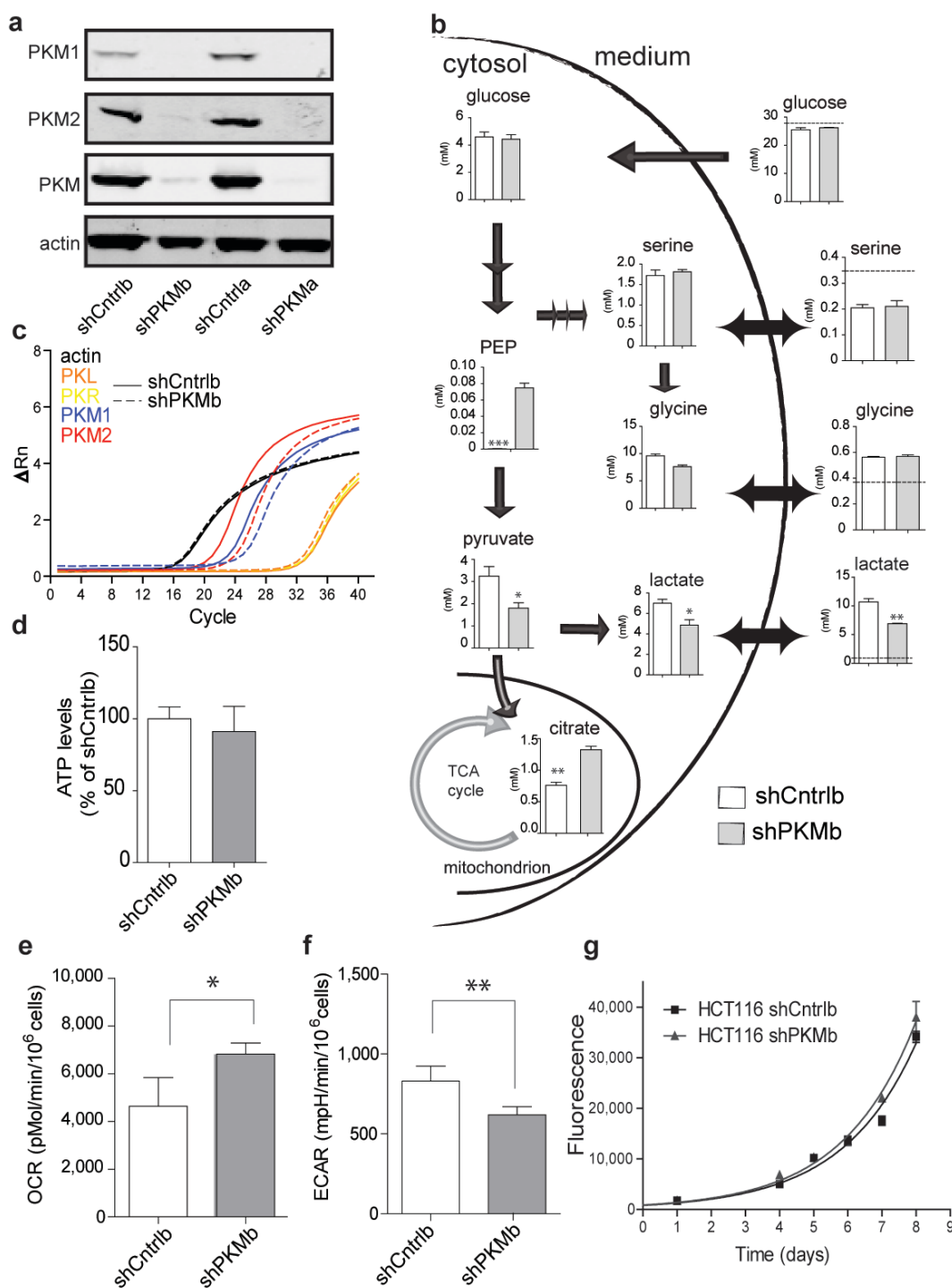


**Figure 3-1: Characterisation of PKM1/2-silenced HCT116 cells**

**a**, Protein levels of PKM1 and PKM2 in the indicated cell lines were detected by western blot. Actin was used as loading control. **b**, Quantified intracellular metabolite concentrations and the uptake or secretion of extracellular metabolites in control and shPKMb\* HCT116 cells. For extracellular metabolites, the dashed line indicates the initial levels in the medium, while the graph represents the levels after 24 hours incubation. **c**, Representative traces of qPCR analysis of the indicated PK isoforms in control and PKM1/2-silenced cells. **d**, Intracellular ATP levels of the indicated cells normalised to protein concentration in the cell extracts. **e-f**, PKM1/2 silencing increased oxygen consumption rate (OCR) and decrease extracellular acidification rate (ECAR). **g**, Proliferation rate

of the indicated cell lines was measured by an Alamar Blue assay. All results are from 3 independent cultures and are presented as mean  $\pm$  s.e.m. \* =  $P < 0.05$ , \*\* =  $P < 0.01$ , \*\*\* =  $P < 0.001$ .

\*HCT116 cells stably expressed either non-targeting control shRNA (shCntrl) or shRNA targeting both PKM isoforms (shPKM). shPKMa and shPKMb refer to two independent HCT116-derived cell lines, in which the expression of both the PKM1 and PKM2 isoforms were simultaneously and stably silenced using discrete shRNA pools, containing non-equivalent shRNAs.

### 3.2.2 Low PK activity and serine deprivation alter $^{13}\text{C}_6$ -glucose metabolism

To examine how changes in PK activity impact the metabolic fate of glucose in cancer cells, we incubated shCntrl and shPKM1/2 HCT116 cells in media containing labelled  $^{13}\text{C}_6$ -glucose and extracted cells at different time points for metabolomic analysis by liquid chromatography-mass spectrometry (LC-MS). Several different glucose-derived metabolites were followed over time (Fig. 3:2a). As observed with unlabelled steady-state metabolite levels, an obvious block in the flux between PEP and pyruvate is seen in shPKM1/2 cells, where PEP accumulated more rapidly and to a much higher level than in control cells (Fig. 3:2a). In the cytosol, pyruvate can be further metabolised to lactate via lactate dehydrogenase (LDH) or to alanine via alanine transaminase (ALT). In both cases, 3 glucose-derived carbons will be detected by LC-MS. In addition, pyruvate can translocate to the mitochondria where it is oxidized and decarboxylated to acetyl-CoA and enter the tricarboxylic acid (TCA) cycle to form citrate - contributing 2 carbon atoms from glucose. Interestingly, blocking PKM1/2 activity shifted the flux of pyruvate from the cytosol (lactate and alanine) to the mitochondria (citrate) (Fig. 3:2a). These results are consistent with the observed increase in oxygen consumption of shPKM1/2 cells (Fig. 3:1e). Finally, an increase in metabolic flux into the serine and glycine biosynthetic pathway was also observed in cells with silenced PK activity (Fig. 3:2a). This is the first indication that lower PK activity can change the fate of glucose metabolism and support anabolic flux, providing an important link between two events that are observed in cancer. However, unlike most metabolites studied, the contribution of glucose-derived carbon to serine and glycine is low (Fig. 3:2b). This is likely due to the fact that the cells are grown in the presence of unlabelled serine and glycine (white bars). Indeed, when cells were incubated for 12 hours in the absence of extracellular serine and glycine, all intracellular serine and glycine were glucose-derived (Fig. 3:2b). Nevertheless, the steady-state level of these amino acids was not rescued to the levels observed in cells grown in the presence of serine and glycine (Fig. 3:2b), indicating that the rate of serine and glycine production from glucose is limiting and is equal to the rate of their use. Nevertheless, serine and glycine deprivation had a pronounced effect on glucose metabolism. In fact, an increase in PEP and a decrease in pyruvate suggest that

serine and glycine deprivation reduces PKM2 activity in these cells (Fig. 3:2b). PKM1/2 activity in cells (predominantly PKM2) may be best represented as the ratio between 3-carbon labelled pyruvate (product) to 3-carbon labelled PEP (substrate) 30 minutes after  $^{13}\text{C}_6$ -glucose addition (Fig. 3:2c). When cells were deprived of serine and glycine for 12 hours and shortly labelled with  $^{13}\text{C}$ -glucose, a sharp decrease in the labelled pyruvate/PEP ratio was observed (Fig. 3:2c). These results indicate that serine/glycine deprivation inhibits PKM2 activity to divert more glucose for serine/glycine biosynthesis. In addition, like PKM1/2 silencing, serine deprivation also lowered lactate production in the cytosol and increased citrate production in the mitochondria Fig. 3:2a- 3:2b).

Although serine hydroxymethyl transferase converts serine to glycine and vice versa, a short (30 minutes) incubation with either serine or glycine, after overnight starvation from both amino acids, was sufficient to increase the intracellular levels of the added amino acid only, without affecting the other amino acid levels. Interestingly, when starved cells were incubated for 30 minutes with serine together with  $^{13}\text{C}_6$ -glucose, an increase in intracellular PK activity was measured as compared to starved cells. On the other hand, glycine alone could not stimulate intracellular PK activity (200).

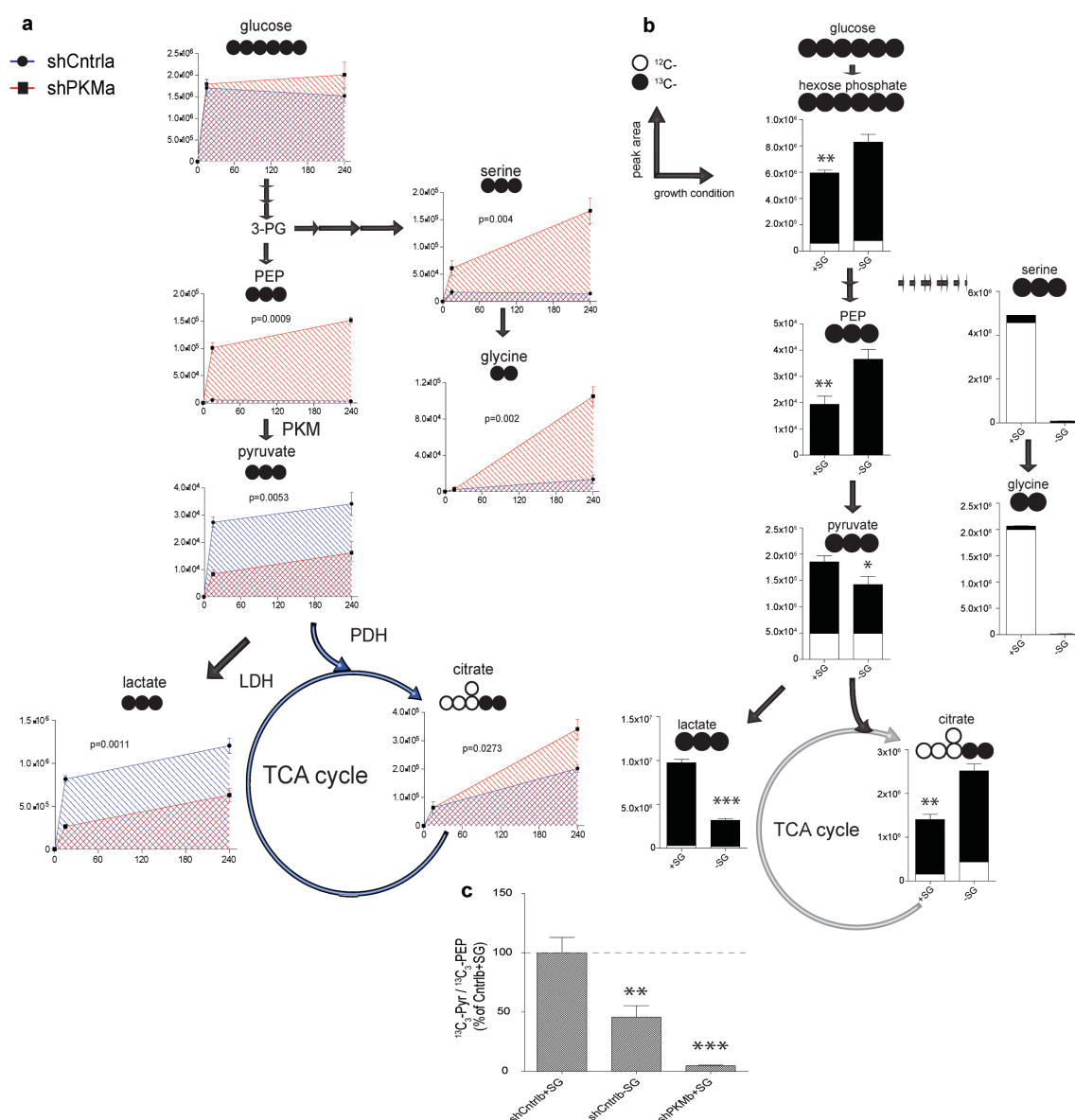


**Figure 3:2- Modulation of central carbon metabolism by PKM1/2-silencing and serine/glycine deprivation**

**a**, HCT116 shCntrl and shPKM cells were incubated with <sup>13</sup>C<sub>6</sub>-glucose and the abundance of the main glucose-derived isotopomer of the indicated metabolites was analysed at the indicated time points. The cumulative intensities of each labelled metabolite analysed in each cell line are presented in blue (shCntrl) or red (shPKM). **b**, Parental HCT116 cells were incubated for 12 hours with <sup>13</sup>C<sub>6</sub>-glucose in the presence (+SG) or absence (-SG) of serine and glycine. The abundance of the main glucose-derived isotopomer (black bars) and the unlabelled fraction (white bars) of the indicated metabolites were analysed. The white and black circles illustrate <sup>12</sup>C- and <sup>13</sup>C-labelling respectively. **c**, PK activity is represented as the ratio between glucose-derived (<sup>13</sup>C<sub>3</sub>-) pyruvate and PEP, 30 minutes after labelling with <sup>13</sup>C<sub>6</sub>-glucose in the presence or absence of serine and glycine in the indicated cell lines. Results were normalised to shCntrl +SG. All results are from 3 independent cultures and they are presented as mean ± s.e.m. \* = P < 0.05, \*\* = P < 0.01, \*\*\* = P < 0.001. 3-PG, 3-phosphoglycerate; PEP, phosphoenolpyruvate; PKM, pyruvate kinase; PDH, pyruvate dehydrogenase; LDH, lactate dehydrogenase; TCA, tricarboxylic acid.

### 3.2.3 Serine binds to, and activates, PKM2

This work was performed at Astex Pharmaceuticals (Cambridge, UK).

Upon observing that serine and glycine deprivation affects central carbon metabolism in a similar fashion as shPKM, we tested whether serine or glycine alone can modulate PKM2 activity *in vitro*. Serine was able to activate recombinant PKM2 with a half maximal effective dose (EC<sub>50</sub>) of ~1 mM (Fig. 3:3a), which is within the physiologic range of intracellular serine concentrations in HCT116 cells (Fig. 3:1b). In addition, isothermal titration calorimetry was used to determine the dissociation constant (K<sub>d</sub>) and stoichiometry of the serine-PKM2 interaction. The K<sub>d</sub> of serine was calculated to be ~0.2 mM (Fig. 3:3b), with a (1:1) PKM2-monomer:serine ratio. These results not only demonstrate direct interactions between serine and PKM2, they also suggest that the concentration of serine required for such interactions is well within the physiological range of its intracellular levels. Furthermore, glycine could not directly activate PKM2 *in vitro* (Fig. 3:3a). Similar to FBP, serine lowered the K<sub>m</sub> of PKM2 for PEP (lowered the required concentration of this substrate) (Fig. 3:3c). Finally an X-ray crystallographic soaking experiment was used to obtain the structure of serine bound to human PKM2. A single serine molecule binds into an amino acid binding-pocket in the middle domain of the PKM2 monomer, and serine binding is facilitated by a reorientation of the side chain of Arg106, which then co-ordinates the carboxylic acid group of the serine (Fig. 3:3d). The amino group of serine forms hydrogen bonds with the side chain of His464, the main chain carbonyl of Leu469 and a water molecule, which interacts with the main chain carbonyls of Tyr466 and His464. In addition, the side chain hydroxyl of the serine forms hydrogen bonds with the main chain carbonyl of Leu469 along with a water molecule that interacts with the main chain carbonyls of Gly468 and Asn44(200).

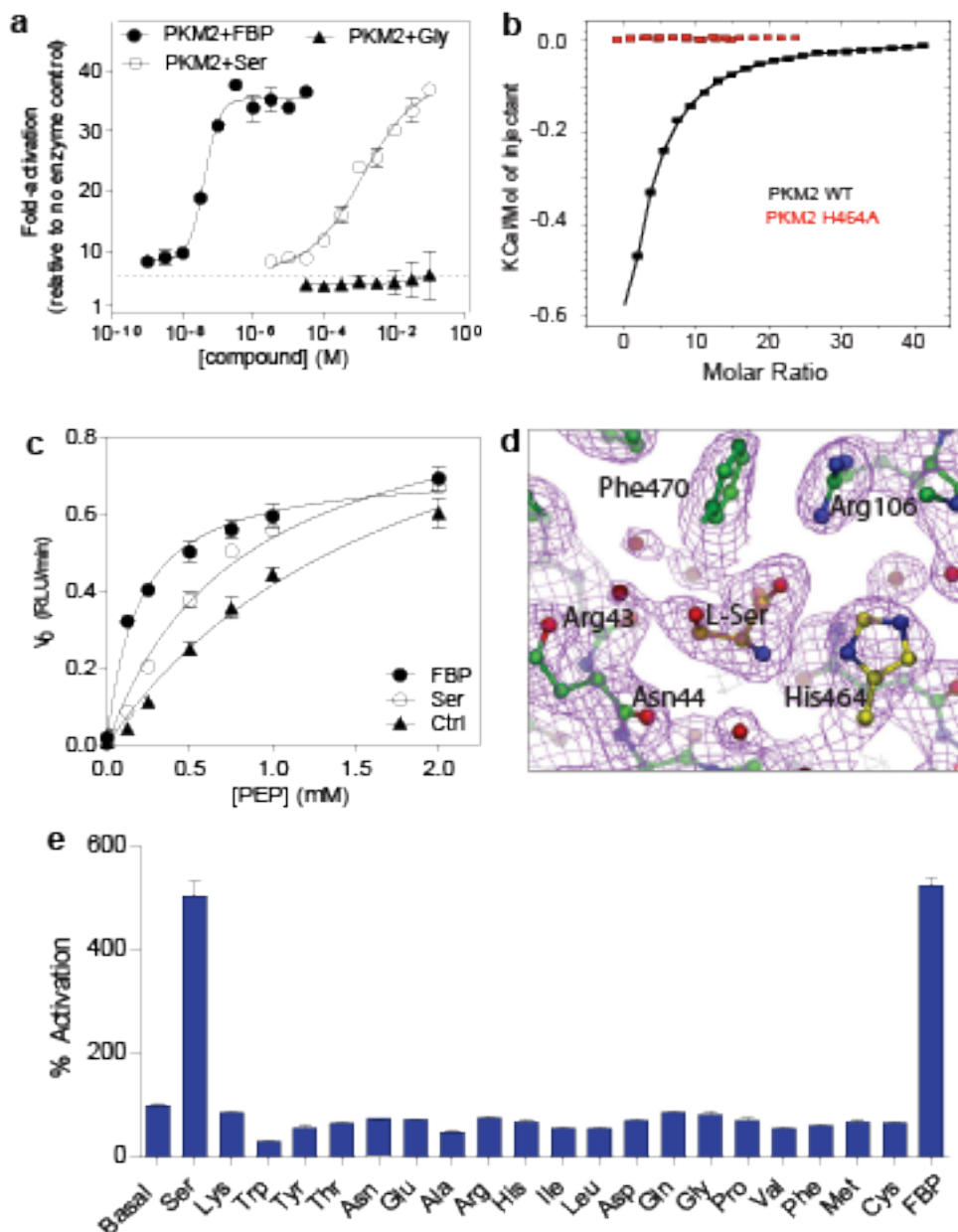


**Figure 3-3- Serine is an allosteric activator of PKM2**

**a**, *In vitro* activity of recombinant human PKM2 was analysed in the presence of increasing concentrations of FBP (●), serine (○) or glycine (▲). **b**, Serine binding to PKM2 wild-type or H464A mutant was measured by isothermal titration calorimetry. The  $K_d$  of serine for wild-type PKM2 was measured as 200  $\mu$ M. No serine binding to H464A PKM2 was detected. **c**, The initial PKM2 reaction ( $V_0$ ) was measured at different PEP concentrations in the presence of 50  $\mu$ M FBP (●), 100  $\mu$ M Serine (○) or vehicle (▲).  $K_m$  values for PEP were determined as 1.9 mM, 0.81 mM and 0.19 mM in the presence of vehicle, serine and FBP, respectively. For **a** and **c**, results are from 3 independent experiments and are presented as mean  $\pm$  s.e.m. FBP, fructose-1,6-bisphosphate. **d**, 2.3 $\text{\AA}$  2Fo-Fc map (purple) contoured at  $1\sigma$  for the final, refined, structure of L-ser (orange) bound to PKM2 (green). The side chain of His464, which was subsequently mutated to alanine, is shown in yellow. **e**, PKM2 activity was measured *in vitro* in the presence of 10 mM of each of the 20 standard amino acids, 50  $\mu$ M FBP or no compound (basal). The signal was normalised to controls containing no enzyme. Data are presented as the mean  $\pm$  s.e.m. of quadruplicates. For **a**,

the signal was normalised to controls containing no enzyme. The basal activity of PKM2 in the presence of vehicle control is indicated by the dotted line. Data are presented as mean  $\pm$  s.e.m. of duplicate determinations and are representative of three independent experiments.

### **3.2.4 PKM2 activation by serine is independent of FBP and does not require tetramerization**

We have shown that serine is able to bind and activate PKM2 via an amino acid-binding pocket present in each PKM2 monomer and as such, it can regulate the usage of glucose carbons for either energy generation or biosynthesis. The molecular mechanism underlying allosteric regulation of PKM2 by serine is, however, poorly understood, especially concerning the ability of serine to induce a switch in the oligomerization state. While it is known that activation of PKM2 by FBP is achieved by a conformational change from a dimer (inactive) to tetramer (active), serine binds to a completely different site of the protein and may not be able to influence PKM2 oligomerization in the same way as FBP. Therefore, we decided to study the biophysics of PKM2 activation by looking at the effect of serine on its oligomeric state by high-pressure liquid chromatography- size exclusion (HPLC-SEC). For this purpose, human recombinant PKM2 proteins were produced and purified. These include, WT PKM2, the H464A mutant that cannot bind serine and the S437Y mutant that cannot bind FBP. We also looked at the effect of these mutations on the enzymatic activity in the absence of activators and in response to increasing concentrations of serine or FBP.

#### **3.2.4.1 *In vitro* activity**

We investigated the *in vitro* activity of WT PKM2, H464A-PKM2, S437Y-PKM2 and PKM1 recombinant proteins in the presence of increasing concentrations of serine or FBP using a luminescent assay (Fig. 3:4a-d). In response to increasing concentrations of serine and FBP, WT PKM2 achieves an approximately 4-fold activation compared to baseline enzyme activity (Fig. 3:4a). H464A-PKM2 achieves an approximately 7-fold activation compared to baseline in the presence of FBP, and approximately 3.5-fold activation in the presence of serine (Fig. 3:4b). S437Y-PKM2 enzyme is unresponsive to FBP, but achieves approximately 3.5-fold activation in the presence of serine (Fig. 3:4c). PKM1 activity is not induced by either serine or FBP (Fig. 3:4d).

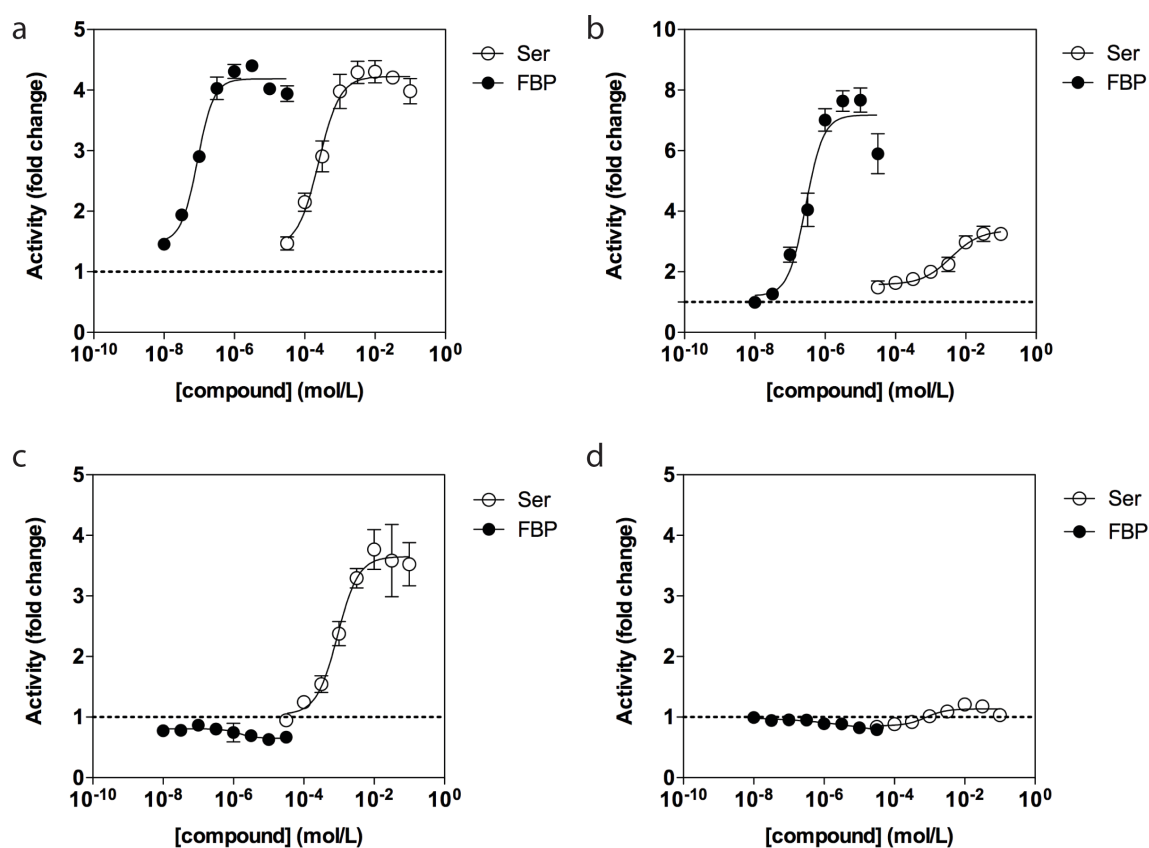


**Figure 3-4- *In vitro* effects of serine and FBP on PKM2 activity**

**a-d,** *In vitro* activity of purified recombinant human wild type PKM2 (a), mutant H464A (b), S437Y (c) and constitutively active PKM1 (d) proteins in the presence of increasing concentrations of FBP (●), serine (○). The basal activity of PKM2 in the presence of vehicle control is indicated by the dotted line. Data are presented as mean  $\pm$  s.e.m. of duplicate determinations and are representative of three independent experiments.

### 3.2.4.2 Conformational analysis by UV HPLC-SEC

The conformational changes of WT PKM2 and mutant proteins in the presence of increasing concentrations of serine and FBP were investigated using HPLC-SEC (Fig. 3:5a-c). WT PKM2 is predominantly in a dimeric conformation when no activator is present but gradually changes conformation towards a tetramer in the presence of increasing concentrations of serine. At a concentration of 5 mM of serine, the enzyme is predominantly tetrameric. Similarly, when 250  $\mu$ M FBP is added, the enzyme is entirely tetrameric (Fig. 3:5a). For the H464A mutant, the presence of increasing concentrations of serine had very little effect on the initial oligomeric distribution of the protein compared to WT PKM2. Initially the H464A mutant presents the same pattern in that at a concentration of 5 mM serine (roughly half of the protein is in a tetrameric conformation) and this does not change dramatically by the addition of 50 mM of serine, whereas full tetramerization is achieved by the addition of 250  $\mu$ M FBP (Fig. 3:5b). For the S437Y mutant, no substantial changes in oligomerization state can be detected and the enzyme remains in its dimeric conformation regardless of the addition of increasing concentrations of serine or FBP (Fig. 3:5c).

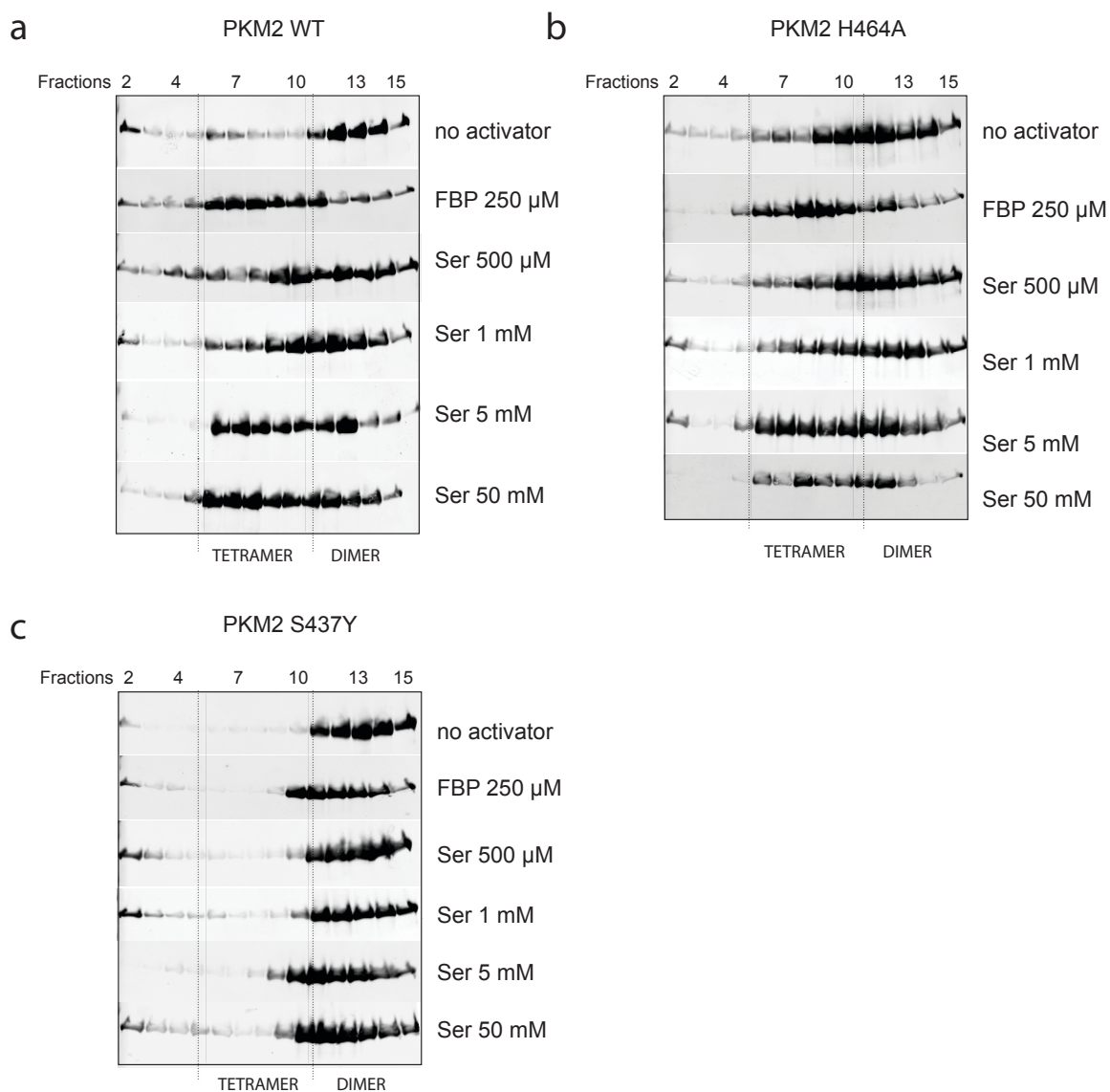


**Figure 3-5- Oligomeric state of PKM2 in the presence of serine or FBP**

**a-c**, Western blot against PKM2 showing the indicated UV HPLC-SEC fractions for PKM2 WT, H464A-PKM2 and S437Y-PKM2 in the absence and presence of increasing concentrations FBP and serine (from top to bottom). The dotted lines delimit the fractions corresponding to tetramer and dimer.

### 3.3 Conclusions

We have identified the conditionally essential amino acid L-serine to be a natural ligand of human PKM2 through the presence of a serine-binding pocket in the enzyme. Our results provide new understanding of the relationship between glucose and amino acid metabolism in cancer cells. Serine biosynthesis is an essential anabolic pathway that supports growth and proliferation(201). However, it takes away glucose-derived carbons that are important for energy production. Therefore, a tight control of the metabolic bifurcations of glycolysis is needed. We have demonstrated for the first time that serine regulation on PKM2 activity provides an important gatekeeping function. When serine is abundant, PKM2 is fully active enabling the production of energy from glucose. However, when the steady-state levels of serine drop below a critical point, an immediate abruption of PKM2 activity occurs, enabling the shuttling of glucose-derived carbons into serine biosynthesis, hence replacing the shortfall in serine supply. By regulating PKM2, serine controls the fate of pyruvate in cells, supporting aerobic glycolysis and lactate production, events that are required for cancer cell growth and survival. In addition, we have demonstrated that serine is able to fully activate PKM2 by inducing its tetramerisation in a dose dependent manner and independent of the presence of FBP.

## **Chapter 4 - Changes in Glucose Metabolism Related to Oncogene-Induced Senescence (OIS)**

## 4.1 Introduction

In recent years, a large body of compelling evidence has shown that oncogene induced- senescence (OIS) acts as a pathophysiologic mechanism suppressing cancer in model systems and humans. Indeed, senescence biomarkers have been reported for a plethora of precancerous lesions including pulmonary adenomas, prostate intraepithelial neoplasia, lymphomas and mammary tumours(202). In these settings, a mutation commonly sparks the activation of an oncogene or loss of a tumour suppressor, initiating a programme that contributes to the formation of a benign lesion. The senescent response manifests after an initial phase of cell proliferation, halting further expansion. Progression towards malignancy can occur only in the context of additional tumorigenic alterations.

Several oncogenic and tumour suppressor pathways are linked to senescence, suggesting that it must, somehow, be mechanistically connected to metabolic dysregulation. Indeed, emerging evidence indicates that p53, which modulates glucose utilization and mitochondrial respiration via the transcriptional control of TIGAR and SCO2, contributes to certain types of OIS (15, 203). Despite the belief that senescent cells remain metabolically active, this matter has not been investigated in detail(204). Therefore, we decided to study the regulation of metabolism in OIS using metabolic flux profiling to screen, in an unbiased fashion, for metabolic changes accompanying OIS. Furthermore, on the basis of the profiles obtained, we studied the contribution of key metabolic enzymes to OIS.

## 4.2 Results

### 4.2.1 BRAF<sup>V600E</sup>-induced senescence increases mitochondrial glucose metabolism

We compared the energy metabolism of human diploid fibroblasts (HDF) undergoing OIS to cycling HDF by studying the metabolic fate of glucose, the primary energy source for cells (205, 206). To study this, we incubated cycling HDF cells and HDF cells overexpressing oncogenic BRAF<sup>V600E</sup>, which has been previously demonstrated to be a strong inducer of OIS(207), with medium containing fully labelled <sup>13</sup>C<sub>6</sub>-glucose for several time points, after which, intracellular metabolites were extracted for metabolomic analysis by LC-MS. The isotopomeric profile showed that <sup>13</sup>C<sub>6</sub>-glucose was quickly incorporated into glycolysis and the TCA cycle. Glycolytic intermediates were fully labelled with either three or six carbons, while the TCA cycle metabolites were mainly labelled with two carbons (derived from acetyl- CoA after the decarboxylation of pyruvate). Several glucose-derived metabolites were measured over time (Fig. 4:1) and a sharp increase in the flux into the TCA cycle was detected in OIS cells when compared to cycling cells (Fig. 4:1). In OIS cells, glucose-derived carbons accumulated faster in TCA cycle intermediates (citrate, α-ketoglutarate and malate), and to a much higher extent than in cycling cells. The same was observed for glucose derived 2-carbon-labeled glutamate, which results from the transamination of α-ketoglutarate (Fig. 4:1). The levels of labeled glycolytic intermediates (G3P and PEP) did not vary between OIS and cycling cells, demonstrating that the flux through glycolysis towards pyruvate remained equal. In addition, as there is enhanced TCA flux in OIS cells, less glucose-derived pyruvate was available, resulting in a decrease in 3-carbon-labeled alanine and lactate (Fig. 4:1).

As the TCA cycle fuels the respiratory chain in the mitochondria, we next determined whether the enhanced flux through the TCA cycle in OIS correlates with an increase in respiration by measuring mitochondria-dependent OCR. Consistent with an increase in TCA flux, OIS cells displayed a significant increase in OCR (Fig. 4.2). We conclude from this metabolic profile that OIS is accompanied by an enhanced flux of glucose-derived carbon into the TCA cycle and increased respiration.

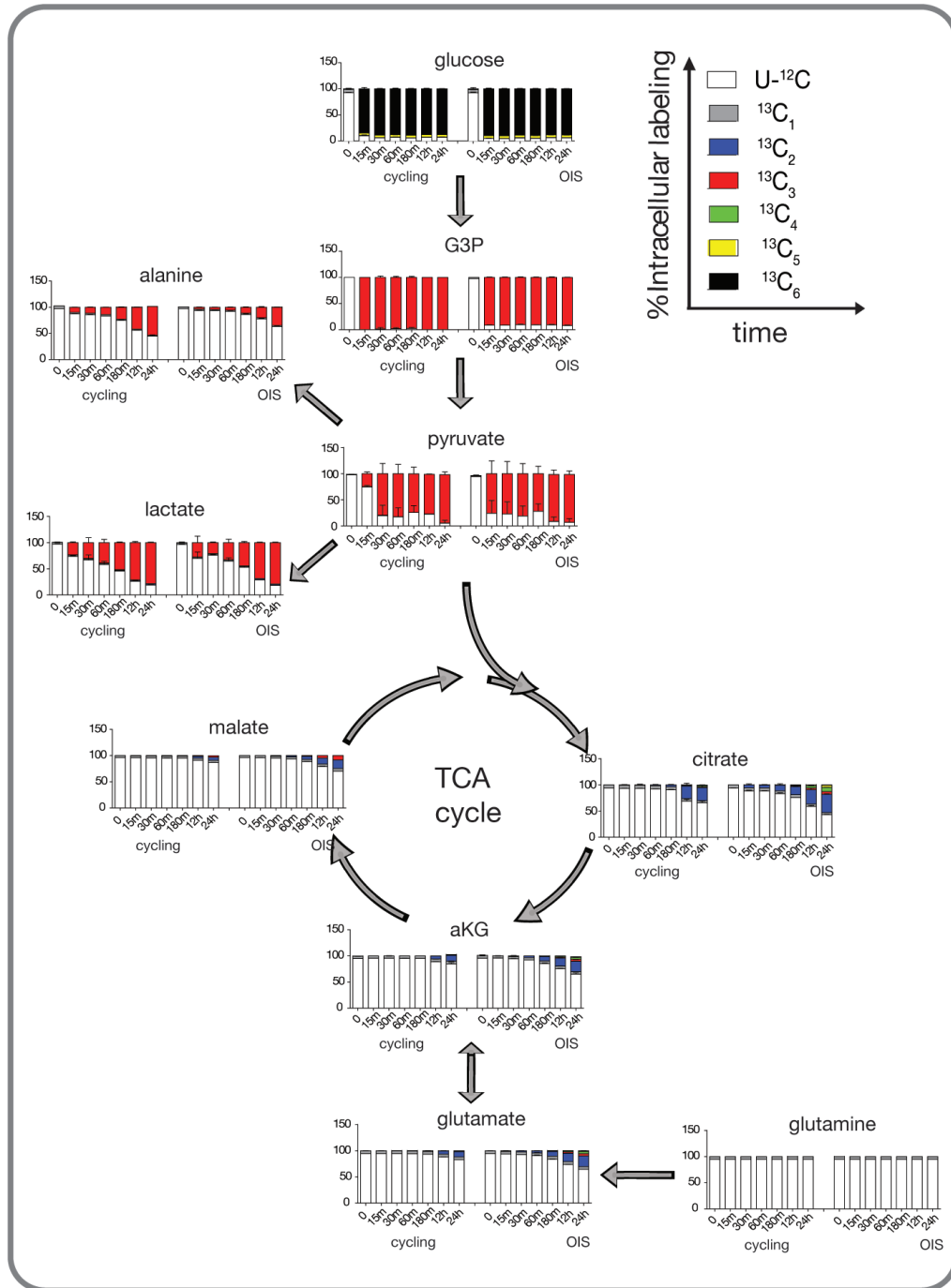


**Figure 4-1- Glucose metabolism in BRAF<sup>V600E</sup>-induced senescence**

Glucose metabolism analysis in cycling HDF and BRAF<sup>V600E</sup> OIS cells upon incubation with uniformly labelled <sup>13</sup>C<sub>6</sub>-glucose for the indicated time points (15 min to 24 hr). The results show the isotopomer distribution (U-<sup>12</sup>C, <sup>13</sup>C<sub>1-6</sub>) for each individual metabolite. All data are represented as mean ± s.d. (n=3). G3P – glyceraldehyde 3-phosphate; aKG – α-ketoglutarate; TCA – tricarboxylic acid cycle.

## 4.2.2 Mass balance analysis

Tomer Shlomi and Vitaly Selivanov performed the calculations and built the computational model.

In order to understand the potential metabolic alterations taking place during OIS, we delineated a mass-balance model utilizing the measured exchange rates of glucose, lactate, glutamine and glutamate as well as that of pyruvate and alanine. Furthermore, the biosynthetic constraint of proliferating cells was translated to the required rate of production and utilization of amino acids, fatty acids and nucleotides. The doubling time of the cycling cells studied is 24 hours and the measured protein concentration is  $165 \mu\text{g}/10^6$  cells. Based on these observations and assuming (for simplicity) there is equal distribution of amino acids in proteins and an average molecular weight of an amino acid of 146 g/mol, we calculated that the required rate for protein synthesis of key amino acids, which are either absent in the medium or directly derived from reactions in the model (alanine, aspartate, asparagine, glutamine and glutamate) to be  $2.3 \text{ nmol}/(10^6 \text{ cells} \times \text{hour})$ . Assuming that the dry mass of cells consists of approximately 60% proteins, 20% lipids and 15% nucleotides [See (1)] and the molecular weight of palmitate (as a readout for fatty acids) is 256 g/mol, the average molecular weight of nucleotides (monophosphate) is 340 g/mol, the rates of lipid (as palmitate equivalents) and nucleotide accumulation as biomass in proliferating cells were calculated to be  $8.8 \text{ nmol}/(10^6 \text{ cells} \times \text{hour})$  and  $5.0 \text{ nmol}/(10^6 \text{ cells} \times \text{hour})$  respectively. Finally, OCR was measured and utilized in this model to account for the oxidation rate of NADH (2 mol NADH per mol  $\text{O}_2$ ) produced in all the studied reactions. These measured and estimated fluxes were fitted into a central carbon metabolism model (Fig. 4:2) and the best possible way to balance those metabolic rates in one consistent model was calculated. Due to the multiple ways to transfer electrons between mitochondrial and cytosolic NAD(P)H/FADH<sub>2</sub>, a single pool representing all of the latter metabolites was assumed. The production (reduction) rate of these reducing equivalents was fitted into all the known reactions in the model (glycolysis, pentose phosphate pathway, malic enzyme and the TCA cycle).

Based on fitting all the above parameters, the mass balance analysis made several predictions:

(1) Glutamine utilization in cycling cells is sufficient to account for the required biosynthesis of pyrimidines and amino acids, which are either derived directly from glutamine (and glutamate) or from the TCA cycle (aspartate and asparagine). In contrast, OIS cells produce and secrete more glutamate from glucose (no net glutaminolysis) and therefore, require active pyruvate carboxylase to support anaplerosis. Indeed, when cells were incubated for 24 hours in uniformly labelled  $^{13}\text{C}_6$ -glucose, and heavy  $^{13}\text{C}$ -isotopes were traced in different metabolites, it was evident that more glutamate was derived from glucose in OIS cells as compared to cycling cells. Moreover, citrate was labelled with 3 and 5  $^{13}\text{C}$  carbons, indicating greater pyruvate carboxylase activity in OIS cells (Fig. 4:2).

(2) The mass balance analysis calculated a large increase in the rate of pyruvate oxidation by PDH in the mitochondria during OIS (Fig. 4:2). Indeed, an increase in OCR during OIS was measured, yet this was insufficient to account for complete oxidation of the excess pyruvate in the mitochondria. Therefore, it was predicted that the citrate/malate shuttle would remove excess acetyl-CoA to the cytosol to be used for fatty acid biosynthesis (calculated in palmitate equivalents). Interestingly, the mass balance predicted that the rate of *de novo* palmitate synthesis in cycling cells is insufficient to support the level of lipid biosynthesis required to sustain the measured proliferation rate and hence cycling cells will require a net uptake of exogenous fatty acids. On the other hand, the higher rate of palmitate production in OIS would require fatty acid secretion. These predictions were experimentally confirmed by LC-MS analysis of extracellular palmitate, oleate and stearate (Fig. 4:2).

To compute the difference in PDH flux between the OIS and cycling cells while accounting for experimental error in the measurement of metabolite uptake and secretion rates, we assumed a Gaussian noise model for each uptake and secretion measurement (considering the experimental mean and standard deviation in uptake and secretion flux measurements). The standard deviation and confidence interval of PDH flux were calculated based on a linear combination of normal distributions. The expected difference in PDH fluxes (presented as  $\text{nmol}/10^6$  cells  $\times$  hour) between OIS and cycling cells are:

OIS: PDH = 307.570

std = 79.937 95% CI = [176.085, 439.055]

Cycling: PDH = 63.050                      std = 43.106 95% CI = [-7.853, 133.953]

PDH difference = 244.520                  std = 90.819 95% CI = [95.136, 393.904]

Metabolic fluxes, which were not measured directly, were determined based on fitting the measured distribution of  $^{13}\text{C}$ -isotopomers of intracellular and secreted metabolites by the isotopomer dynamics method(208). This method is based on the simulation of isotopomer distribution dynamics and does not require reaching isotopic steady state. Application of this method was justified by the measured slow dynamics of metabolite labelling. The model consists of a system of ordinary differential equations describing the time course of concentrations of all the measured isotopomers. The algorithms for data fitting and determination of confidence intervals for metabolic fluxes are described in de Mas et al. (209).

As the secreted lactate, pyruvate and alanine with respect to consumed glucose is less in OIS cells compared to cycling cells, the former convert much more pyruvate into acetyl-CoA via PDH, followed by citrate synthesis. This is clearly demonstrated by the fact that OIS cells have higher concentration of citrate, which is labelled faster than in cycling cells (Fig. 4:2). The intervals calculated for cycling and OIS cells are based on fitting the measured fluxes and distribution of isotopomers using  $\chi^2$  (sum of normalized squared deviation between measured and computed data) criterion as described by de Mas et al., 2011. Oxygen consumption is calculated as the combined metabolic rates of PDH + (aKG  $\rightarrow$  Mal) + (Cit  $\rightarrow$  aKG)/2 + MDH/2. This calculation takes into account that conversion of 1 mol of glyceraldehyde-3-phosphate into acetyl-CoA results in the reduction of 2 mol of NAD<sup>+</sup> into NADH (one by GAPDH in the cytosol and another by PDH); further conversion in combined reactions (aKG  $\rightarrow$  Mal) result in 1 mol NADH and 1 mol reduced FAD; the reactions (Cit  $\rightarrow$  aKG) and MDH result in reduction of 1 mol NAD<sup>+</sup> each. Oxidation of 2 mol NADH or FADH<sub>2</sub> results in the reduction of one mol of oxygen.

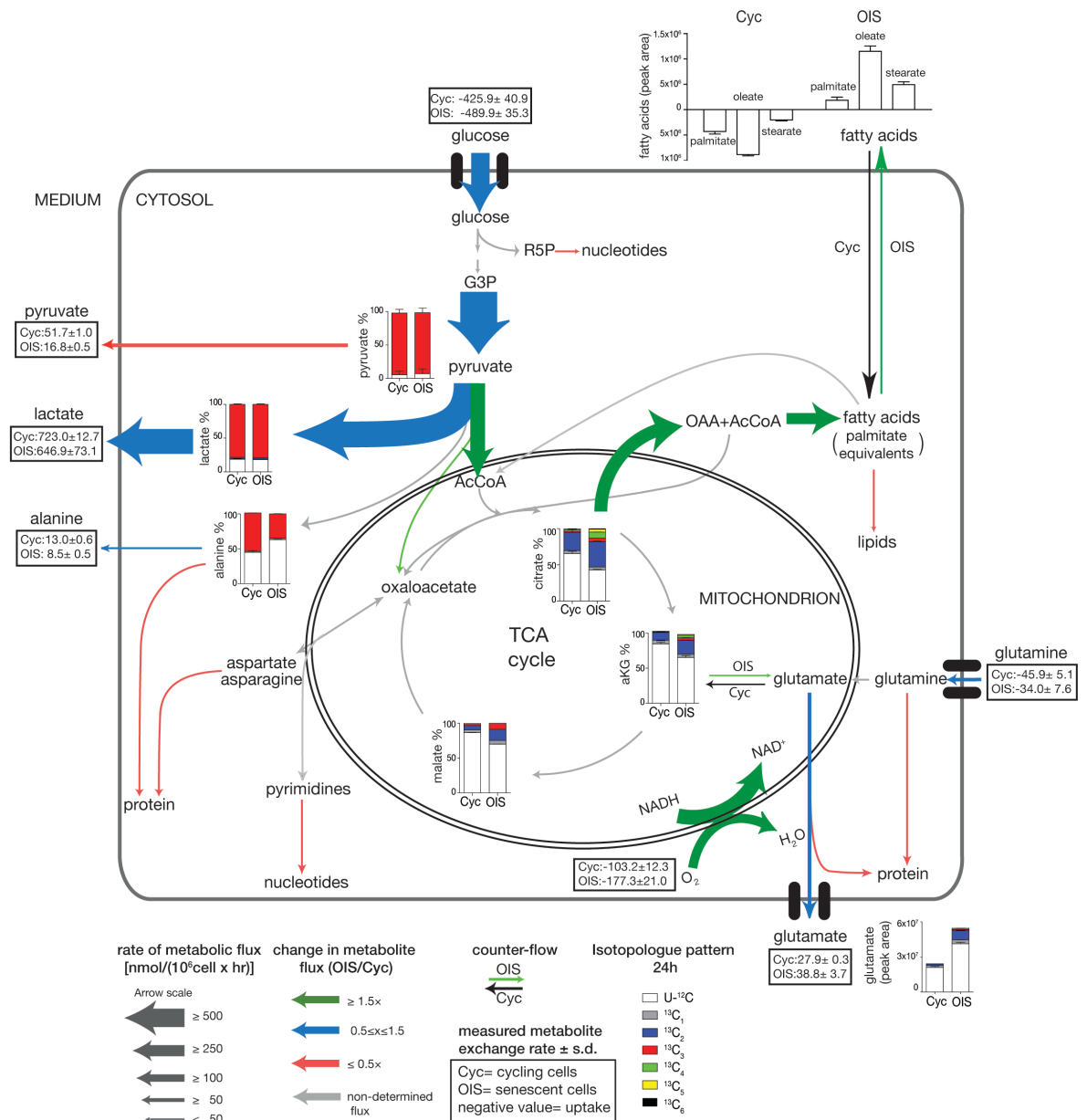


**Figure 4-2- Metabolic model for concerted activation of PDH necessary to drive OIS**

In response to an oncogenic trigger (BRAF<sup>V600E</sup>), primary cells up-regulate PDP2 and down-regulate PDK1, causing the activation of PDH, the gatekeeper enzyme linking glycolysis and the TCA cycle. Its activation during OIS promotes the flux of glucose-derived pyruvate to the TCA cycle, increasing cellular respiration and representing an essential element of the OIS program. Enforced normalization of PDP2 or PDK1 expression levels abrogates OIS, reactivating cell proliferation.

### 4.2.3 Effect of K-RAS<sup>G12V</sup>-induced senescence on glucose metabolism

We then went on and performed the same metabolic analysis using <sup>13</sup>C<sub>6</sub>-glucose in HDF overexpressing K-RAS<sup>G12V</sup> and obtained comparable results to the ones observed in cells undergoing BRAF<sup>V600E</sup>-induced senescence. K-RAS<sup>G12V</sup>-senescent cells have an increased rate of accumulation of glucose-derived carbons into TCA cycle metabolites compared to cycling cells (Fig. 4:3). However, this is less pronounced than in BRAF<sup>V600E</sup>-induced senescence. Therefore, this oxidative phenotype is not unique to BRAF<sup>V600E</sup>-induced senescence, but rather are characteristic of the senescent status.

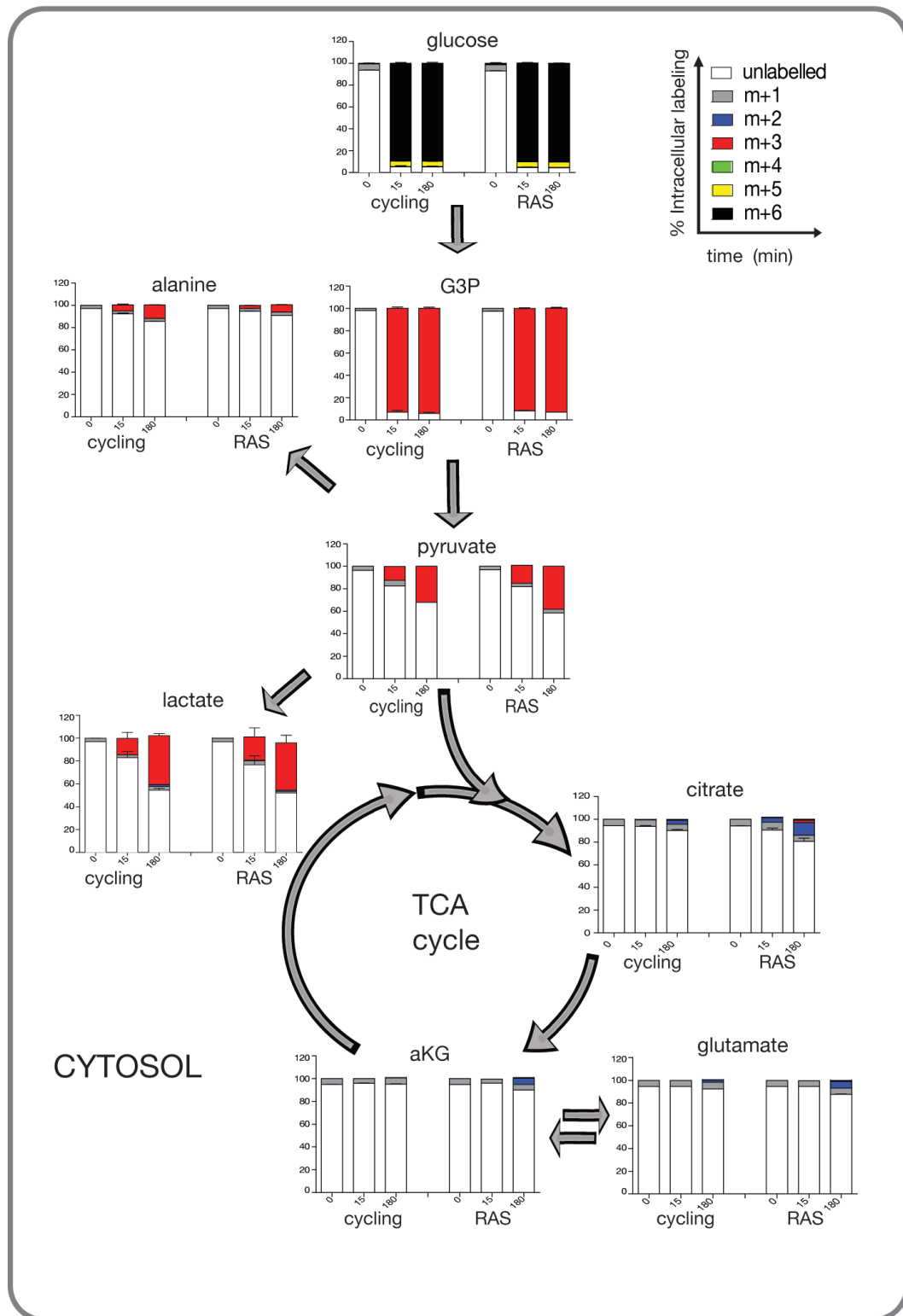


**Figure 4-3- Glucose metabolism in K-RAS<sup>G12V</sup>-induced senescence**

Glucose metabolism analysis in cycling HDF and K-RAS<sup>G12V</sup> OIS cells after 0, 15 and 180 minutes of labelling with <sup>13</sup>C<sub>6</sub>-glucose. Results show the distribution of the different isotopomers (U-<sup>12</sup>C, <sup>13</sup>C<sub>1-6</sub>) of each metabolite presented over time. All data are represented as mean ± s.d. (n=3). G3P – glyceraldehyde 3-phosphate; aKG – α-ketoglutarate; TCA –tricarboxylic acid cycle.

#### 4.2.4 Effect of cell cycle arrest on glucose metabolism

To identify whether the changes in glucose metabolism upon OIS were due to a block in proliferation, characteristic of the senescent state, or part of a particular set of features that characterize the senescent phenotype, quiescent cells (obtained through contact inhibition of HDF and confirmed by BrdU incorporation) were also fed with  $^{13}\text{C}_6$ -glucose. However, unlike senescent cells, quiescent cells accumulated  $^{13}\text{C}_6$ -glucose-derived carbons faster into pyruvate and alanine as well as into TCA cycle intermediates like citrate and glutamate, compared to proliferating cells (Fig. 4:4). This labelling pattern indicates an overall increase in cell metabolism during quiescence, unlike the specific increase in glucose-driven TCA metabolism observed during senescence. In addition, a similar increase in metabolic activity in quiescent fibroblasts has also been previously described(210).

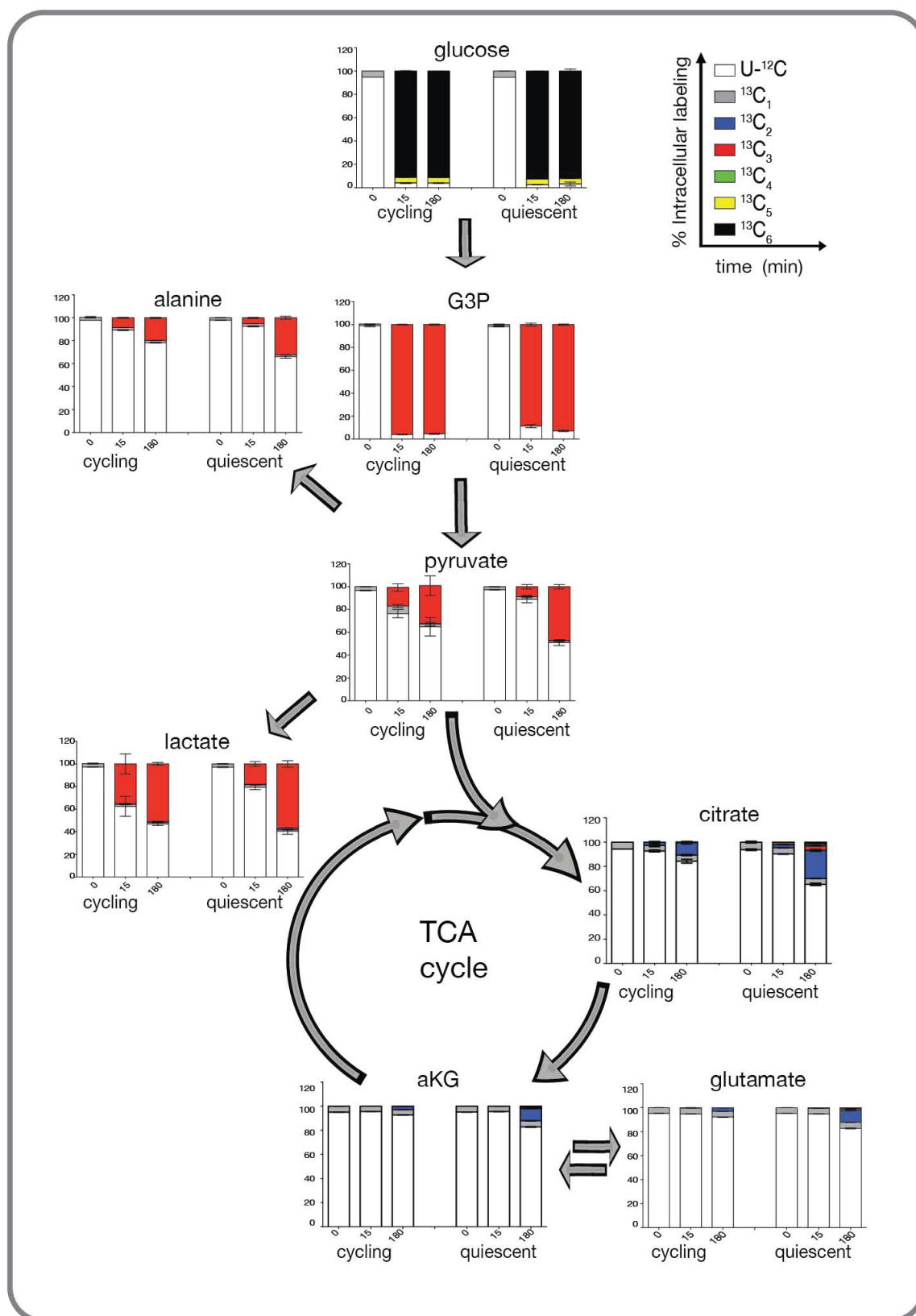


**Figure 4-4- Glucose metabolism in quiescent cells**

Comparison of the glucose metabolism in quiescent and cycling HDF analysed after 0, 15 and 180 minutes of labelling with  $^{13}\text{C}_6$ -glucose. Results show the distribution of the different isotopomers ( $\text{U-}^{12}\text{C}$ ,  $^{13}\text{C}_{1-6}$ ) of each metabolite presented over time. Data are represented as mean  $\pm$  s.d. ( $n=3$ ). G3P – glyceraldehyde 3-phosphate; aKG –  $\alpha$ -ketoglutarate; TCA –tricarboxylic acid cycle.

## 4.3 Conclusions

In recent years, the study of the deregulation of cellular metabolism during oncogenic transformation has received increasing interest. The development of sensitive analytic tools to monitor metabolism in living cells has allowed us to increase our understanding of metabolic regulation. However, despite the widely recognized importance of OIS as a tumour suppressive mechanism, little is known about the regulation and role of cellular metabolism in this context, in particular, how metabolic fluxes change when cells undergo OIS and whether they are functionally connected to the senescent programme.

In order to solve this question, we performed an unbiased and comprehensive analysis of the metabolic fluxes in cells undergoing OIS. Our results revealed that a profound switch in metabolic fluxes accompany the establishment of OIS. In OIS, glucose, the primary energy source for these cells, was primarily oxidized in the TCA cycle following its conversion to pyruvate, which was associated with increased mitochondrial respiration. Furthermore, we identified PDH, the enzyme linking glycolysis and TCA cycle, as the central component of this switch. During OIS, PDH activation drives pyruvate into the TCA cycle for oxidation at the expense lactate and alanine production. Finally, we demonstrated that this process is not mere consequence of a block in proliferation, as quiescent cells do not have the same metabolic phenotype.

## **Chapter 5 - Resistance to BRAFV600E Inhibition Induces Glutamine Dependency in Melanoma Cell Lines**

## 5.1 Introduction

Melanoma is a heterogeneous disease with multiple subtypes driven by specific genetic alterations. About half of cutaneous melanomas possess the BRAF<sup>V600E</sup> mutation that results in the constitutive activation of the MAPK signalling pathway(211-213). The recently developed specific BRAF<sup>V600E</sup> inhibitors vemurafenib and dabrafenib improve the overall survival of patients harbouring mutant BRAF melanoma by 6-8 months(214, 215). Unfortunately, intrinsic, and secondary or acquired resistance limits the overall response rate as well as the therapeutic benefit of this personalised treatment(216-220). Although most of these studies have focused on cancer-specific alterations in kinases or transcription factors, it has recently emerged that metabolic rewiring can also contribute to such resistant phenotypes(221, 222).

It has been described that melanoma cells display aerobic glycolysis and use glutamine for anaplerosis(223, 224). Recent studies have also identified the microphthalmia-associated transcription factor (MITF)/ peroxisome proliferator-activated receptor gamma coactivator 1- $\alpha$  (PGC1 $\alpha$ ) axis to be responsible for the oxidative metabolism displayed by certain melanomas and that MAPK activity suppresses this oxidative phenotype(225, 226). Moreover, vemurafenib-resistant cell lines display increased mitochondrial respiration, which makes them more vulnerable to oxidative stress-induced cell death(227). Therefore, understanding the metabolic response and adaptive mechanisms in melanoma towards targeted therapies could assist in identifying key targets to use in combined therapeutic strategies in order to prevent the onset of resistance or how to overcome it. In this study, we examined the metabolic consequences upon BRAF<sup>V600E</sup> inhibition that result in (or support) the acquisition of resistance in melanoma cells.

## 5.2 Results

This work was done in collaboration with Franziska Baenke at the Cancer Research UK Manchester Institute.

### 5.2.1 BRAF<sup>V600E</sup> inhibition stimulates mitochondrial biogenesis and oxidative metabolism

In order to study the metabolic changes that occur upon BRAF<sup>V600E</sup> inhibition, we utilised an analogue of vemurafenib, the BRAF<sup>V600E</sup> inhibitor commonly used for melanoma treatment, named PLX4720. We generated PLX4720 resistant cell lines (hereof PLX-resistant) from the well established BRAF<sup>V600E</sup>-expressing melanoma cell lines A375 and Colo829, by continuously culturing them in the presence of 1  $\mu$ M PLX4720 and designated them as A375/R and Colo829/R respectively. It has been recently reported that BRAF inhibitors increase PGC1 $\alpha$  expression in melanoma cell lines(225, 226). In line with these findings, we observed a significant increase in PGC1 $\alpha$  mRNA levels in A375/R and Colo829/R cells (Fig. 5:1a). A375/R cells also have increased mitochondrial mass, as shown by the higher expression of the mitochondrial-encoded genes cytochrome B2 (CYTB2), cytochrome c oxidase subunit 2 (COXII) and ATP synthase protein 8 (ATP8) (Fig. 5:1b). Furthermore, in A375/R and Colo829/R cells, basal and maximal oxygen consumption rates (OCR) were significantly higher compared to parental cells with a consistent decrease in extracellular acidification rate (ECAR) (Fig. 5:1c).

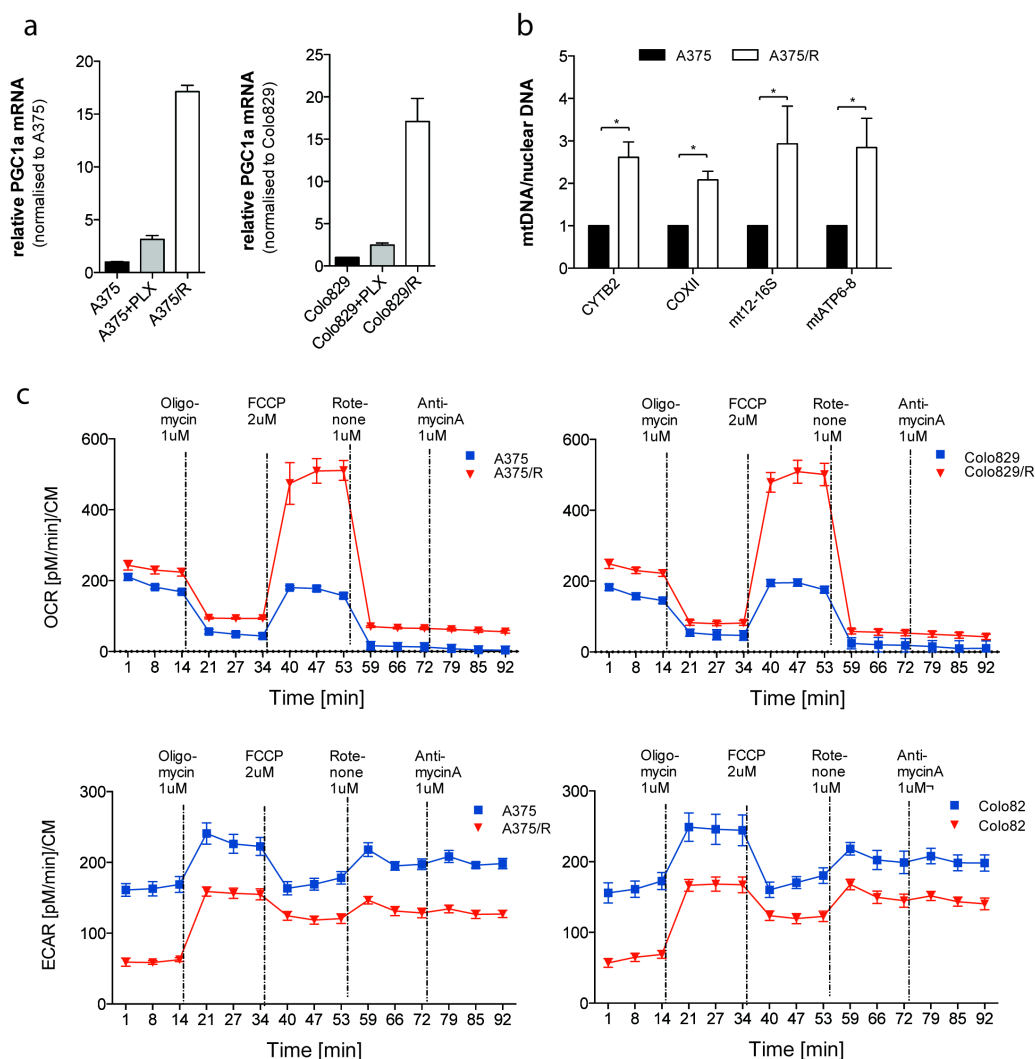


**Figure 5-1: BRAF<sup>V600E</sup> inhibition increases mitochondria and the oxidative phenotype in melanoma cell lines**

**a**, PGC1α mRNA expression levels in A375, A375/R, Colo829 and Colo829/R melanoma cell lines in the absence or presence of 1 μM PLX4720 for 24 hours. **b**, Comparison of mitochondrial encoded genes CYTB2, COXII and mtATP6-8, normalised to nuclear encoded genes in A375 ± 1 μM PLX4720 and A375/R for 24 hours (mean ± SEM of n=3) (N=2) \*p<0.05, \*\*p<0.01 and \*\*\*p<0.001. **c**, Oxygen consumption rate (OCR) and extracellular acidification rate (ECAR) in A375, A375/R and Colo829 and Colo829/R cells in the absence or presence of 1 μM PLX4720 after 18 hours using the Seahorse Analyser. OCR was measured under basal conditions, followed by injections of 1 μM oligomycin, 2 μM FCCP, 1 μM rotenone and 1 μM antimycin A. Raw values were normalised to protein content. Experiments were at least performed three times. A representative experiment is shown here. Error bars represent the SEM of n=5.

### 5.2.2 BRAF<sup>V600E</sup> inhibition reduces glycolytic flux

Aerobic glycolysis is one of the most prominent features of cancer cells, which display dysregulated glucose metabolism and the associated increase in lactate secretion (9, 228). In order to explore the contribution of glucose to the oxidative phenotype of PLX-resistant cells, uniformly labelled <sup>13</sup>C<sub>6</sub>-glucose was used to trace glucose-derived intracellular metabolites. No significant effects on glycolysis were observed in parental cells treated with PLX4720 for 24 hours, whereas PLX-resistant cells had significantly lower levels of intracellular glucose and lactate (Fig. 5:2a). Furthermore, by measuring extracellular exchange rates, we confirmed that glucose consumption, and pyruvate and lactate secretion were reduced in PLX-resistant cells compared to parental cells (Fig. 5:2b).

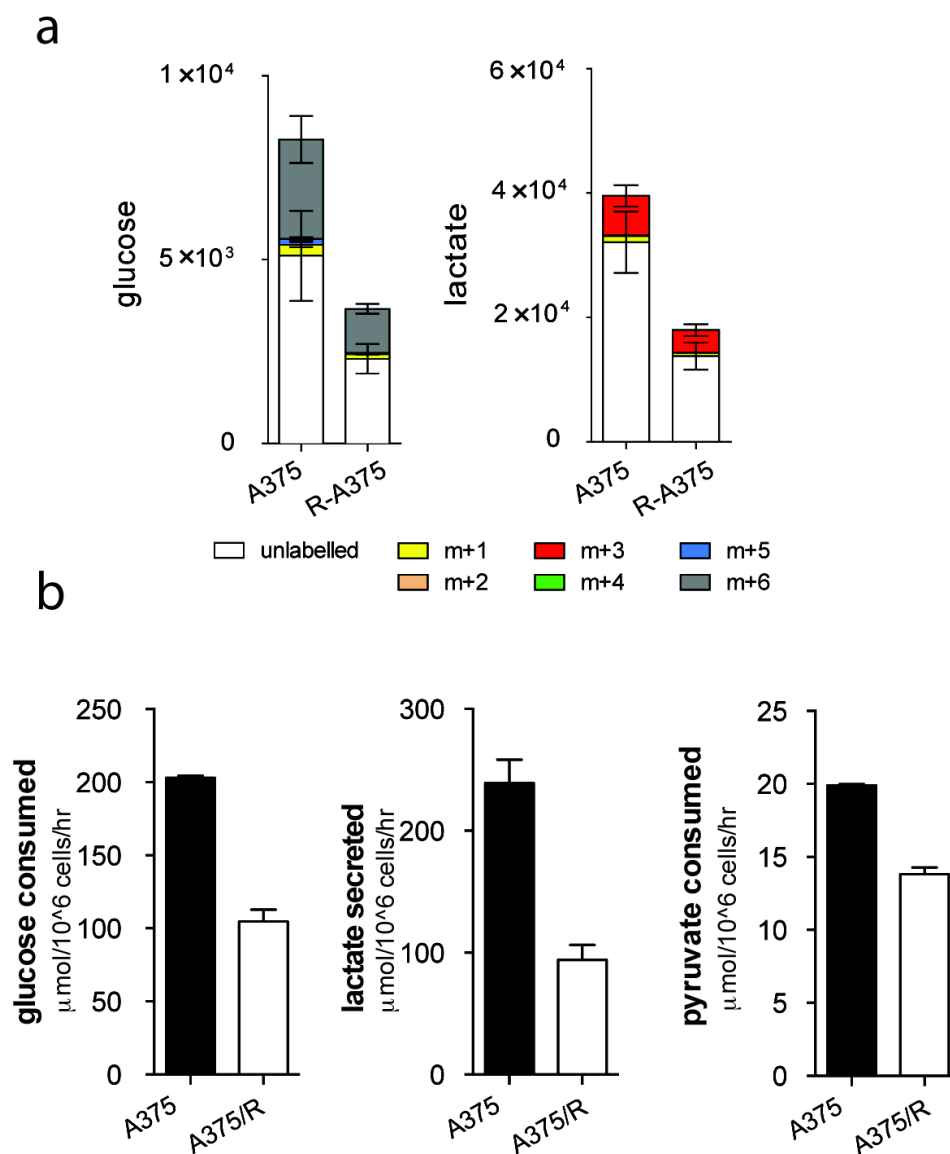


**Figure 5:2- BRAFV600E inhibition results in decreased glycolytic flux**

**a**, A375 and A375/R cells were incubated in full RPMI media with 5mM  $^{13}\text{C}_6$ -glucose for 3 hours and several intracellular glucose-derived metabolites were measured by LC-MS. The graphs show a representative experiment (mean  $\pm$  SEM of  $n=6$ ) ( $N=2$ ). **b**, Extracellular exchange rates were determined for glucose, lactate and pyruvate (mean  $\pm$  SEM of  $n=6$ ) ( $N=3$ ).

### 5.2.3 PLX4720-resistant cells display increased glutaminolysis

The observation that PLX-resistant cells were less dependent on glucose, despite showing increased oxidative metabolism, suggested the use of an alternative carbon source. Glutamine is the most abundant amino acid in the blood and it has been shown to be an important carbon as well as nitrogen source for cancer cells(146, 229). In order to analyse the glutamine-derived carbon flux, cells were cultured with uniformly labelled  $^{13}\text{C}_5$ -glutamine for 24hr and intracellular metabolites were extracted and analysed by LC-MS. Higher intracellular levels of  $^{13}\text{C}_5$ -glutamine and  $^{13}\text{C}_5$ -glutamate were detected in PLX-resistant cells (Fig. 5:3a). By measuring extracellular exchange rates for glutamine and glutamate, we also confirmed an increase in glutamine uptake in PLX-resistant cells as well as increased glutaminolytic activity as shown by increased glutamate secretion (Fig. 5:3b). Many oncogenic events are associated with an elevated expression of genes involved in glutaminolysis(229). By qPCR we confirmed that the mRNA levels of glutaminases (GLS and GLS2) and glutamic pyruvate transaminases (GPT and GPT2) were elevated in PLX-resistant cells (Fig. 5:3c). Together, these results demonstrate that glutamine is an important carbon source for PLX-resistant cells.

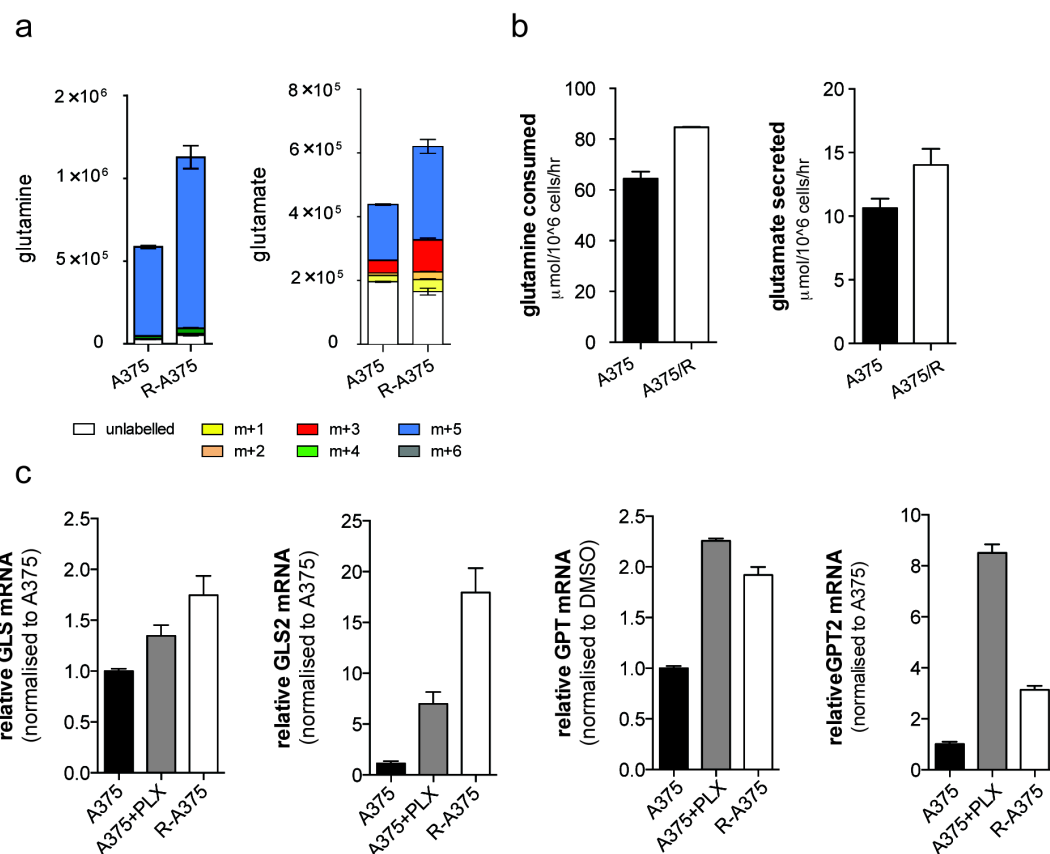


**Figure 5-3- PLX4720-resistance increases glutamine metabolism**

**a**, A375 and A375/R cells were incubated with  $^{13}\text{C}_5$ -glutamine, and intracellular glutamine and glutamate levels were determined. The graphs show a representative experiment (mean  $\pm$  SEM n=6) (N=2). **b**, Extracellular exchange rates for glutamine and glutamate were measured. Graphs show a representative experiment (mean  $\pm$  SEM of n=6) (N=3). **c**, mRNA levels of various enzymes (GLS, GLS2, GPT and GPT2) involved in glutaminolysis were determined after 24 hours of PLX4720 treatment (mean  $\pm$  SEM n=3) (N=3). \*p<0.05, \*\*p<0.01, \*\*\*p<0.001 and n.s. = not significant.

#### **5.2.4 Inhibition of glutaminolysis sensitizes PLX4720-resistant cells to PLX4720**

Given the increased glutamine metabolism displayed by PLX-resistant cells, we decided to test their dependency on glutaminolysis for survival and proliferation by treatment with the glutaminase inhibitor BPTES. BPTES did not affect the OCR in parental cells, but was significantly reduced in A375/R and Colo829/R cells (Fig. 5:4a). Furthermore, ATP levels were only decreased following the inhibition of glutaminolysis in PLX-resistant cells (Fig. 5:4b), suggesting they are unable to adapt to the inhibition of glutaminolysis and undergo an energy crisis. Indeed, the viability of PLX-resistant cells was significantly affected by glutaminase inhibition (Fig. 5:4c). In addition, BPTES-induced inhibition of proliferation is partially rescued by dimethyl- $\alpha$ -ketoglutarate, a cell-permeable analogue of  $\alpha$ -ketoglutarate that enters the TCA cycle downstream of glutaminase (Fig. 5:4c). Taken together, these findings confirm that PLX-resistant cells rely on glutamine as a major carbon source for energy production and are unable to overcome the inhibition of glutaminolysis.

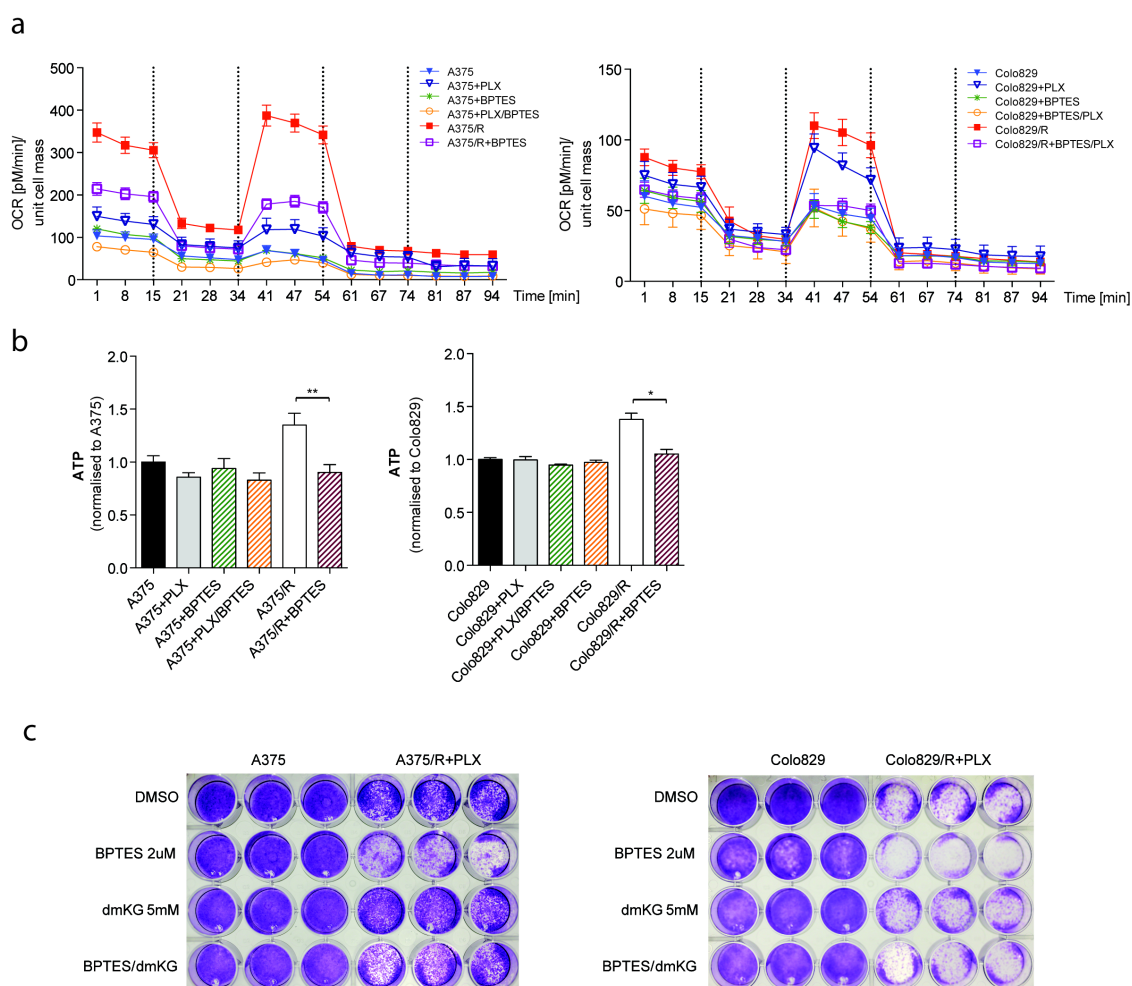


**Figure 5:4- Inhibition of glutaminolysis hampers oxidative metabolism and cell viability of PLX4720-resistant cell lines**

**a**, Measurement of oxygen consumption rate (OCR) in A375, A375/R, Colo829 and Colo829/R cells in the absence or presence of 1  $\mu$ M PLX4720 and/or 2  $\mu$ M BPTES after 18 hours using the Seahorse Analyser. OCR was measured under basal conditions, followed by injections of 1  $\mu$ M oligomycin, 2  $\mu$ M FCCP, 1  $\mu$ M rotenone and 1  $\mu$ M antimycin A. Raw values were normalised to protein content. **b**, ATP levels were determined for A375, A375/R, Colo829 and Colo829/R treated with PLX4720 and/or BPTES. Error bars represent SEM of  $n=3$ ,  $N=2$ . \* $p<0.05$  and \*\* $p<0.01$ . **c**, Indicated parental and PLX-resistant cells were seeded at a low density either alone, in the presence of BPTES, dimethyl- $\alpha$ -KG or a combination of both, and colony formation was analysed after 10 days using crystal violet.

## 5.3 Conclusions

BRAF inhibition results in an extended overall disease-free survival in melanoma patients harbouring a BRAF<sup>V600E</sup> mutation. However, all patients eventually develop resistance to the drug and recurrence of the disease. It has previously been reported that a subset of BRAF<sup>V600E</sup> mutant melanomas display increased PGC1 $\alpha$  expression (the master regulator of mitochondrial biogenesis and function) as well as high basal oxidative phosphorylation(226) and that acute treatment with the BRAF inhibitor PLX4720 induces PGC1 $\alpha$  in melanoma cell lines(225). We have confirmed these observations and furthermore, established that PGC1 $\alpha$  is greatly upregulated in PLX-resistant cells. In addition, this is associated with a rewiring of cellular metabolic pathways as demonstrated by a decrease in glucose consumption and lactate secretion in PLX-resistant cells. A compensatory increase in glutamine consumption is also observed, which allows for the sustained high rates of mitochondrial oxidative metabolism displayed by these cells. This metabolic reprogramming in PLX-resistant cells is further accompanied by an elevated expression of the mitochondrial genes CYTB2, COXII, and ATP8, and an increase in mitochondrial mass. These changes in mitochondrial biogenesis are accompanied by an increase in both oxidative phosphorylation and in the dependence on mitochondrial function for survival. However, this did not coincide with a rise in glucose consumption. On the contrary, PLX-resistant cells were more dependent on glutamine metabolism.

By measuring metabolic exchange rates and metabolic fluxes we have shown that PLX-resistant cells display increased oxidative metabolism, which is fuelled by glutamine. Moreover, PLX-resistant cells are sensitised to PLX4720 by the inhibition of glutaminase. Our findings show that the switch from glucose to glutamine utilisation during the acquisition of resistance could provide a therapeutic strategy that combines inhibitors of mitochondrial respiration or glutamine metabolism with the use of vemurafenib for the treatment of BRAF<sup>V600E</sup> melanoma.

## **Chapter 6 - Discussion and Final Remarks**

## 6.1 Discussion

Nutrients can follow several pathways to ultimately produce energy as ATP or anabolic constituents for cell growth. In malignant cells, they are preferentially utilised to maintain uncontrolled cell growth. Several alterations within the complex metabolic network of mammalian cells seem to be associated with tumorigenesis, among them, the truncated oxidation of pyruvate and its diversion to lactate are well known paradigms of metabolic transformation. Indeed the enhanced glucose uptake imposed by this phenotype is common to the vast majority of tumours and has been successfully exploited for diagnostic by FDG-PET. On the contrary, the attempt to target therapeutically glucose metabolism has been limited, on the one hand, by the presence of multiple redundant alternative pathways, and on the other, by a narrow therapeutic window due to the overlap with normal physiological process. For this reason, few glycolytic inhibitors have reached clinical trials and none of them has been approved for clinical use(230). In recent years a better understanding of the genetic and molecular events that underlie this functional phenotype has been achieved. Several oncogenes and few tumour suppressor genes are known to regulate glucose uptake and glycolysis. Nonetheless, the demonstration that different types of cancer depend on glucose to different extent is of fundamental importance to design therapeutic agents targeting glycolysis (69, 231).

Together with glycolysis, the TCA cycle and OXPHOS control the cellular balance between energy production and anabolism. Tumours with impaired OXPHOS due to hypoxia, mitochondrial DNA mutation, or drugs, enhance glycolysis and rewire the TCA cycle to enable growth. This rationale supported the design of a small molecule targeting the energetic requirement of lung cancer cells with a non-functional electron transport chain (232).

While energetic and anabolic demands are important modulators of tumour metabolism, they cannot entirely explain the metabolic features displayed by many tumours. The microenvironment related to the tissue of origin, as well as stochastic genetic/epigenetic alterations, can qualitatively and quantitatively

affect the cellular metabolic network. Integrated signals deriving from intracellular and extracellular environments finely tune cancer cell metabolism. Few mutations that can directly affect metabolic enzymes are known, while it has been postulated that the dysregulation of cell energetics is one of the cancer hallmarks(233). This assumption implies that the metabolic switch that supports uncontrolled growth is often triggered by mutations in signalling pathways that reset the whole anabolic and energetic homeostasis. Therefore we focused our work in understanding how growth signalling pathways, such as the MAPK, regulate metabolism in order to support growth and proliferation and how this interaction can be exploited therapeutically.

### **6.1.1 Identification of a new mechanism of allosteric regulation for PKM2**

In the past few years there has been a substantial increase in the understanding of the mechanism by which PKM2 modulates metabolic rearrangement during cancer progression. This involvement is thought to be multifaceted and to include contributions to anabolism and regulation of aerobic glycolysis. Counter-intuitively, despite the glycolytic phenotype displayed by cancer cells, PKM2 is a rather slow enzyme compared to the PKM1 iso-enzyme. But in fact, its lower activity may contribute to cell growth and proliferation by favouring the accumulation of glycolytic intermediates that can be used for biosynthetic purposes. Our knowledge on PKM2 regulation has been significantly enriched by functional, structural and metabolomic studies. Nevertheless, there are still many open questions regarding the multiple roles that PKM2 may have in metabolic regulation and other, non-glycolytic functions of the enzyme.

PKM2 activation by serine is especially interesting in the context of cancer, because cancer cells rely heavily on serine biosynthesis to proliferate and grow (90-92). In proliferating cells, serine is the source of one-carbon units for *de novo* synthesis of purines and pyrimidines, and additionally, it provides precursors for the synthesis of other amino acids, lipid messengers, and neuromodulators(201). This sparked interest in a possible link between glycolysis and serine biosynthesis mediated by PKM2 in cancer cells. Indeed, we have shown that cells with low PK activity have increased serine and glycine biosynthesis. When cells were deprived of these amino acids, PK activity was

decreased and a consequent increase in serine biosynthesis was observed. Simultaneously, cells displayed a pronounced switch from glycolytic to oxidative metabolism, suggesting that PK activity is reduced in the absence of serine and glycine to redirect glucose-derived carbon away from glycolytic ATP production and towards serine and glycine biosynthesis. Although serine and glycine can be interconverted, only serine was able to induce PK activity both in isolated proteins and cells. Similar to the mechanism of action of FBP, serine was able to increase the affinity of PKM2 for PEP. Importantly, this occurred at physiologically relevant concentrations of serine, indicating that serine and FBP can activate PKM2 to help cells adapt to changes in serine and glucose availability, respectively. The PKM1, PKL, and PKR isoforms did not display activation by serine, indicating this is a specific trait to rapidly proliferating cells that express PKM2 (200). Together, this demonstrates an exciting rheostat-like function of PKM2 that enables cancer cells to partition glucose-derived carbon towards energy generation and serine biosynthesis depending on their needs, thereby sustaining optimal proliferation and growth.

We have further confirmed the importance of histidine-464 in the amino acid binding pocket of PKM2 for serine binding by mutagenesis. The H464A mutation reduces the activation of PKM2 by serine while retaining its activation by FBP. However, the effect of H464A on serine induced PKM2 tetramerisation is not clear. Furthermore, a serine residue in position 437 of PKM2, which is in close proximity to the FBP binding region, seems to be essential for tetramerisation. In addition, serine was able to activate PKM2 even when tetramerisation is impaired by the S437Y mutation. These results improve our understanding on the molecular basis of PKM2 regulation and provide a different perspective from the current view in which PKM2 activation is mediated by its tetramerisation only. However, further crystallographic and structural modelling studies of mutants that cannot bind serine, like the H464A, need to be performed in order to fully understand the mechanism by which serine can activate PKM2 independently of its oligomeric state.

### 6.1.2 Therapeutic targeting of metabolic regulators to reactivate senescence

PDH has been shown to be a central metabolic regulator in diabetes, heart disease and it has been recently suggested to contribute to cancer (20, 234-238). However, its regulation and function in the context of cellular senescence have not been recognised. Based on the analysis of the consumption and production of nutrients and metabolites, others previously reported that a decrease in glucose-derived lactate parallels replicative senescence (239). Similarly, it has been shown that overexpression of some glycolytic enzymes can interfere with senescence(240). Using metabolic flux analysis we measured the fate of glucose-derived metabolites into glycolysis and the TCA cycle, showing that the metabolic fate of pyruvate diverges in OIS and cycling cells: during OIS, pyruvate oxidation by the TCA cycle increased at the expense of lactate and alanine production. Interference with this shift from glycolysis to the TCA cycle, by PDP2 depletion or restoration of PDK1 (both resulting in inhibition of PDH) prevents the onset of OIS (22).

To date, a limited number of biomarkers for detecting senescence are available, and even fewer that are causally involved in the process(241). PDK1 has been shown to be up-regulated in cancer and its high levels associate with poor prognosis for HNSCC patients (242). Our results unmask the three constituents of the mitochondrial PDK1-PDP2-PDH axis as a new series of potential senescence biomarkers, at least in the context of BRAF<sup>V600E</sup>-induced senescence.

It has been previously shown that senescent cells display a robust inflammatory transcriptome signature (207, 243, 244). Interestingly, PDH regulation influenced the inflammatory transcriptome: inhibition of PDH activity resulted in a sharp decrease in the expression levels of interleukins 6 (IL6) and 8 (IL8) transcripts, two prominent biomarkers of OIS (22). Altogether, these findings demonstrate a close communication between metabolic regulation and the senescence-associated secretory phenotype. Specifically, our findings suggest the existence of a complex auto-stimulatory feedback mechanism, in which cytokines, metabolic regulators and transcription factors operate to control OIS.

Our results on metabolic regulation in OIS not only provide a novel insight into the regulation of cellular senescence, but also explain former observations on the potentially therapeutic effect of PDK inhibition on tumorigenesis. Previous analysis of a cell culture model of stepwise malignant transformation showed that increasing tumorigenicity correlates with a shift from OXPHOS towards glycolysis (245). Since we showed that PDH activation in the context of an oncogenic signal (BRAFV<sup>600E</sup>) has the opposite effect, PDH regulation likely represents a barrier against tumorigenesis. Consistent with this idea is the finding that DCA, a PDK inhibitor, inhibits xenograft tumour growth (20). Similar decrease in invasiveness and tumour growth was observed upon PDK1 depletion (238). We showed that PDH reactivation by PDK1 depletion is sufficient to mount a senescence response in primary cells (22). This raises the possibility that PDH represents a pro-senescence therapeutic target. Over the past few years, the concept of pro-senescence therapy as a novel clinical approach to treat cancers has attracted increasing interest(246). In summary, our findings provide a rationale to further explore the feasibility of targeting key metabolic enzymes such as PDK1 for clinical intervention in cancer.

### **6.1.3 Inhibition of glutamine metabolism as a therapeutic strategy in PLX-resistant melanoma**

Half of the patients affected by metastatic melanoma present a gain of function mutation in the BRAF gene; hence, BRAF inhibitors are highly effective in this pathology. However, an increased occurrence of squamous cell carcinomas and keratoacanthomas as a consequence of BRAF inhibitor treatment has been observed. This observation highlights a potential pitfall of targeting specific oncogenic addiction (alone) and can prospect the occurrence of a “synthetic tumorigenesis” as a response to a specific treatment. Therefore the need of finding therapeutic combinations that will target different pathways in the tumour in order to kill it faster and more efficiently.

The switch from OXPHOS to aerobic glycolysis in cancer cells and the possible reasons behind this process are well described. However, cancer cell metabolism is far more complex than a change in glucose utilization and many other metabolic pathways are tightly interconnected to support growth and proliferation. Beyond glucose, other metabolites, from amino acids to fatty

acids, can be utilised for ATP generation and anabolic purposes(64). Indeed, in the last decade, substantial attention was paid to glutamine, the most abundant amino acid in human blood. The requirement of glutamine for the growth of cancer cells was clearly established more than 50 years ago(247). However, it is only thanks to recent technologies that its anabolic role is increasingly appreciated and it is now clear that glutamine, which is avidly consumed by cancer cells, is an important anaplerotic substrate used by mitochondria for bioenergetics and for macromolecular biosynthesis(130). In particular, it was demonstrated that glutamine has the flexibility to be converted both in a oxidative and reductive fashion in the TCA cycle, providing cells with important anabolic metabolites such as citrate for lipid biosynthesis, aspartate for nucleotides biosynthesis and NADH to feed OXPHOS when mitochondria are partially dysfunctional due to mutations or to low oxygen levels (78, 248).

Melanoma cells can be highly glycolytic and have flexible metabolic pathways that allow them to adapt to stressful environments (223). Our work complements a recent report showing that BRAF<sup>V600E</sup> inhibition results in reduced glucose consumption and expression of glycolytic enzymes (249). Intriguingly, in that study it was reported that oncogenic NRAS (NRAS<sup>Q61K</sup>) rendered A375 cells resistant to BRAF inhibitors and restored the expression of glycolytic enzymes, suggesting that ectopic expression of NRAS<sup>Q61K</sup> restored metabolism to its original state. However, here we showed that melanoma cells, in which resistance was induced by continuous exposure to a BRAF inhibitor, switched from glucose to glutamine dependency. In addition, PLX-resistant cells were more sensitive to glutamine starvation and inhibition of glutaminolysis.

A shift towards glutamine metabolism in resistant cells may allow cells to sustain proliferation as the influx of glucose-derived carbons into the TCA cycle is diminished (248, 250). Glutaminolysis can effectively sustain TCA cycle metabolite levels and provide nitrogen for nucleotide biosynthesis. This may convey particular advantage to PLX-resistant cells, as they require more carbon in the TCA cycle for oxidative metabolism and more carbon and nitrogen to sustain growth and proliferation. These findings are in agreement with recent studies that determined metabolic flexibility of cancer cells (78, 82).

Inhibition of glutaminolysis can suppress cell growth in some cancers such as, Burkitt lymphoma and other cancers driven by c-Myc (7, 69). We showed that PLX-resistant cells are also more sensitive to glutaminase inhibition, suggesting that glutaminase may be a therapeutic target in BRAF-inhibitor resistant melanoma cells. Notably, PGC1 $\alpha$  was recently shown to be important for glutamine metabolism in *ERBB2* positive breast cancer(251) and it was recently suggested that glutamine transporters might also be important therapeutic targets in melanoma again highlighting the therapeutic potential of addressing this metabolic pathway in this disease (252).

We have shown that PLX-resistant cells are more dependent on mitochondrial function than their parental counterpart. Therefore, additional approaches including the use of mitochondrial inhibitors such as biguanides could be considered. Metformin has been reported to have antitumour activity in melanoma and many other cancers(253). Biguanides activate AMPK by inhibiting complex I of the mitochondrial electron transport chain. This is in line with reports that PLX-resistant melanoma cell lines are more sensitive to metformin and phenformin(254).

Developing effective treatments to delay or overcome resistance in melanoma is a clinical and biological challenge due to the complexity of multiple resistance mechanisms that sustain MAPK/ERK signalling. Our work shows that melanoma cells surviving PLX4720 treatment switch from a glycolytic to an oxidative phenotype using glutamine as main carbon source. Thus, combining the use of BRAF inhibitors with inhibitors of glutaminolysis may be a useful strategy for the treatment of melanoma.

## 6.2 Final Remarks

The range of metabolic adaptations found in cancer cells has been subject of intense research in the last decade becoming one of the hallmarks of cancer(233). Several factors have contributed to the tremendous progress of this field. The first was the inability of genomics and proteomics to fully describe the process of tumorigenesis. While sequencing entire cancer genomes has revealed areas of genetic susceptibility and discovered genes linked to tumour formation, these results have yielded moderate progress and additional work to determine the functional basis for the observed genetic associations is required(255). The second factor was the development of analytical techniques that allowed for the reliable identification and quantification of metabolites present in tumour cells as well as in their environment. Despite the fact that individual metabolites have been analysed for decades by nuclear magnetic resonance (NMR) and mass spectrometry (MS), it was the development of the high-throughput analyses, metabolomics, which made the study of the global metabolic profile of a cancer cell possible. In addition, thanks to the parallel progress in systems biology, metabolic fluxes in cancer cells can now be explored and the data from different “omics” approaches can be integrated to obtain a clearer picture of the metabolic transformation in cancer cells.

Metabolomics is now playing a crucial role in dissecting the possible metabolic rearrangements operating in cancer cells. Indeed, since intra-tumour heterogeneity has been characterised by deep sequencing, a different metabolic behaviour among cancer cells belonging to the same tumour can be expected. In addition, most cancers are composed of multiple cells types, which engage in several homo- and heterotypic interactions. Therefore, the current and future challenge of the field of cancer metabolism is to dissect these complex metabolic changes and, at the same time, interpret them as result of global metabolic interactions between different cell types, tissues and organs so that we can more efficiently identify targets that are efficacious and specific for tumours with minimal toxicity for normal cells.

## Bibliography

1. Dang CV. Links between metabolism and cancer. *Genes & development*. 2012;26(9):877-90.
2. Ward PS, Thompson CB. Metabolic reprogramming: a cancer hallmark even warburg did not anticipate. *Cancer cell*. 2012;21(3):297-308.
3. Semenza GL. HIF-1: upstream and downstream of cancer metabolism. *Current opinion in genetics & development*. 2010;20(1):51-6.
4. Shaw RJ, Cantley LC. Ras, PI(3)K and mTOR signalling controls tumour cell growth. *Nature*. 2006;441(7092):424-30.
5. Guertin DA, Sabatini DM. Defining the role of mTOR in cancer. *Cancer cell*. 2007;12(1):9-22.
6. Shackelford DB, Shaw RJ. The LKB1-AMPK pathway: metabolism and growth control in tumour suppression. *Nature reviews Cancer*. 2009;9(8):563-75.
7. Wise DR, DeBerardinis RJ, Mancuso A, Sayed N, Zhang XY, Pfeiffer HK, et al. Myc regulates a transcriptional program that stimulates mitochondrial glutaminolysis and leads to glutamine addiction. *Proceedings of the National Academy of Sciences of the United States of America*. 2008;105(48):18782-7.
8. Cantor JR, Sabatini DM. Cancer cell metabolism: one hallmark, many faces. *Cancer discovery*. 2012;2(10):881-98.
9. Warburg O. On the origin of cancer cells. *Science*. 1956;123(3191):309-14.
10. Macheda ML, Rogers S, Best JD. Molecular and cellular regulation of glucose transporter (GLUT) proteins in cancer. *Journal of cellular physiology*. 2005;202(3):654-62.
11. Dang CV, Lewis BC, Dolde C, Dang G, Shim H. Oncogenes in tumor metabolism, tumorigenesis, and apoptosis. *Journal of bioenergetics and biomembranes*. 1997;29(4):345-54.
12. Yoon DY, Buchler P, Saarikoski ST, Hines OJ, Reber HA, Hankinson O. Identification of genes differentially induced by hypoxia in pancreatic cancer cells. *Biochemical and biophysical research communications*. 2001;288(4):882-6.
13. Minchenko A, Leshchinsky I, Opentanova I, Sang N, Srinivas V, Armstead V, et al. Hypoxia-inducible factor-1-mediated expression of the 6-phosphofructo-2-kinase/fructose-2,6-bisphosphatase-3 (PFKFB3) gene. Its possible role in the Warburg effect. *The Journal of biological chemistry*. 2002;277(8):6183-7.
14. Ros S, Santos CR, Moco S, Baenke F, Kelly G, Howell M, et al. Functional metabolic screen identifies 6-phosphofructo-2-kinase/fructose-2,6-bisphosphatase 4 as an important regulator of prostate cancer cell survival. *Cancer discovery*. 2012;2(4):328-43.
15. Bensaad K, Tsuruta A, Selak MA, Vidal MN, Nakano K, Bartrons R, et al. TIGAR, a p53-inducible regulator of glycolysis and apoptosis. *Cell*. 2006;126(1):107-20.
16. Hitosugi T, Zhou L, Elf S, Fan J, Kang HB, Seo JH, et al. Phosphoglycerate mutase 1 coordinates glycolysis and biosynthesis to promote tumor growth. *Cancer cell*. 2012;22(5):585-600.
17. Fantin VR, St-Pierre J, Leder P. Attenuation of LDH-A expression uncovers a link between glycolysis, mitochondrial physiology, and tumor maintenance. *Cancer cell*. 2006;9(6):425-34.
18. Kim JW, Tchernyshyov I, Semenza GL, Dang CV. HIF-1-mediated expression of pyruvate dehydrogenase kinase: a metabolic switch required for cellular adaptation to hypoxia. *Cell Metab*. 2006;3(3):177-85.

19. Papandreou I, Cairns RA, Fontana L, Lim AL, Denko NC. HIF-1 mediates adaptation to hypoxia by actively downregulating mitochondrial oxygen consumption. *Cell metabolism*. 2006;3(3):187-97.
20. Bonnet S, Archer SL, Allalunis-Turner J, Haromy A, Beaulieu C, Thompson R, et al. A mitochondria-K<sup>+</sup> channel axis is suppressed in cancer and its normalization promotes apoptosis and inhibits cancer growth. *Cancer cell*. 2007;11(1):37-51.
21. Pearson H. Cancer patients opt for unapproved drug. *Nature*. 2007;446(7135):474-5.
22. Kaplon J, Zheng L, Meissl K, Chaneton B, Selivanov VA, Mackay G, et al. A key role for mitochondrial gatekeeper pyruvate dehydrogenase in oncogene-induced senescence. *Nature*. 2013;498(7452):109-12.
23. Noguchi T, Inoue H, Tanaka T. The M1- and M2-type isozymes of rat pyruvate kinase are produced from the same gene by alternative RNA splicing. *The Journal of biological chemistry*. 1986;261(29):13807-12.
24. Takenaka M, Yamada K, Lu T, Kang R, Tanaka T, Noguchi T. Alternative splicing of the pyruvate kinase M gene in a minigene system. *European journal of biochemistry / FEBS*. 1996;235(1-2):366-71.
25. Dombrauckas JD, Santarsiero BD, Mesecar AD. Structural basis for tumor pyruvate kinase M2 allosteric regulation and catalysis. *Biochemistry*. 2005;44(27):9417-29.
26. Clower CV, Chatterjee D, Wang Z, Cantley LC, Vander Heiden MG, Krainer AR. The alternative splicing repressors hnRNP A1/A2 and PTB influence pyruvate kinase isoform expression and cell metabolism. *Proceedings of the National Academy of Sciences of the United States of America*. 2010;107(5):1894-9.
27. David CJ, Chen M, Assanah M, Canoll P, Manley JL. HnRNP proteins controlled by c-Myc deregulate pyruvate kinase mRNA splicing in cancer. *Nature*. 2010;463(7279):364-8.
28. Chen M, Zhang J, Manley JL. Turning on a fuel switch of cancer: hnRNP proteins regulate alternative splicing of pyruvate kinase mRNA. *Cancer research*. 2010;70(22):8977-80.
29. Oremek GM, Teigelkamp S, Kramer W, Eigenbrodt E, Usadel KH. The pyruvate kinase isoenzyme tumor M2 (Tu M2-PK) as a tumor marker for renal carcinoma. *Anticancer research*. 1999;19(4A):2599-601.
30. Christofk HR, Vander Heiden MG, Harris MH, Ramanathan A, Gerszten RE, Wei R, et al. The M2 splice isoform of pyruvate kinase is important for cancer metabolism and tumour growth. *Nature*. 2008;452(7184):230-3.
31. Bluemlein K, Gruning NM, Feichtinger RG, Lehrach H, Kofler B, Ralser M. No evidence for a shift in pyruvate kinase PKM1 to PKM2 expression during tumorigenesis. *Oncotarget*. 2011;2(5):393-400.
32. Muirhead H. Isoenzymes of pyruvate kinase. *Biochemical Society transactions*. 1990;18(2):193-6.
33. Brinck U, Eigenbrodt E, Oehmke M, Mazurek S, Fischer G. L- and M2-pyruvate kinase expression in renal cell carcinomas and their metastases. *Virchows Archiv : an international journal of pathology*. 1994;424(2):177-85.
34. Steinberg P, Klingelhoffer A, Schafer A, Wust G, Weisse G, Oesch F, et al. Expression of pyruvate kinase M2 in preneoplastic hepatic foci of N-nitrosomorpholine-treated rats. *Virchows Archiv : an international journal of pathology*. 1999;434(3):213-20.
35. Eigenbrodt E, Reinacher M, Scheefers-Borchel U, Scheefers H, Friis R. Double role for pyruvate kinase type M2 in the expansion of phosphometabolite pools found in tumor cells. *Critical reviews in oncogenesis*. 1992;3(1-2):91-115.

36. Mazurek S, Boschek CB, Hugo F, Eigenbrodt E. Pyruvate kinase type M2 and its role in tumor growth and spreading. *Seminars in cancer biology*. 2005;15(4):300-8.
37. Bailey E, Stirpe F, Taylor CB. Regulation of rat liver pyruvate kinase. The effect of preincubation, pH, copper ions, fructose 1,6-diphosphate and dietary changes on enzyme activity. *The Biochemical journal*. 1968;108(3):427-36.
38. Ashizawa K, Willingham MC, Liang CM, Cheng SY. In vivo regulation of monomer-tetramer conversion of pyruvate kinase subtype M2 by glucose is mediated via fructose 1,6-bisphosphate. *The Journal of biological chemistry*. 1991;266(25):16842-6.
39. Christofk HR, Vander Heiden MG, Wu N, Asara JM, Cantley LC. Pyruvate kinase M2 is a phosphotyrosine-binding protein. *Nature*. 2008;452(7184):181-6.
40. Gruning NM, Rinnerthaler M, Bluemlein K, Mulleder M, Wamelink MM, Lehrach H, et al. Pyruvate kinase triggers a metabolic feedback loop that controls redox metabolism in respiring cells. *Cell metabolism*. 2011;14(3):415-27.
41. Anastasiou D, Poulogiannis G, Asara JM, Boxer MB, Jiang JK, Shen M, et al. Inhibition of pyruvate kinase M2 by reactive oxygen species contributes to cellular antioxidant responses. *Science*. 2011;334(6060):1278-83.
42. Wang Q, Zhang Y, Yang C, Xiong H, Lin Y, Yao J, et al. Acetylation of metabolic enzymes coordinates carbon source utilization and metabolic flux. *Science*. 2010;327(5968):1004-7.
43. Lv L, Li D, Zhao D, Lin R, Chu Y, Zhang H, et al. Acetylation targets the M2 isoform of pyruvate kinase for degradation through chaperone-mediated autophagy and promotes tumor growth. *Molecular cell*. 2011;42(6):719-30.
44. Imamura K, Taniuchi K, Tanaka T. Multimolecular forms of pyruvate kinase. II. Purification of M<sub>2</sub>-type pyruvate kinase from Yoshida ascites hepatoma 130 cells and comparative studies on the enzymological and immunological properties of the three types of pyruvate kinases, L, M<sub>1</sub>, and M<sub>2</sub>. *Journal of biochemistry*. 1972;72(4):1001-15.
45. Carbonell J, Feliu JE, Marco R, Sols A. Pyruvate kinase. Classes of regulatory isoenzymes in mammalian tissues. *European journal of biochemistry / FEBS*. 1973;37(1):148-56.
46. Berglund L, Humble E. Kinetic properties of pig pyruvate kinases type A from kidney and type M from muscle. *Archives of biochemistry and biophysics*. 1979;195(2):347-61.
47. Eigenbrodt E, Leib S, Kramer W, Friis RR, Schoner W. Structural and kinetic differences between the M<sub>2</sub> type pyruvate kinases from lung and various tumors. *Biomedica biochimica acta*. 1983;42(11-12):S278-82.
48. Dabrowska A, Pietkiewicz J, Dabrowska K, Czapinska E, Danielewicz R. Interaction of M<sub>1</sub> and M<sub>2</sub> isozymes pyruvate kinase from human tissues with phospholipids. *Biochimica et biophysica acta*. 1998;1383(1):123-9.
49. Presek P, Reinacher M, Eigenbrodt E. Pyruvate kinase type M<sub>2</sub> is phosphorylated at tyrosine residues in cells transformed by Rous sarcoma virus. *FEBS letters*. 1988;242(1):194-8.
50. Zwerschke W, Mazurek S, Massimi P, Banks L, Eigenbrodt E, Jansen-Durr P. Modulation of type M<sub>2</sub> pyruvate kinase activity by the human papillomavirus type 16 E7 oncoprotein. *Proceedings of the National Academy of Sciences of the United States of America*. 1999;96(4):1291-6.
51. Le Mellay V, Houben R, Troppmair J, Hagemann C, Mazurek S, Frey U, et al. Regulation of glycolysis by Raf protein serine/threonine kinases. *Advances in enzyme regulation*. 2002;42:317-32.

52. Mazurek S, Drexler HC, Troppmair J, Eigenbrodt E, Rapp UR. Regulation of pyruvate kinase type M2 by A-Raf: a possible glycolytic stop or go mechanism. *Anticancer research*. 2007;27(6B):3963-71.
53. Hitosugi T, Kang S, Vander Heiden MG, Chung TW, Elf S, Lythgoe K, et al. Tyrosine phosphorylation inhibits PKM2 to promote the Warburg effect and tumor growth. *Science signaling*. 2009;2(97):ra73.
54. Mazurek S, Hugo F, Failing K, Eigenbrodt E. Studies on associations of glycolytic and glutaminolytic enzymes in MCF-7 cells: role of P36. *Journal of cellular physiology*. 1996;167(2):238-50.
55. Mazurek S, Zwerschke W, Jansen-Durr P, Eigenbrodt E. Effects of the human papilloma virus HPV-16 E7 oncoprotein on glycolysis and glutaminolysis: role of pyruvate kinase type M2 and the glycolytic-enzyme complex. *The Biochemical journal*. 2001;356(Pt 1):247-56.
56. Gao X, Wang H, Yang JJ, Liu X, Liu ZR. Pyruvate kinase M2 regulates gene transcription by acting as a protein kinase. *Molecular cell*. 2012;45(5):598-609.
57. Stetak A, Veress R, Ovadi J, Csermely P, Keri G, Ullrich A. Nuclear translocation of the tumor marker pyruvate kinase M2 induces programmed cell death. *Cancer research*. 2007;67(4):1602-8.
58. Hoshino A, Hirst JA, Fujii H. Regulation of cell proliferation by interleukin-3-induced nuclear translocation of pyruvate kinase. *The Journal of biological chemistry*. 2007;282(24):17706-11.
59. Spoden GA, Morandell D, Eehalt D, Fiedler M, Jansen-Durr P, Hermann M, et al. The SUMO-E3 ligase PIAS3 targets pyruvate kinase M2. *Journal of cellular biochemistry*. 2009;107(2):293-302.
60. Lee J, Kim HK, Han YM, Kim J. Pyruvate kinase isozyme type M2 (PKM2) interacts and cooperates with Oct-4 in regulating transcription. *The international journal of biochemistry & cell biology*. 2008;40(5):1043-54.
61. Yang W, Xia Y, Ji H, Zheng Y, Liang J, Huang W, et al. Nuclear PKM2 regulates beta-catenin transactivation upon EGFR activation. *Nature*. 2011;480(7375):118-22.
62. Luo W, Hu H, Chang R, Zhong J, Knabel M, O'Meally R, et al. Pyruvate kinase M2 is a PHD3-stimulated coactivator for hypoxia-inducible factor 1. *Cell*. 2011;145(5):732-44.
63. Curi R, Lagranha CJ, Doi SQ, Sellitti DF, Procopio J, Pithon-Curi TC, et al. Molecular mechanisms of glutamine action. *Journal of cellular physiology*. 2005;204(2):392-401.
64. DeBerardinis RJ, Lum JJ, Hatzivassiliou G, Thompson CB. The biology of cancer: metabolic reprogramming fuels cell growth and proliferation. *Cell metabolism*. 2008;7(1):11-20.
65. Lobo C, Ruiz-Bellido MA, Aledo JC, Marquez J, Nunez De Castro I, Alonso FJ. Inhibition of glutaminase expression by antisense mRNA decreases growth and tumourigenicity of tumour cells. *The Biochemical journal*. 2000;348 Pt 2:257-61.
66. Gao P, Tchernyshyov I, Chang TC, Lee YS, Kita K, Ochi T, et al. c-Myc suppression of miR-23a/b enhances mitochondrial glutaminase expression and glutamine metabolism. *Nature*. 2009;458(7239):762-5.
67. Wang JB, Erickson JW, Fuji R, Ramachandran S, Gao P, Dinavahi R, et al. Targeting mitochondrial glutaminase activity inhibits oncogenic transformation. *Cancer cell*. 2010;18(3):207-19.
68. Robinson MM, McBryant SJ, Tsukamoto T, Rojas C, Ferraris DV, Hamilton SK, et al. Novel mechanism of inhibition of rat kidney-type glutaminase by bis-2-(5-phenylacetamido-1,2,4-thiadiazol-2-yl)ethyl sulfide (BPTES). *The Biochemical journal*. 2007;406(3):407-14.

69. Le A, Lane AN, Hamaker M, Bose S, Gouw A, Barbi J, et al. Glucose-independent glutamine metabolism via TCA cycling for proliferation and survival in B cells. *Cell metabolism*. 2012;15(1):110-21.
70. Baysal BE, Ferrell RE, Willett-Brozick JE, Lawrence EC, Myssiorek D, Bosch A, et al. Mutations in SDHD, a mitochondrial complex II gene, in hereditary paraganglioma. *Science*. 2000;287(5454):848-51.
71. Tomlinson IP, Alam NA, Rowan AJ, Barclay E, Jaeger EE, Kelsell D, et al. Germline mutations in FH predispose to dominantly inherited uterine fibroids, skin leiomyomata and papillary renal cell cancer. *Nature genetics*. 2002;30(4):406-10.
72. Frezza C, Gottlieb E. Mitochondria in cancer: not just innocent bystanders. *Seminars in cancer biology*. 2009;19(1):4-11.
73. Gimenez-Roqueplo AP, Favier J, Rustin P, Mourad JJ, Plouin PF, Corvol P, et al. The R22X mutation of the SDHD gene in hereditary paraganglioma abolishes the enzymatic activity of complex II in the mitochondrial respiratory chain and activates the hypoxia pathway. *American journal of human genetics*. 2001;69(6):1186-97.
74. Pollard PJ, Briere JJ, Alam NA, Barwell J, Barclay E, Wortham NC, et al. Accumulation of Krebs cycle intermediates and over-expression of HIF1alpha in tumours which result from germline FH and SDH mutations. *Human molecular genetics*. 2005;14(15):2231-9.
75. Isaacs JS, Jung YJ, Mole DR, Lee S, Torres-Cabala C, Chung YL, et al. HIF overexpression correlates with biallelic loss of fumarate hydratase in renal cancer: novel role of fumarate in regulation of HIF stability. *Cancer cell*. 2005;8(2):143-53.
76. Koivunen P, Hirsila M, Remes AM, Hassinen IE, Kivirikko KI, Myllyharju J. Inhibition of hypoxia-inducible factor (HIF) hydroxylases by citric acid cycle intermediates: possible links between cell metabolism and stabilization of HIF. *The Journal of biological chemistry*. 2007;282(7):4524-32.
77. Selak MA, Armour SM, MacKenzie ED, Boulahbel H, Watson DG, Mansfield KD, et al. Succinate links TCA cycle dysfunction to oncogenesis by inhibiting HIF-alpha prolyl hydroxylase. *Cancer cell*. 2005;7(1):77-85.
78. Frezza C, Zheng L, Folger O, Rajagopalan KN, MacKenzie ED, Jerby L, et al. Haem oxygenase is synthetically lethal with the tumour suppressor fumarate hydratase. *Nature*. 2011;477(7363):225-8.
79. Ashrafian H, Czibik G, Bellahcene M, Aksentijevic D, Smith AC, Mitchell SJ, et al. Fumarate is cardioprotective via activation of the Nrf2 antioxidant pathway. *Cell metabolism*. 2012;15(3):361-71.
80. Parsons DW, Jones S, Zhang X, Lin JC, Leary RJ, Angenendt P, et al. An integrated genomic analysis of human glioblastoma multiforme. *Science*. 2008;321(5897):1807-12.
81. Mardis ER, Ding L, Dooling DJ, Larson DE, McLellan MD, Chen K, et al. Recurring mutations found by sequencing an acute myeloid leukemia genome. *The New England journal of medicine*. 2009;361(11):1058-66.
82. Dang L, White DW, Gross S, Bennett BD, Bittinger MA, Driggers EM, et al. Cancer-associated IDH1 mutations produce 2-hydroxyglutarate. *Nature*. 2009;462(7274):739-44.
83. Choi C, Ganji SK, DeBerardinis RJ, Hatanpaa KJ, Rakheja D, Kovacs Z, et al. 2-hydroxyglutarate detection by magnetic resonance spectroscopy in IDH-mutated patients with gliomas. *Nature medicine*. 2012;18(4):624-9.
84. Elkhalel A, Jalbert LE, Phillips JJ, Yoshihara HA, Parvataneni R, Srinivasan R, et al. Magnetic resonance of 2-hydroxyglutarate in IDH1-mutated low-grade gliomas. *Science translational medicine*. 2012;4(116):116ra5.

85. Andronesi OC, Kim GS, Gerstner E, Batchelor T, Tzika AA, Fantin VR, et al. Detection of 2-hydroxyglutarate in IDH-mutated glioma patients by in vivo spectral-editing and 2D correlation magnetic resonance spectroscopy. *Science translational medicine*. 2012;4(116):116ra4.
86. Turcan S, Rohle D, Goenka A, Walsh LA, Fang F, Yilmaz E, et al. IDH1 mutation is sufficient to establish the glioma hypermethylator phenotype. *Nature*. 2012;483(7390):479-83.
87. Lu C, Ward PS, Kapoor GS, Rohle D, Turcan S, Abdel-Wahab O, et al. IDH mutation impairs histone demethylation and results in a block to cell differentiation. *Nature*. 2012;483(7390):474-8.
88. Noushmehr H, Weisenberger DJ, Diefes K, Phillips HS, Pujara K, Berman BP, et al. Identification of a CpG island methylator phenotype that defines a distinct subgroup of glioma. *Cancer cell*. 2010;17(5):510-22.
89. Rohle D, Popovici-Muller J, Palaskas N, Turcan S, Grommes C, Campos C, et al. An inhibitor of mutant IDH1 delays growth and promotes differentiation of glioma cells. *Science*. 2013;340(6132):626-30.
90. Pollari S, Kakonen SM, Edgren H, Wolf M, Kohonen P, Sara H, et al. Enhanced serine production by bone metastatic breast cancer cells stimulates osteoclastogenesis. *Breast cancer research and treatment*. 2011;125(2):421-30.
91. Possemato R, Marks KM, Shaul YD, Pacold ME, Kim D, Birsoy K, et al. Functional genomics reveal that the serine synthesis pathway is essential in breast cancer. *Nature*. 2011;476(7360):346-50.
92. Locasale JW, Grassian AR, Melman T, Lyssiotis CA, Mattaini KR, Bass AJ, et al. Phosphoglycerate dehydrogenase diverts glycolytic flux and contributes to oncogenesis. *Nature genetics*. 2011;43(9):869-74.
93. Maddocks OD, Berkers CR, Mason SM, Zheng L, Blyth K, Gottlieb E, et al. Serine starvation induces stress and p53-dependent metabolic remodelling in cancer cells. *Nature*. 2013;493(7433):542-6.
94. Labuschagne CF, van den Broek NJ, Mackay GM, Vousden KH, Maddocks OD. Serine, but not glycine, supports one-carbon metabolism and proliferation of cancer cells. *Cell reports*. 2014;7(4):1248-58.
95. Shaw RJ, Bardeesy N, Manning BD, Lopez L, Kosmatka M, DePinho RA, et al. The LKB1 tumor suppressor negatively regulates mTOR signaling. *Cancer cell*. 2004;6(1):91-9.
96. Oshiro N, Yoshino K, Hidayat S, Tokunaga C, Hara K, Eguchi S, et al. Dissociation of raptor from mTOR is a mechanism of rapamycin-induced inhibition of mTOR function. *Genes to cells : devoted to molecular & cellular mechanisms*. 2004;9(4):359-66.
97. Sarbassov DD, Sabatini DM. Redox regulation of the nutrient-sensitive raptor-mTOR pathway and complex. *The Journal of biological chemistry*. 2005;280(47):39505-9.
98. Sarbassov DD, Ali SM, Sabatini DM. Growing roles for the mTOR pathway. *Current opinion in cell biology*. 2005;17(6):596-603.
99. Brugarolas J, Lei K, Hurley RL, Manning BD, Reiling JH, Hafen E, et al. Regulation of mTOR function in response to hypoxia by REDD1 and the TSC1/TSC2 tumor suppressor complex. *Genes & development*. 2004;18(23):2893-904.
100. Wullschleger S, Loewith R, Hall MN. TOR signaling in growth and metabolism. *Cell*. 2006;124(3):471-84.
101. Sancak Y, Peterson TR, Shaul YD, Lindquist RA, Thoreen CC, Bar-Peled L, et al. The Rag GTPases bind raptor and mediate amino acid signaling to mTORC1. *Science*. 2008;320(5882):1496-501.

102. Sheen JH, Zoncu R, Kim D, Sabatini DM. Defective regulation of autophagy upon leucine deprivation reveals a targetable liability of human melanoma cells in vitro and in vivo. *Cancer cell*. 2011;19(5):613-28.
103. Cantley LC, Neel BG. New insights into tumor suppression: PTEN suppresses tumor formation by restraining the phosphoinositide 3-kinase/AKT pathway. *Proceedings of the National Academy of Sciences of the United States of America*. 1999;96(8):4240-5.
104. Tee AR, Fingar DC, Manning BD, Kwiatkowski DJ, Cantley LC, Blenis J. Tuberous sclerosis complex-1 and -2 gene products function together to inhibit mammalian target of rapamycin (mTOR)-mediated downstream signaling. *Proceedings of the National Academy of Sciences of the United States of America*. 2002;99(21):13571-6.
105. Mavrakis KJ, Zhu H, Silva RL, Mills JR, Teruya-Feldstein J, Lowe SW, et al. Tumorigenic activity and therapeutic inhibition of Rheb GTPase. *Genes & development*. 2008;22(16):2178-88.
106. LoPiccolo J, Blumenthal GM, Bernstein WB, Dennis PA. Targeting the PI3K/Akt/mTOR pathway: effective combinations and clinical considerations. *Drug resistance updates : reviews and commentaries in antimicrobial and anticancer chemotherapy*. 2008;11(1-2):32-50.
107. Majumder PK, Febbo PG, Bikoff R, Berger R, Xue Q, McMahon LM, et al. mTOR inhibition reverses Akt-dependent prostate intraepithelial neoplasia through regulation of apoptotic and HIF-1-dependent pathways. *Nature medicine*. 2004;10(6):594-601.
108. Saal LH, Johansson P, Holm K, Gruvberger-Saal SK, She QB, Maurer M, et al. Poor prognosis in carcinoma is associated with a gene expression signature of aberrant PTEN tumor suppressor pathway activity. *Proceedings of the National Academy of Sciences of the United States of America*. 2007;104(18):7564-9.
109. Tennant DA, Duran RV, Gottlieb E. Targeting metabolic transformation for cancer therapy. *Nature reviews Cancer*. 2010;10(4):267-77.
110. Chan DA, Sutphin PD, Nguyen P, Turcotte S, Lai EW, Banh A, et al. Targeting GLUT1 and the Warburg effect in renal cell carcinoma by chemical synthetic lethality. *Science translational medicine*. 2011;3(94):94ra70.
111. Gautier EL, Westerterp M, Bhagwat N, Cremers S, Shih A, Abdel-Wahab O, et al. HDL and Glut1 inhibition reverse a hypermetabolic state in mouse models of myeloproliferative disorders. *The Journal of experimental medicine*. 2013;210(2):339-53.
112. Yun J, Rago C, Cheong I, Pagliarini R, Angenendt P, Rajagopalan H, et al. Glucose deprivation contributes to the development of KRAS pathway mutations in tumor cells. *Science*. 2009;325(5947):1555-9.
113. Ying H, Kimmelman AC, Lyssiotis CA, Hua S, Chu GC, Fletcher-Sananikone E, et al. Oncogenic Kras maintains pancreatic tumors through regulation of anabolic glucose metabolism. *Cell*. 2012;149(3):656-70.
114. Di Cosimo S, Ferretti G, Papaldo P, Carlini P, Fabi A, Cognetti F. Lonidamine: efficacy and safety in clinical trials for the treatment of solid tumors. *Drugs of today*. 2003;39(3):157-74.
115. Cao X, Bloomston M, Zhang T, Frankel WL, Jia G, Wang B, et al. Synergistic antipancreatic tumor effect by simultaneously targeting hypoxic cancer cells with HSP90 inhibitor and glycolysis inhibitor. *Clinical cancer research : an official journal of the American Association for Cancer Research*. 2008;14(6):1831-9.
116. Ko YH, Smith BL, Wang Y, Pomper MG, Rini DA, Torbenson MS, et al. Advanced cancers: eradication in all cases using 3-bromopyruvate therapy to

- deplete ATP. *Biochemical and biophysical research communications*. 2004;324(1):269-75.
117. Maschek G, Savaraj N, Priebe W, Braunschweiger P, Hamilton K, Tidmarsh GF, et al. 2-deoxy-D-glucose increases the efficacy of adriamycin and paclitaxel in human osteosarcoma and non-small cell lung cancers in vivo. *Cancer research*. 2004;64(1):31-4.
118. Rosbe KW, Brann TW, Holden SA, Teicher BA, Frei E, 3rd. Effect of lonidamine on the cytotoxicity of four alkylating agents in vitro. *Cancer chemotherapy and pharmacology*. 1989;25(1):32-6.
119. Singh D, Banerji AK, Dwarakanath BS, Tripathi RP, Gupta JP, Mathew TL, et al. Optimizing cancer radiotherapy with 2-deoxy-d-glucose dose escalation studies in patients with glioblastoma multiforme. *Strahlentherapie und Onkologie : Organ der Deutschen Rontgengesellschaft [et al.]*. 2005;181(8):507-14.
120. Anastasiou D, Yu Y, Israelsen WJ, Jiang JK, Boxer MB, Hong BS, et al. Pyruvate kinase M2 activators promote tetramer formation and suppress tumorigenesis. *Nature chemical biology*. 2012;8(10):839-47.
121. Clem B, Telang S, Clem A, Yalcin A, Meier J, Simmons A, et al. Small-molecule inhibition of 6-phosphofructo-2-kinase activity suppresses glycolytic flux and tumor growth. *Molecular cancer therapeutics*. 2008;7(1):110-20.
122. Spoden GA, Mazurek S, Morandell D, Bacher N, Ausserlechner MJ, Jansen-Durr P, et al. Isozyme-specific inhibitors of the glycolytic key regulator pyruvate kinase subtype M2 moderately decelerate tumor cell proliferation. *International journal of cancer Journal international du cancer*. 2008;123(2):312-21.
123. Vander Heiden MG, Christofk HR, Schuman E, Subtelny AO, Sharfi H, Harlow EE, et al. Identification of small molecule inhibitors of pyruvate kinase M2. *Biochemical pharmacology*. 2010;79(8):1118-24.
124. Kung C, Hixon J, Choe S, Marks K, Gross S, Murphy E, et al. Small molecule activation of PKM2 in cancer cells induces serine auxotrophy. *Chemistry & biology*. 2012;19(9):1187-98.
125. Israelsen WJ, Dayton TL, Davidson SM, Fiske BP, Hosios AM, Bellinger G, et al. PKM2 isoform-specific deletion reveals a differential requirement for pyruvate kinase in tumor cells. *Cell*. 2013;155(2):397-409.
126. Boxer MB, Jiang JK, Vander Heiden MG, Shen M, Skoumbourdis AP, Southall N, et al. Evaluation of substituted N,N'-diarylsulfonamides as activators of the tumor cell specific M2 isoform of pyruvate kinase. *Journal of medicinal chemistry*. 2010;53(3):1048-55.
127. Jiang JK, Boxer MB, Vander Heiden MG, Shen M, Skoumbourdis AP, Southall N, et al. Evaluation of thieno[3,2-b]pyrrole[3,2-d]pyridazinones as activators of the tumor cell specific M2 isoform of pyruvate kinase. *Bioorganic & medicinal chemistry letters*. 2010;20(11):3387-93.
128. Auld D, Shen M, Skoumbourdis AP, Jiang J, Boxer M, Southall N, et al. Identification of activators for the M2 isoform of human pyruvate kinase. *Probe Reports from the NIH Molecular Libraries Program*. Bethesda (MD)2010.
129. Walsh MJ, Brimacombe KR, Veith H, Bougie JM, Daniel T, Leister W, et al. 2-Oxo-N-aryl-1,2,3,4-tetrahydroquinoline-6-sulfonamides as activators of the tumor cell specific M2 isoform of pyruvate kinase. *Bioorganic & medicinal chemistry letters*. 2011;21(21):6322-7.
130. DeBerardinis RJ, Cheng T. Q's next: the diverse functions of glutamine in metabolism, cell biology and cancer. *Oncogene*. 2010;29(3):313-24.
131. Semenza GL, Jiang BH, Leung SW, Passantino R, Concordet JP, Maire P, et al. Hypoxia response elements in the aldolase A, enolase 1, and lactate

- dehydrogenase A gene promoters contain essential binding sites for hypoxia-inducible factor 1. *J Biol Chem.* 1996;271(51):32529-37.
132. Sun W, Zhou S, Chang SS, McFate T, Verma A, Califano JA. Mitochondrial mutations contribute to HIF1 $\alpha$  accumulation via increased reactive oxygen species and up-regulated pyruvate dehydrogenase kinase 2 in head and neck squamous cell carcinoma. *Clinical cancer research : an official journal of the American Association for Cancer Research.* 2009;15(2):476-84.
133. Michelakis ED, Webster L, Mackey JR. Dichloroacetate (DCA) as a potential metabolic-targeting therapy for cancer. *British journal of cancer.* 2008;99(7):989-94.
134. Stuwe L, Muller M, Fabian A, Waning J, Mally S, Noel J, et al. pH dependence of melanoma cell migration: protons extruded by NHE1 dominate protons of the bulk solution. *The Journal of physiology.* 2007;585(Pt 2):351-60.
135. Wong P, Kleemann HW, Tannock IF. Cytostatic potential of novel agents that inhibit the regulation of intracellular pH. *British journal of cancer.* 2002;87(2):238-45.
136. Sonveaux P, Vegran F, Schroeder T, Wergin MC, Verrax J, Rabbani ZN, et al. Targeting lactate-fueled respiration selectively kills hypoxic tumor cells in mice. *The Journal of clinical investigation.* 2008;118(12):3930-42.
137. Bhujwala ZM, Aboagye EO, Gillies RJ, Chacko VP, Mendola CE, Backer JM. Nm23-transfected MDA-MB-435 human breast carcinoma cells form tumors with altered phospholipid metabolism and pH: a <sup>31</sup>P nuclear magnetic resonance study in vivo and in vitro. *Magnetic resonance in medicine : official journal of the Society of Magnetic Resonance in Medicine / Society of Magnetic Resonance in Medicine.* 1999;41(5):897-903.
138. Martinez-Zaguilan R, Seftor EA, Seftor RE, Chu YW, Gillies RJ, Hendrix MJ. Acidic pH enhances the invasive behavior of human melanoma cells. *Clinical & experimental metastasis.* 1996;14(2):176-86.
139. Baumann F, Leukel P, Doerfelt A, Beier CP, Dettmer K, Oefner PJ, et al. Lactate promotes glioma migration by TGF- $\beta$ 2-dependent regulation of matrix metalloproteinase-2. *Neuro-oncology.* 2009;11(4):368-80.
140. Gatenby RA, Gawlinski ET, Gmitro AF, Kaylor B, Gillies RJ. Acid-mediated tumor invasion: a multidisciplinary study. *Cancer research.* 2006;66(10):5216-23.
141. Gillies RJ, Gatenby RA. Hypoxia and adaptive landscapes in the evolution of carcinogenesis. *Cancer metastasis reviews.* 2007;26(2):311-7.
142. Supuran CT, Briganti F, Tilli S, Chegwiddden WR, Scozzafava A. Carbonic anhydrase inhibitors: sulfonamides as antitumor agents? *Bioorganic & medicinal chemistry.* 2001;9(3):703-14.
143. Supuran CT. Indisulam: an anticancer sulfonamide in clinical development. *Expert opinion on investigational drugs.* 2003;12(2):283-7.
144. Supuran CT. Carbonic anhydrases: novel therapeutic applications for inhibitors and activators. *Nature reviews Drug discovery.* 2008;7(2):168-81.
145. Chiche J, Ilc K, Laferriere J, Trottier E, Dayan F, Mazure NM, et al. Hypoxia-inducible carbonic anhydrase IX and XII promote tumor cell growth by counteracting acidosis through the regulation of the intracellular pH. *Cancer research.* 2009;69(1):358-68.
146. DeBerardinis RJ, Mancuso A, Daikhin E, Nissim I, Yudkoff M, Wehrli S, et al. Beyond aerobic glycolysis: transformed cells can engage in glutamine metabolism that exceeds the requirement for protein and nucleotide synthesis. *Proceedings of the National Academy of Sciences of the United States of America.* 2007;104(49):19345-50.

147. Szeliga M, Obara-Michlewska M. Glutamine in neoplastic cells: focus on the expression and roles of glutaminases. *Neurochemistry international*. 2009;55(1-3):71-5.
148. Samid D, Yeh A, Prasanna P. Induction of erythroid differentiation and fetal hemoglobin production in human leukemic cells treated with phenylacetate. *Blood*. 1992;80(6):1576-81.
149. Samid D, Shack S, Myers CE. Selective growth arrest and phenotypic reversion of prostate cancer cells in vitro by nontoxic pharmacological concentrations of phenylacetate. *The Journal of clinical investigation*. 1993;91(5):2288-95.
150. Samid D, Ram Z, Hudgins WR, Shack S, Liu L, Walbridge S, et al. Selective activity of phenylacetate against malignant gliomas: resemblance to fetal brain damage in phenylketonuria. *Cancer research*. 1994;54(4):891-5.
151. Dang CV. MYC, microRNAs and glutamine addiction in cancers. *Cell cycle*. 2009;8(20):3243-5.
152. Rosenfeld H, Roberts J. Enhancement of antitumor activity of glutamine antagonists 6-diazo-5-oxo-L-norleucine and acivicin in cell culture by glutaminase-asparaginase. *Cancer research*. 1981;41(4):1324-8.
153. Seltzer MJ, Bennett BD, Joshi AD, Gao P, Thomas AG, Ferraris DV, et al. Inhibition of glutaminase preferentially slows growth of glioma cells with mutant IDH1. *Cancer research*. 2010;70(22):8981-7.
154. Haskell CM, Canellos GP, Leventhal BG, Carbone PP, Block JB, Serpick AA, et al. L-asparaginase: therapeutic and toxic effects in patients with neoplastic disease. *The New England journal of medicine*. 1969;281(19):1028-34.
155. Masetti R, Pession A. First-line treatment of acute lymphoblastic leukemia with pegasparaginase. *Biologics : targets & therapy*. 2009;3:359-68.
156. Feun L, Savaraj N. Pegylated arginine deiminase: a novel anticancer enzyme agent. *Expert opinion on investigational drugs*. 2006;15(7):815-22.
157. Izzo F, Marra P, Beneduce G, Castello G, Vallone P, De Rosa V, et al. Pegylated arginine deiminase treatment of patients with unresectable hepatocellular carcinoma: results from phase I/II studies. *Journal of clinical oncology : official journal of the American Society of Clinical Oncology*. 2004;22(10):1815-22.
158. Alo PL, Visca P, Marci A, Mangoni A, Botti C, Di Tondo U. Expression of fatty acid synthase (FAS) as a predictor of recurrence in stage I breast carcinoma patients. *Cancer*. 1996;77(3):474-82.
159. Rashid A, Pizer ES, Moga M, Milgraum LZ, Zahurak M, Pasternack GR, et al. Elevated expression of fatty acid synthase and fatty acid synthetic activity in colorectal neoplasia. *The American journal of pathology*. 1997;150(1):201-8.
160. Pizer ES, Lax SF, Kuhajda FP, Pasternack GR, Kurman RJ. Fatty acid synthase expression in endometrial carcinoma: correlation with cell proliferation and hormone receptors. *Cancer*. 1998;83(3):528-37.
161. Li JN, Gorospe M, Chrest FJ, Kumaravel TS, Evans MK, Han WF, et al. Pharmacological inhibition of fatty acid synthase activity produces both cytostatic and cytotoxic effects modulated by p53. *Cancer research*. 2001;61(4):1493-9.
162. Vazquez-Martin A, Ropero S, Brunet J, Colomer R, Menendez JA. Inhibition of Fatty Acid Synthase (FASN) synergistically enhances the efficacy of 5-fluorouracil in breast carcinoma cells. *Oncology reports*. 2007;18(4):973-80.
163. Hatzivassiliou G, Zhao F, Bauer DE, Andreadis C, Shaw AN, Dhanak D, et al. ATP citrate lyase inhibition can suppress tumor cell growth. *Cancer cell*. 2005;8(4):311-21.

164. Clem BF, Clem AL, Yalcin A, Goswami U, Arumugam S, Telang S, et al. A novel small molecule antagonist of choline kinase-alpha that simultaneously suppresses MAPK and PI3K/AKT signaling. *Oncogene*. 2011;30(30):3370-80.
165. Beckers A, Organe S, Timmermans L, Scheys K, Peeters A, Brusselmans K, et al. Chemical inhibition of acetyl-CoA carboxylase induces growth arrest and cytotoxicity selectively in cancer cells. *Cancer research*. 2007;67(17):8180-7.
166. Nomura DK, Long JZ, Niessen S, Hoover HS, Ng SW, Cravatt BF. Monoacylglycerol lipase regulates a fatty acid network that promotes cancer pathogenesis. *Cell*. 2010;140(1):49-61.
167. Cao Z, Fan-Minogue H, Bellovin DI, Yevtodiyeenko A, Arzeno J, Yang Q, et al. MYC phosphorylation, activation, and tumorigenic potential in hepatocellular carcinoma are regulated by HMG-CoA reductase. *Cancer research*. 2011;71(6):2286-97.
168. Wilson WR, Hay MP. Targeting hypoxia in cancer therapy. *Nature reviews Cancer*. 2011;11(6):393-410.
169. Engelman JA. Targeting PI3K signalling in cancer: opportunities, challenges and limitations. *Nature reviews Cancer*. 2009;9(8):550-62.
170. Cushman SW, Wardzala LJ. Potential mechanism of insulin action on glucose transport in the isolated rat adipose cell. Apparent translocation of intracellular transport systems to the plasma membrane. *The Journal of biological chemistry*. 1980;255(10):4758-62.
171. Suzuki K, Kono T. Evidence that insulin causes translocation of glucose transport activity to the plasma membrane from an intracellular storage site. *Proceedings of the National Academy of Sciences of the United States of America*. 1980;77(5):2542-5.
172. Deprez J, Vertommen D, Alessi DR, Hue L, Rider MH. Phosphorylation and activation of heart 6-phosphofructo-2-kinase by protein kinase B and other protein kinases of the insulin signaling cascades. *The Journal of biological chemistry*. 1997;272(28):17269-75.
173. Majewski N, Nogueira V, Robey RB, Hay N. Akt inhibits apoptosis downstream of BID cleavage via a glucose-dependent mechanism involving mitochondrial hexokinases. *Molecular and cellular biology*. 2004;24(2):730-40.
174. Dankort D, Curley DP, Carlidge RA, Nelson B, Karnezis AN, Damsky WE, Jr., et al. Braf(V600E) cooperates with Pten loss to induce metastatic melanoma. *Nature genetics*. 2009;41(5):544-52.
175. Brachmann S, Fritsch C, Maira SM, Garcia-Echeverria C. PI3K and mTOR inhibitors: a new generation of targeted anticancer agents. *Current opinion in cell biology*. 2009;21(2):194-8.
176. Abraham RT, Eng CH. Mammalian target of rapamycin as a therapeutic target in oncology. *Expert opinion on therapeutic targets*. 2008;12(2):209-22.
177. Um SH, Frigerio F, Watanabe M, Picard F, Joaquin M, Sticker M, et al. Absence of S6K1 protects against age- and diet-induced obesity while enhancing insulin sensitivity. *Nature*. 2004;431(7005):200-5.
178. Esteve-Puig R, Canals F, Colome N, Merlino G, Recio JA. Uncoupling of the LKB1-AMPKalpha energy sensor pathway by growth factors and oncogenic BRAF. *PloS one*. 2009;4(3):e4771.
179. Zheng B, Jeong JH, Asara JM, Yuan YY, Granter SR, Chin L, et al. Oncogenic B-RAF negatively regulates the tumor suppressor LKB1 to promote melanoma cell proliferation. *Molecular cell*. 2009;33(2):237-47.
180. Appleyard MV, Murray KE, Coates PJ, Wullschleger S, Bray SE, Kernohan NM, et al. Phenformin as prophylaxis and therapy in breast cancer xenografts. *British journal of cancer*. 2012;106(6):1117-22.

181. Shackelford DB, Abt E, Gerken L, Vasquez DS, Seki A, Leblanc M, et al. LKB1 inactivation dictates therapeutic response of non-small cell lung cancer to the metabolism drug phenformin. *Cancer cell*. 2013;23(2):143-58.
182. Libby G, Donnelly LA, Donnan PT, Alessi DR, Morris AD, Evans JM. New users of metformin are at low risk of incident cancer: a cohort study among people with type 2 diabetes. *Diabetes care*. 2009;32(9):1620-5.
183. Anisimov VN, Berstein LM, Egorin PA, Piskunova TS, Popovich IG, Zabezhinski MA, et al. Effect of metformin on life span and on the development of spontaneous mammary tumors in HER-2/neu transgenic mice. *Experimental gerontology*. 2005;40(8-9):685-93.
184. Dowling RJ, Zakikhani M, Fantus IG, Pollak M, Sonenberg N. Metformin inhibits mammalian target of rapamycin-dependent translation initiation in breast cancer cells. *Cancer research*. 2007;67(22):10804-12.
185. Foretz M, Hebrard S, Leclerc J, Zarrinpashneh E, Soty M, Mithieux G, et al. Metformin inhibits hepatic gluconeogenesis in mice independently of the LKB1/AMPK pathway via a decrease in hepatic energy state. *The Journal of clinical investigation*. 2010;120(7):2355-69.
186. El-Mir MY, Nogueira V, Fontaine E, Averet N, Rigoulet M, Leverve X. Dimethylbiguanide inhibits cell respiration via an indirect effect targeted on the respiratory chain complex I. *The Journal of biological chemistry*. 2000;275(1):223-8.
187. Dunn WB, Bailey NJ, Johnson HE. Measuring the metabolome: current analytical technologies. *The Analyst*. 2005;130(5):606-25.
188. Griffiths WJ, Koal T, Wang Y, Kohl M, Enot DP, Dignier HP. Targeted metabolomics for biomarker discovery. *Angewandte Chemie*. 2010;49(32):5426-45.
189. Buscher JM, Czernik D, Ewald JC, Sauer U, Zamboni N. Cross-platform comparison of methods for quantitative metabolomics of primary metabolism. *Analytical chemistry*. 2009;81(6):2135-43.
190. Lu W, Bennett BD, Rabinowitz JD. Analytical strategies for LC-MS-based targeted metabolomics. *Journal of chromatography B, Analytical technologies in the biomedical and life sciences*. 2008;871(2):236-42.
191. Zamboni N, Sauer U. Novel biological insights through metabolomics and <sup>13</sup>C-flux analysis. *Current opinion in microbiology*. 2009;12(5):553-8.
192. Vichai V, Kirtikara K. Sulforhodamine B colorimetric assay for cytotoxicity screening. *Nature protocols*. 2006;1(3):1112-6.
193. Chaneton B, Gottlieb E. Rocking cell metabolism: revised functions of the key glycolytic regulator PKM2 in cancer. *Trends in biochemical sciences*. 2012;37(8):309-16.
194. Noguchi T, Yamada K, Inoue H, Matsuda T, Tanaka T. The L- and R-type isozymes of rat pyruvate kinase are produced from a single gene by use of different promoters. *The Journal of biological chemistry*. 1987;262(29):14366-71.
195. Altenberg B, Greulich KO. Genes of glycolysis are ubiquitously overexpressed in 24 cancer classes. *Genomics*. 2004;84(6):1014-20.
196. Imamura K, Tanaka T. Multimolecular forms of pyruvate kinase from rat and other mammalian tissues. I. Electrophoretic studies. *Journal of biochemistry*. 1972;71(6):1043-51.
197. Wooll JO, Friesen RH, White MA, Watowich SJ, Fox RO, Lee JC, et al. Structural and functional linkages between subunit interfaces in mammalian pyruvate kinase. *Journal of molecular biology*. 2001;312(3):525-40.

198. Mazurek S. Pyruvate kinase type M2: a key regulator within the tumour metabolome and a tool for metabolic profiling of tumours. *Ernst Schering Foundation symposium proceedings*. 2007(4):99-124.
199. Mazurek S. Pyruvate kinase type M2: a key regulator of the metabolic budget system in tumor cells. *The international journal of biochemistry & cell biology*. 2011;43(7):969-80.
200. Chaneton B, Hillmann P, Zheng L, Martin AC, Maddocks OD, Chokkathukalam A, et al. Serine is a natural ligand and allosteric activator of pyruvate kinase M2. *Nature*. 2012;491(7424):458-62.
201. de Koning TJ, Snell K, Duran M, Berger R, Poll-The BT, Surtees R. L-serine in disease and development. *The Biochemical journal*. 2003;371(Pt 3):653-61.
202. Collado M, Serrano M. Senescence in tumours: evidence from mice and humans. *Nature reviews Cancer*. 2010;10(1):51-7.
203. Matoba S, Kang JG, Patino WD, Wragg A, Boehm M, Gavrilova O, et al. p53 regulates mitochondrial respiration. *Science*. 2006;312(5780):1650-3.
204. Campisi J. Replicative senescence: an old lives' tale? *Cell*. 1996;84(4):497-500.
205. Pardee AB. A restriction point for control of normal animal cell proliferation. *Proceedings of the National Academy of Sciences of the United States of America*. 1974;71(4):1286-90.
206. Rolfe DF, Brown GC. Cellular energy utilization and molecular origin of standard metabolic rate in mammals. *Physiological reviews*. 1997;77(3):731-58.
207. Kuilman T, Michaloglou C, Vredeveld LC, Douma S, van Doorn R, Desmet CJ, et al. Oncogene-induced senescence relayed by an interleukin-dependent inflammatory network. *Cell*. 2008;133(6):1019-31.
208. Selivanov VA, Marin S, Lee PW, Cascante M. Software for dynamic analysis of tracer-based metabolomic data: estimation of metabolic fluxes and their statistical analysis. *Bioinformatics*. 2006;22(22):2806-12.
209. de Mas IM, Selivanov VA, Marin S, Roca J, Oresic M, Agius L, et al. Compartmentation of glycogen metabolism revealed from <sup>13</sup>C isotopologue distributions. *BMC systems biology*. 2011;5:175.
210. Lemons JM, Feng XJ, Bennett BD, Legesse-Miller A, Johnson EL, Raitman I, et al. Quiescent fibroblasts exhibit high metabolic activity. *PLoS biology*. 2010;8(10):e1000514.
211. Hodis E, Watson IR, Kryukov GV, Arold ST, Imielinski M, Theurillat JP, et al. A landscape of driver mutations in melanoma. *Cell*. 2012;150(2):251-63.
212. Berger MF, Hodis E, Heffernan TP, Deribe YL, Lawrence MS, Protopopov A, et al. Melanoma genome sequencing reveals frequent PREX2 mutations. *Nature*. 2012;485(7399):502-6.
213. Krauthammer M, Kong Y, Ha BH, Evans P, Bacchicocchi A, McCusker JP, et al. Exome sequencing identifies recurrent somatic RAC1 mutations in melanoma. *Nature genetics*. 2012;44(9):1006-14.
214. Sosman JA, Kim KB, Schuchter L, Gonzalez R, Pavlick AC, Weber JS, et al. Survival in BRAF V600-mutant advanced melanoma treated with vemurafenib. *The New England journal of medicine*. 2012;366(8):707-14.
215. Hauschild A, Grob JJ, Demidov LV, Jouary T, Gutzmer R, Millward M, et al. Dabrafenib in BRAF-mutated metastatic melanoma: a multicentre, open-label, phase 3 randomised controlled trial. *Lancet*. 2012;380(9839):358-65.
216. Poulidakos PI, Zhang C, Bollag G, Shokat KM, Rosen N. RAF inhibitors transactivate RAF dimers and ERK signalling in cells with wild-type BRAF. *Nature*. 2010;464(7287):427-30.

217. Girotti MR, Pedersen M, Sanchez-Laorden B, Viros A, Turajlic S, Niculescu-Duvaz D, et al. Inhibiting EGF receptor or SRC family kinase signaling overcomes BRAF inhibitor resistance in melanoma. *Cancer discovery*. 2013;3(2):158-67.
218. Shi H, Moriceau G, Kong X, Lee MK, Lee H, Koya RC, et al. Melanoma whole-exome sequencing identifies (V600E)B-RAF amplification-mediated acquired B-RAF inhibitor resistance. *Nature communications*. 2012;3:724.
219. Nazarian R, Shi H, Wang Q, Kong X, Koya RC, Lee H, et al. Melanomas acquire resistance to B-RAF(V600E) inhibition by RTK or N-RAS upregulation. *Nature*. 2010;468(7326):973-7.
220. Johannessen CM, Johnson LA, Piccioni F, Townes A, Frederick DT, Donahue MK, et al. A melanocyte lineage program confers resistance to MAP kinase pathway inhibition. *Nature*. 2013;504(7478):138-42.
221. Komurov K, Tseng JT, Muller M, Seviour EG, Moss TJ, Yang L, et al. The glucose-deprivation network counteracts lapatinib-induced toxicity in resistant ErbB2-positive breast cancer cells. *Molecular systems biology*. 2012;8:596.
222. Zhao Y, Liu H, Liu Z, Ding Y, Ledoux SP, Wilson GL, et al. Overcoming trastuzumab resistance in breast cancer by targeting dysregulated glucose metabolism. *Cancer research*. 2011;71(13):4585-97.
223. Scott DA, Richardson AD, Filipp FV, Knutzen CA, Chiang GG, Ronai ZA, et al. Comparative metabolic flux profiling of melanoma cell lines: beyond the Warburg effect. *The Journal of biological chemistry*. 2011;286(49):42626-34.
224. Hall A, Meyle KD, Lange MK, Klima M, Sanderhoff M, Dahl C, et al. Dysfunctional oxidative phosphorylation makes malignant melanoma cells addicted to glycolysis driven by the (V600E)BRAF oncogene. *Oncotarget*. 2013;4(4):584-99.
225. Haq R, Shoag J, Andreu-Perez P, Yokoyama S, Edelman H, Rowe GC, et al. Oncogenic BRAF regulates oxidative metabolism via PGC1alpha and MITF. *Cancer cell*. 2013;23(3):302-15.
226. Vazquez F, Lim JH, Chim H, Bhalla K, Girnun G, Pierce K, et al. PGC1alpha expression defines a subset of human melanoma tumors with increased mitochondrial capacity and resistance to oxidative stress. *Cancer cell*. 2013;23(3):287-301.
227. Corazao-Rozas P, Guerreschi P, Jendoubi M, Andre F, Jonneaux A, Scalbert C, et al. Mitochondrial oxidative stress is the Achilles' heel of melanoma cells resistant to Braf-mutant inhibitor. *Oncotarget*. 2013;4(11):1986-98.
228. Sauer LA, Stayman JW, 3rd, Dauchy RT. Amino acid, glucose, and lactic acid utilization in vivo by rat tumors. *Cancer research*. 1982;42(10):4090-7.
229. Dang CV. Glutaminolysis: supplying carbon or nitrogen or both for cancer cells? *Cell cycle*. 2010;9(19):3884-6.
230. Hamanaka RB, Chandel NS. Cell biology. Warburg effect and redox balance. *Science*. 2011;334(6060):1219-20.
231. Kwee TC, Basu S, Saboury B, Ambrosini V, Torigian DA, Alavi A. A new dimension of FDG-PET interpretation: assessment of tumor biology. *European journal of nuclear medicine and molecular imaging*. 2011;38(6):1158-70.
232. Ulanovskaya OA, Cui J, Kron SJ, Kozmin SA. A pairwise chemical genetic screen identifies new inhibitors of glucose transport. *Chemistry & biology*. 2011;18(2):222-30.
233. Hanahan D, Weinberg RA. Hallmarks of cancer: the next generation. *Cell*. 2011;144(5):646-74.
234. Wu P, Inskip K, Bowker-Kinley MM, Popov KM, Harris RA. Mechanism responsible for inactivation of skeletal muscle pyruvate dehydrogenase complex in starvation and diabetes. *Diabetes*. 1999;48(8):1593-9.

235. Sugden MC, Holness MJ. Therapeutic potential of the mammalian pyruvate dehydrogenase kinases in the prevention of hyperglycaemia. *Current drug targets Immune, endocrine and metabolic disorders*. 2002;2(2):151-65.
236. Lewandowski ED, White LT. Pyruvate dehydrogenase influences postischemic heart function. *Circulation*. 1995;91(7):2071-9.
237. Terrand J, Papageorgiou I, Rosenblatt-Velin N, Lerch R. Calcium-mediated activation of pyruvate dehydrogenase in severely injured postischemic myocardium. *American journal of physiology Heart and circulatory physiology*. 2001;281(2):H722-30.
238. McFate T, Mohyeldin A, Lu H, Thakar J, Henriques J, Halim ND, et al. Pyruvate dehydrogenase complex activity controls metabolic and malignant phenotype in cancer cells. *The Journal of biological chemistry*. 2008;283(33):22700-8.
239. Zwerschke W, Mazurek S, Stockl P, Hutter E, Eigenbrodt E, Jansen-Durr P. Metabolic analysis of senescent human fibroblasts reveals a role for AMP in cellular senescence. *The Biochemical journal*. 2003;376(Pt 2):403-11.
240. Kondoh H, Lleonart ME, Gil J, Wang J, Degan P, Peters G, et al. Glycolytic enzymes can modulate cellular life span. *Cancer research*. 2005;65(1):177-85.
241. Kuilman T, Michaloglou C, Mooi WJ, Peeper DS. The essence of senescence. *Genes & development*. 2010;24(22):2463-79.
242. Wigfield SM, Winter SC, Giatromanolaki A, Taylor J, Koukourakis ML, Harris AL. PDK-1 regulates lactate production in hypoxia and is associated with poor prognosis in head and neck squamous cancer. *British journal of cancer*. 2008;98(12):1975-84.
243. Rodier F, Coppe JP, Patil CK, Hoesijmakers WA, Munoz DP, Raza SR, et al. Persistent DNA damage signalling triggers senescence-associated inflammatory cytokine secretion. *Nature cell biology*. 2009;11(8):973-9.
244. Kuilman T, Peeper DS. Senescence-messaging secretome: SMS-ing cellular stress. *Nature reviews Cancer*. 2009;9(2):81-94.
245. Ramanathan A, Wang C, Schreiber SL. Perturbational profiling of a cell-line model of tumorigenesis by using metabolic measurements. *Proceedings of the National Academy of Sciences of the United States of America*. 2005;102(17):5992-7.
246. Nardella C, Clohessy JG, Alimonti A, Pandolfi PP. Pro-senescence therapy for cancer treatment. *Nature reviews Cancer*. 2011;11(7):503-11.
247. Eagle H. Nutrition needs of mammalian cells in tissue culture. *Science*. 1955;122(3168):501-14.
248. Metallo CM, Gameiro PA, Bell EL, Mattaini KR, Yang J, Hiller K, et al. Reductive glutamine metabolism by IDH1 mediates lipogenesis under hypoxia. *Nature*. 2012;481(7381):380-4.
249. Parmenter TJ, Kleinschmidt M, Kinross KM, Bond ST, Li J, Kaadige MR, et al. Response of BRAF-mutant melanoma to BRAF inhibition is mediated by a network of transcriptional regulators of glycolysis. *Cancer discovery*. 2014;4(4):423-33.
250. Vander Heiden MG, Lunt SY, Dayton TL, Fiske BP, Israelsen WJ, Mattaini KR, et al. Metabolic pathway alterations that support cell proliferation. *Cold Spring Harbor symposia on quantitative biology*. 2011;76:325-34.
251. McGuirk S, Gravel SP, Deblois G, Papadopoli DJ, Faubert B, Wegner A, et al. PGC-1alpha supports glutamine metabolism in breast cancer. *Cancer & metabolism*. 2013;1(1):22.
252. Wang Q, Beaumont KA, Otte NJ, Font J, Bailey CG, van Geldermalsen M, et al. Targeting glutamine transport to suppress melanoma cell growth.

International journal of cancer Journal international du cancer.  
2014;135(5):1060-71.

253. Pollak MN. Investigating metformin for cancer prevention and treatment: the end of the beginning. *Cancer discovery*. 2012;2(9):778-90.

254. Yuan P, Ito K, Perez-Lorenzo R, Del Guzzo C, Lee JH, Shen CH, et al. Phenformin enhances the therapeutic benefit of BRAF(V600E) inhibition in melanoma. *Proceedings of the National Academy of Sciences of the United States of America*. 2013;110(45):18226-31.

255. Weinberg R. Point: Hypotheses first. *Nature*. 2010;464(7289):678.

# Appendices